21

RE-ORDER NO. 66-933

06988-6002-R000

TEMPERATURE CONTROL FLUX MONITOR FOR MARINER MARS 1969

FINAL REPORT

CONTRACT NO. 951726

DECEMBER 9, 1966

Prepared for

JET PROPULSION LABORATORY

This work was performed for the Jet Propulsion Laboratory, California Institute of Technology, sponsored by the National Aeronautics and Space Administration under Contract NAS7-100.

TRW SYSTEMS
AN OPERATING GROUP OF TRW INC.

CONTENTS

CONTENTS (Continued)

ILLUSTRATIONS

TABLES

1. INTRODUCTION

This document constitutes the Final Report on the definition study and preliminary design of the Temperature Control Flux Monitor (TCFM) for Mariner Mars 1969. It is a compendium of preliminary design requirements and supportive analyses generated during the study and design phases. This report is intended to supplement the previously submitted Definition Study Report, TRW Document No. 06988-6001-R000, which contains a detailed description of the recommended control and measurement approach for adapting the JPL Absolute Cavity Radiometer concept to the Mariner Mars 1969 spacecraft application.

Taken together, these two documents contain the essential body of preliminary design information required to proceed with the detailed design and hardware development phases.

As a result of the completed initial design effort, it is concluded that the essential target requirements set forth for the TCFM can be met within the existing state-of-the-art techniques. Further, the target requirements can be achieved without imposition of additional or undue constraints on the Mariner spacecraft system.

2. DESIGN CONSIDERATIONS

2.1 Transducer Preliminary Design Considerations

The preliminary design of the TCFM transducer retains the essential features of the JPL Absolute Cavity Radiometer laboratory prototype, as shown in the layout of Figure 2-1.

The conical receptor element will be a cone of 23.5° included apex angle with a base aperture of 0.96 cm^2. Inasmuch as analyses and experimental tests by JPL have shown this to be an acceptable design, there is no significant basis for altering these dimensions. The conical element is to be electro-deposited silver machined on its exterior surface to achieve a uniform metal thickness of 0.005-inch. The cone will contain two bifilar windings, one to serve as a heater and one as a temperature sensor.

The heater winding of 0.002-inch dia Evanohm wire will occupy the forward 25% of the cone length. This location improves the isothermality of the cone as shown by prior JPL analysis.

The sensor winding of either CP platinum or CP nickel, will have a nominal room temperature resistance of 600 ohms. In order to assume precise tracking between the cone temperature sensor and the thermal guard temperature sensor, it is important that these be precisely matched in resistance at the operating reference temperature. A matching tolerance of 0.05% will be required. The selection of the type of wire (platinum or nickel) to be utilized for the temperature sensors is not entirely clear. Although the stability and low strain coefficient of platinum is desirable, the increased sensitivity of nickel is attractive from the control standpoint. Platinum sensors should be utilized if the sensitivity requirements of the control system permit.

The thermal guard temperature sensors will be wound on a 0.005-inch thick cylindrical silver spool. Three separate windings will be required for the thermal-guard set point control, the cone-guard differential temperature control, and the guard absolute temperature measurement.

The guard absolute temperature measurement sensor is intended to be of a resistance (100 ohms) that is compatible with most precision

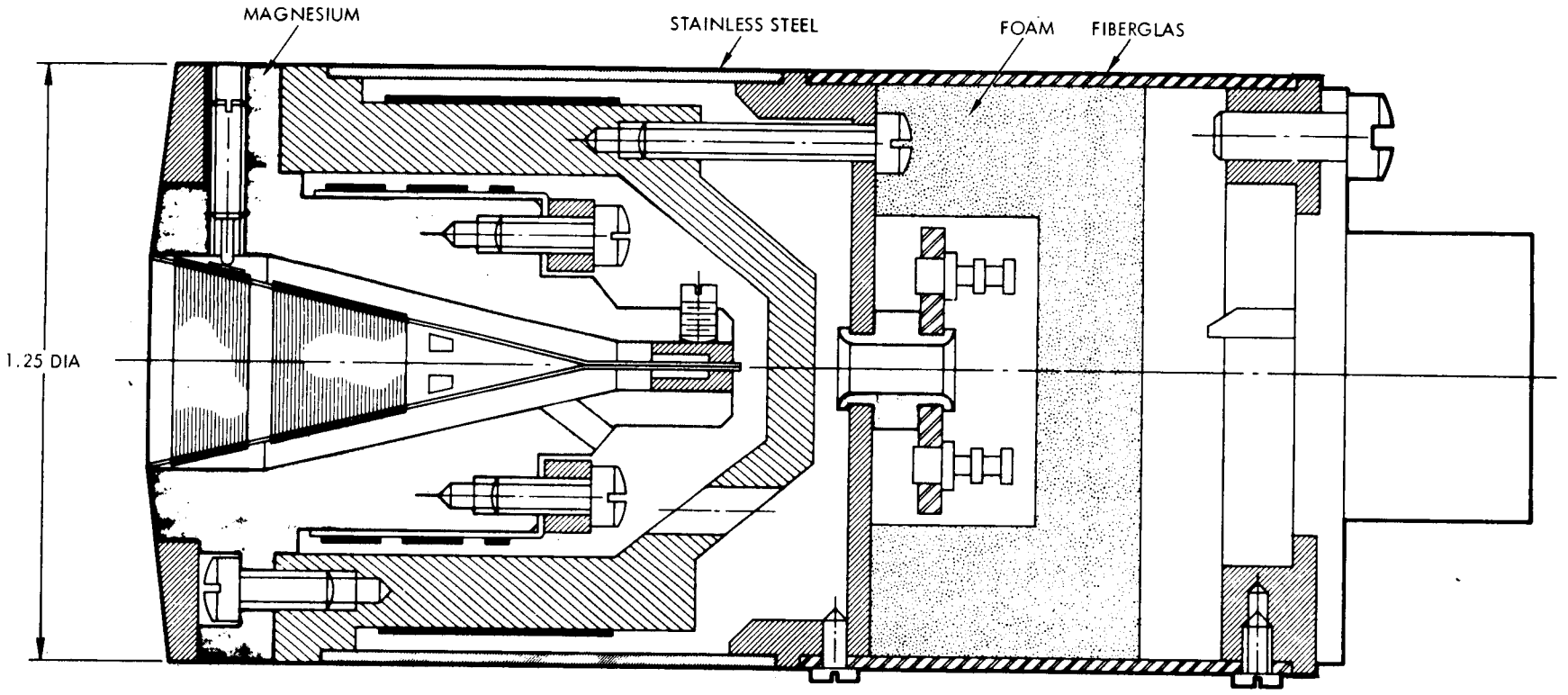

Figure 2-1. Transducer and Mounting Fixture

temperature measurement laboratory equipment, such as standard Mueller bridges. If a decision is made to measure the absolute temperature of the transducer inflight, a higher resistance winding for this sensor will be required.

The design of the thermal guard sensor spool is such that more intimate thermal contrast with the guard structure is possible. The spool incorporates a flange which is attached to the guard by means of six No. 0 screws, with an interface filler of RTV-11 approximately 0.001-inch thick. This arrangement improves the dynamic control stability of the system.

In order to minimize the thermal strain differential between the cone sensor and the guard sensors, the guard sensor spool will also be formed by electro-deposition of silver, 0.005-inch thick.

All windings on either the cone or the guard sensor spool will be terminated at small insulated tabs to permit the attachment of lead wires. The selection of material and diameter of lead wires is critical. In order to reduce parasitic power loss, a low conductivity material is desired; on the other hand low resistance, thermal EMF, and temperature coefficient must be considered in the selection. All things considered, the best choice at present appears to be copper wire of a diameter between 0.003-inch and 0.005-inch.

The most significant change in the transducer design involves the use of a magnesium alloy for the thermal guard structure. ASTM type ZE 10A-H24 or HM 21A-T8 appear to be best suited due to their higher thermal conductivity (78 Btu/hr/ft^2/°F/ft). The use of magnesium has required a mechanically joined, two-piece thermal guard structure. The thermal interface between the two pieces will be filled with a film of RTV-11 so that the differential temperature across the joint at a flux of 0.200 watt will be no greater than 0.10°C.

A significant weight reduction in the transducer is possible by use of magnesium alloy. Shown in Table 2-1 are the weights of the transducer components.

Table 2-1. Transducer Weights

	in^3	lb
Case-stainless steel	0.056	0.016
Outer guard - magnesium	0.58	
Inner guard - magnesium	0.31	
Back plate - magnesium	0.11	
Mounting flange - magnesium	0.19	
Total	1.19	0.077
Support - Fiberglas	0.056	0.011
Connector receptacle, Microdot RMD 53		0.040
Total		0.144
Misc. wires, screws, adhesives		0.01
Total		0.154

In order to reduce the annular gap loss from the conical element, it will be necessary to design to a gap width of 0.0005 inch. It is anticipated that this can be accomplished by overplating the guard aperture internal diameter then reaming the opening after all polishing operations have been performed. This will assure a sharp gap edge. In addition, an effort must be made to reduce the emissivity of the external surface of the cone by the application of vacuum deposited coatings. By masking difficult areas of the cone during the VDA process, it is anticipated that the majority of the cone surface can be reduced to a low emissivity. Because of the differential thermal expansion between the guard opening and the cone rim, the annular gap increases in width at the reference operating temperature of the tranducer so that in spite of a close fit of these parts at room temperature, a correction must still be applied to the aperture area value. If a successful procedure for reducing the emissivity of the cone external surface can be inplemented, the significance of the gap width can be greatly reduced.

As noted previously, the conical receptor is to be formed by electro-depositing silver on a metal mandrel which is later etched out of the cone. It is anticipated that this procedure will result in better control of alignment and concentricity of the form than the rolled sheet method of fabrication. While the electro-deposition method of forming the

receptor permits consideration of shapes other than a right cone, the external surface machining which is later required would present formidable difficulty. Furthermore, the analytical treatment(determination of effective emittance and absorptance) increases vastly in complexity for other than a linear form.

The selection of materials will be based on a continuous operating temperature of 200°C for the transducer with a short term cability of operation to 230°C. Although the choice of materials for operation at these temperatures is not wide, no difficulty is presently foreseen in selecting non-metals where these are required by the design. Silicone varnishes or polymide resins will be utilized for electrical wire insulation. Structural insulator will be made of glass cloth-silicone-resin laminations and high temperature epoxys will be used as structural adhesives backed up by screws for added structural reliability. To insure against outgassing contamination from the non-metals, all parts must be vacuum baked at 200°C for several hours prior to and after assembly.

2.2 Electronic System

The electronic system described in the Definition Study report previously submitted to JPL has not basically changed. Reference to this report is necessary for a detailed description. Further system design and error analysis has shown that the systems concept and accuracy design goals are both practical and sound.

The electronic system consists of two servo loops with integration (reset) and proportional control to accurately regulate the temperature of the thermal guard and cone, and to provide for inflight measurements of cone power and error (unbalance). Thermal guard power and temperature set point will be monitored in system ground tests.

Briefly, the control loop is essentially digital, the square-wave error signal is sampled and converted to pulses which control a 10-bit binary register. The number contained in the register accurately represents heater power. The power to the heater is controlled by register by changing the duty cycle of a constant amplitude pulse. A difference in the amount of power being supplied and the amount of power required to maintain the heated element (cone or guard) at the predetermined temperature will cause a change in the error signal. The system continues to change until the error signal is zero and the system is stable.

2.2.1 Alternate Systems

The required features of the systems are:

a. Bridge error amplification and detection

b. Power measurement and power readout

c. Supply heater power

d. Integration or reset

An additional highly desirable feature would be the ability to determine when the system is stable.

The performance requirements of the system limits the total error due to the electronics to ± 0.5%. Therefore, the power readout portion of the total error should be less than ± 0.2%. Since the telemetry channels are limited to ± 1% accuracy, it is apparent that a digital readout, using a register, is the only reasonable approach. The digital register automatically provides a means of integration and therefore satisfies this requirement.

2.2.2 A/D Versus Pulse Heater Power

If the remaining portions of the system are DC or analog, a 10 or 11-bit A/D converter would have to be used. A study of the A/D converter appears in the appendix. Included in the study is the hardware complexity error allocation, and a man loading estimate of the circuit design time. A comparison of the A/D converter approach and the all digital system shows the latter approach to be far simpler, fewer parts and shorter design cycle because of the less complex circuitry involved.

2.2.3 A2. Bridge Error Amplifiers and Detectors

The present configuration of the JPL laboratory model of the flux monitor utilizes a DC bridge temperature sensor and a DC amplifier to control the AC heater power source. The sense resistor and the heater are the same element. The DC bridge and AC heater arrangement has several drawbacks. Because of the low level error signals from the sensor, DC drift in the amplifier becomes a serious problem. In addition to the drift characteristics of the amplifier itself, thermoelectric (thermocouple) effects involving the wiring from the sensor to the amplifier input can also cause offset errors. To provide the desired system accuracy (cone temperature constant to within about 0.1°C), the DC error amplifier would most likely need to be kept at a constant temperature by means of an oven. Although this is certainly possible, the oven would add to the size, weight and power consumption of the equipment. Even with constant temperature, the DC voltage long term drift would be ±20μv/day. For a 280 day mission this drift voltage would be prohibitive. The use of AC power for the heater has the disadvantage that it requires an AC to DC conversion of the voltage and/or current to produce signals usable by the telemetry system. In the JPL lab model this was done

using vacuum thermocouples followed by DC amplifiers. This method of measurement introduces the possibility of additional errors in the system.

It is believed that the use of AC excitation for the bridge and DC power for the heater will result in both a simpler system and superior performance. A simplified diagram of this scheme is shown in Figure 2-2. The 600 cps bridge excitation signal is derived from the 2400 cps spacecraft power source by a two-stage counter. The power source is used because it precludes the necessity for generating the excitation signal by other means, it introduces no new sources of interference, and it provides a simple means of obtaining the sample pulse. The AC bridge has the disadvantage that an ambiguity exists in that it is not possible to determine in which direction the bridge is unbalanced by amplitude measurement alone. (In a DC bridge, the error signals are either positive or negative depending on the direction of the error). In the AC bridge, an error signal phase reversal takes place and this phase change must be sensed. This is done in the sample and hold circuit by always sensing inphase with the bridge excitation signal as shown in the timing diagrams of Figure 2-2. With the bridge at null and no AC signal in the sample and hold circuit, the circuit would be arranged to provide some standing output from the power amplifier to the heater. In this manner, an error in one direction would increase the output to the heater, and an error in the other direction would decrease the output. The sample and hold circuit effectively changes the AC error signal out of the error amplifier into a DC signal to drive the power amplifier. Under steady-state conditions, the voltage across the heater resistor is a steady DC voltage that can be delivered directly to the telemetry circuitry for processing as an accurate indication of the heater input power. The sample pulse occurs during the middle of the square-wave error signal; therefore, rise time, fall time, and overshoot of the error signal waveform are of little or no concern. R1, C1 and associated feedback network reduce the DC response of the amplifier to insure that DC input drifts do not cause the amplifier to saturate due to these drifts. The R2-C2 network reduces the high frequency response of the amplifier. A reasonable low corner frequency on the order of 1/100 of the signal frequency or 6 cps and a high corner frequency of about 2 kc seem reasonable.

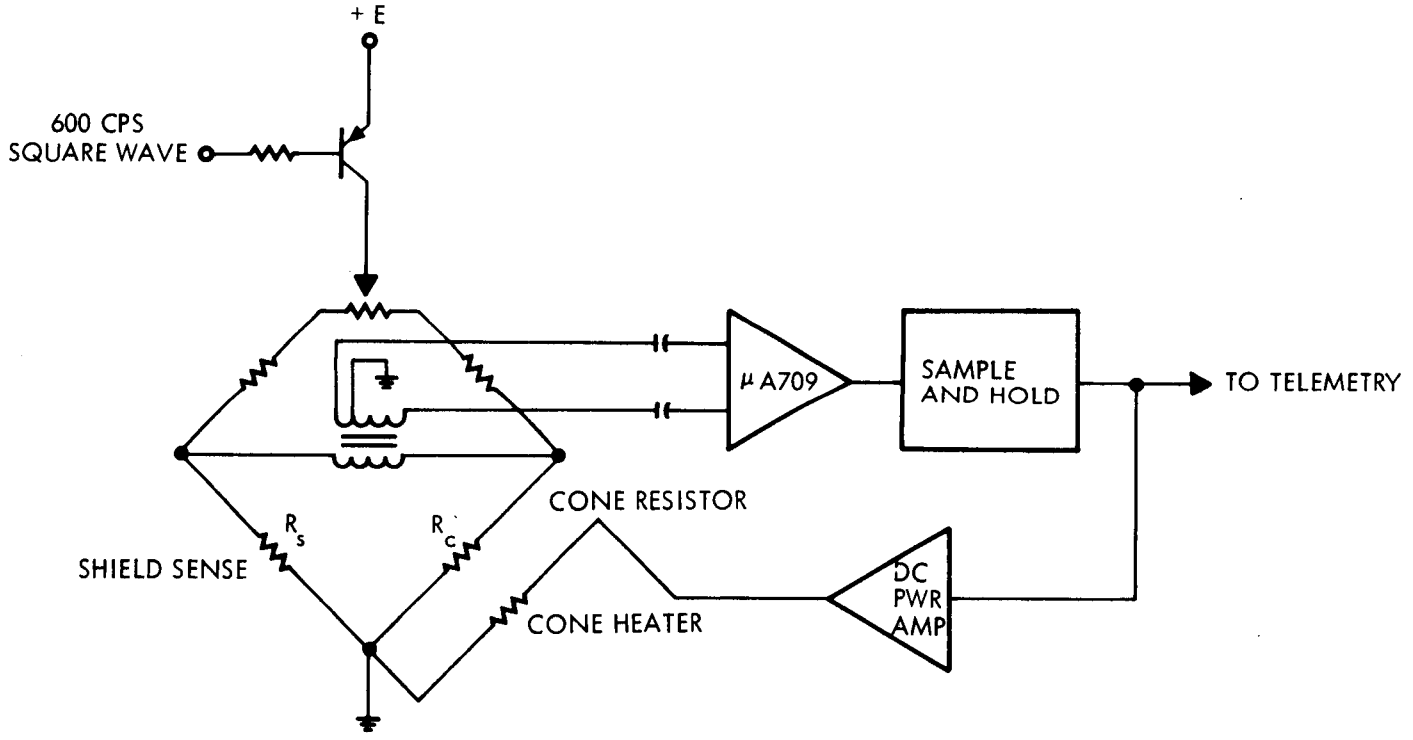

Figure 2-2. AC Sense for TCFM

Although the described system has several advantages over the present JPL scheme, it has one fault not present in the DC bridge system. In the AC bridge scheme, a common mode signal exists that is simply the bridge excitation signal that appears at the output arms of the bridge. For the circuit of Figure 2-2, this voltage is 1V p-p or 0.5 V rms. The μA 709 is a typical integrated diff amp with a common mode rejection ratio (CM_{RR}) of 70 db min. where CM_{RR} is defined as 20 log $\frac{ACM}{ADiff}$. For the circuit shown the minimum differential discernable signal (output equal to common mode signal contribution) is $(0.5)/\log^{-1} 3.5 = 158$ μv. It will be shown that this figure should be on the order of 10 μv or less.

Figure 2-2 shows a means by which the common mode signal can be greatly reduced by transformer coupling from the bridge to the amplifier input. A rejection ratio of something greater than 20 db is required. A rejection ratio for a transformer of 120 db is not unreasonable. Since both the input signal level and transformer primary DC current are low, the transformer can be made small (≈ 1-inch cube).

The hold-to-aperture time ratio for the sample and hold circuit is 8. This is a mild requirement since ratios of 1000 are common.

The circuit of Figure 2-2 could be used for both the cone and shield heaters. When used to control the shield temperature, one side of the bridge would have stable fixed resistors.

It should be noted that with the described scheme the sense resistor and heater must be separate coils. This appears to pose no problem.

2.2.4 A Discussion of the Sensor Bridge Characteristics

Of interest is the differential to common mode signal ratio and what it is dependent upon.

The bridge circuit of Figure 2-2 can be redrawn as two resistors in series as follows:

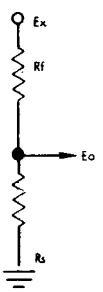

The only assumption made is that the other half of the bridge is stable. This is true by definition because the other half of the bridge is the reference.

In the equivalent circuit above, Rs is the temperature variable sense resistor, Rf is the stable resistor in the upper AM, Ex is the excitation voltage, and Eo is the common mode voltage.

$$TC = \frac{DR}{R} = \frac{\Omega/\Omega}{OC}$$

dEo is the error signal

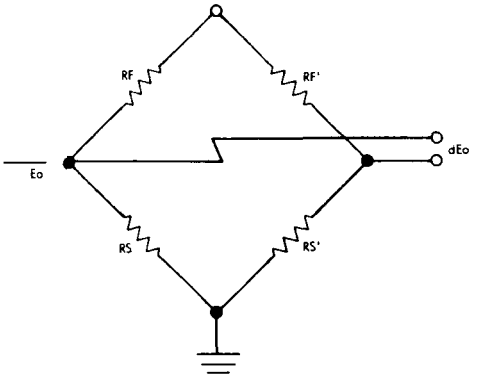

$$Eo = \frac{RS\ Ex}{(Rs + RF)} \tag{1}$$

$$dEo = \frac{(Rs + RF)\ ExdRs - RsExdRs}{(Rs + RF)^2} - \frac{RsExdRF}{(Rs + RF)^2}$$

$$= \frac{RFExdRs}{(Rs + RF)^2} - \frac{RsExdRF}{(RS + RF)^2} \tag{2}$$

Neglect the second term for now. Ratio $\frac{dEo}{Eo}$ or signal to CM signal.

$$\frac{dEo}{Eo} = \frac{RF\ dRs}{(Rs + RF)Rs} = \left(\frac{1}{\frac{Rs}{RF} + 1}\right) \frac{dRs}{Rs} \tag{3}$$

Let Rs = 1K

then TC = 0.003 $\Omega/\Omega/^{o}C$(1k)

= $3\Omega/^{o}C$

signal for 0.1^{o}C change will be RF = Rs Ex = 4V

$$dE = \frac{RF\ Ex\ dRs}{(Rs + RF)^2} = \frac{ExdRs}{4Rs} = \frac{4(0.003)}{4} = 0.3\ mv = 300\ \mu v$$

2.2.5 A. Bridge Errors

It is important that the total contribution of bridge errors does not exceed the one-bit sensitivity level established by the analog-digital converter. (See Table 2-2.)

2.2.6 A. Bridge (all signals refer to the input)

1. Noise

   a. 1/f noise for DC bridge at the bandwidth required is $\simeq 10\mu v$. At sample rates of approximately 600 cps 1/f would be $\simeq 1\mu v$.

   b. Differential offset current $\simeq 0.1$ Na/C°, for 100K impedance voltage referred to input would be

$$V_I = 1 \times 10^{-10} \times 1 \times 10^{5}$$

$$= 10\mu v$$

   c. Offset voltage drift/day

$$T \pm 20\mu v/day$$

   d. Offset temp coefficient $2\text{-}10\mu v/^{o}C$

   e. Offset current charge/day

$$I = 0.01 \text{ Na/day}$$

$$V = 1\mu v/day$$

   f. Johnson noise

$$E^2 = 4KTROf$$

$$K = \text{Boltzmann's constant } 1.38 \times 10^{-23} \text{ j/°K}$$

$$T = 410^{o}K \quad B\omega = 100 \text{ cps} \quad R = 1K$$

$$E_N = \sqrt{4x410x100x1.38.10^{-23}.10^{3}}$$

$$= \sqrt{2300x10^{-9}} \text{ volts}$$

$$= 50 \times 10^{-9} = 0.34\mu\text{volts}$$

Table 2-2. Bridge Errors

Errors	Integrated	FET Input	Chopper Stab.
*Differential offset Current temp coeff	Doubles/10°C	Doubles/10°C	±0.002 Na/°C
Differential offset volt Temp coeff	10 μv/°C	±5 μv/°C (Initial 500 μv)	±2 μv°/°C
*Offset current aging Offset voltage aging	20-50 Na/6 mo	0.5 Na (assume)	0.5 Na (assume)
Noise 1/f Thermal	10-20 μv	6 μv	
Offset voltage aging or drift/day	-50 μv ±20 μv/day	Initial 500 μv Assume 50 μv	Initial 50 μv Assume 10 μv
*Initial offset current will be adjusted	(200 Na) / 145 μv+	0.1 Na / 56 μv	±0.1 Na / 11 μv

*Assume 1K source impedance for DC case

$$\text{Total error} = \left[\text{I} + \text{V offset drift}\right] + \text{noise} + \left[\text{I} + \text{V offset temp change}\right] + \text{power supply effects}$$

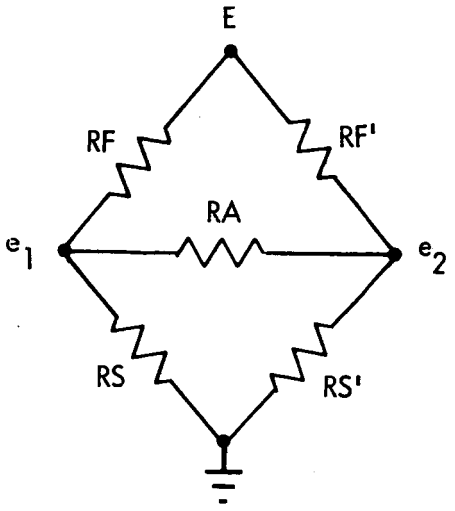

Bridge analysis to account for the input impedance of the amplifier RA

1) $$0 = e_1 \left(\frac{1}{RF} + \frac{1}{RA} + \frac{1}{RS}\right) - \frac{e_2}{RA} - \frac{E}{RF}$$

2) $$0 = \frac{-e_1}{RA} + e_2 \left(\frac{1}{RF'} + \frac{1}{RA} + \frac{1}{RS'}\right) - \frac{E}{RF'}$$

3) $$e_2 = \frac{\frac{e_1}{RA} + \frac{E}{RF'}}{\left(\frac{1}{RF'} + \frac{1}{RA'} + \frac{1}{RS'}\right)}$$

4) $$de_2 = \frac{+\left(\frac{e_1}{RA} + \frac{E}{RF'}\right) dRS'}{RS^2\left(\frac{1}{RF'} + \frac{1}{RA'} + \frac{1}{RS'}\right)^2}$$

5) From 1) $$e_1 = \frac{\frac{e_2}{RA} + \frac{E}{RF}}{\left(\frac{1}{RF} + \frac{1}{RA} + \frac{1}{RS}\right)}$$

6) $$0 = -\frac{e_2}{RA^2} - \frac{E}{RFRA} + X$$

7) $$0 = e_2 \left(\frac{1}{RF'} + \frac{1}{RA} + \frac{1}{RS'}\right)\left(\frac{1}{RF} + \frac{1}{RA} + \frac{1}{RS}\right) - \frac{E}{RF}\left(\frac{1}{RF} + \frac{1}{RA} + \frac{1}{RS}\right) - X$$

Add 6) and 7)

8) $e_2 \left[(\quad)(\quad) - \frac{1}{RA^2} \right] - E \left[\frac{1}{RF\ RA} + \frac{1}{RF'} \left(\frac{1}{RF} + \frac{1}{RA} + \frac{1}{RS} \right) \right]$

$$e_2 = \frac{E\left[\frac{1}{RF\ RA} + \frac{1}{RF'} \left(\frac{1}{RF} + \frac{1}{RA} + \frac{1}{RS} \right) \right]}{\left[\left(\frac{1}{RF'} + \frac{1}{RA} + \frac{1}{RS'} \right)\left(\frac{1}{RF} + \frac{1}{RA} + \frac{1}{RS} \right) - \frac{1}{RA^2} \right]}$$

$$= \frac{E\left[\frac{1}{RF\ RA} + \frac{1}{RF'} (A) \right]}{\left[A \left(\frac{1}{RF'} + \frac{1}{RA} + \frac{1}{RS'} \right) - \frac{1}{RA^2} \right]} = \frac{B}{\left[\quad\right]}$$

$$de_2 = - \frac{B\ d\left(\frac{A}{RS'} \right)}{\left[A \left(\frac{1}{RF'} + \frac{1}{RA} + \frac{1}{RS'} \right) - \frac{1}{RA^2} \right]^2}$$

$$\frac{de_2}{dRS'} = + \frac{BA}{RS'^2 \left[A \left(\frac{1}{RF'} + \frac{1}{RA} + \frac{1}{RS'} \right) - \frac{1}{RA^2} \right]^2}$$

$$E\left[\frac{1}{RF\ RA} + \frac{1}{RF'} \left(\frac{1}{RF} + \frac{1}{RA} + \frac{1}{RS} \right) \right]$$

$$= \frac{\cdot \left[\frac{1}{RF} + \frac{1}{RA} + \frac{1}{RS} \right]}{RS'^2 \left[\left(\frac{1}{RF} + \frac{1}{RA} + \frac{1}{RS} \right)\left(\frac{1}{RF'} + \frac{1}{RA} + \frac{1}{RS'} \right) - \frac{1}{RA^2} \right]^2}$$

Determine R' = R

Let RA $\rightarrow \infty$ to check equations

$$\frac{de_2}{dRS} = \frac{\frac{E}{RF} \left(\frac{1}{RF} + \frac{1}{RS} \right)^2}{RS^2 \left(\frac{1}{RF} + \frac{1}{RS} \right)^4} = \frac{E}{RS\ (RS)^2}$$

$$\left(\frac{1}{RF} + \frac{1}{RS} \right)^2$$

$RA \rightarrow \infty$

$$e_2 = \frac{E \frac{1}{RF'} \left(\frac{1}{RF} + \frac{1}{RS}\right)}{\left(\frac{1}{RF} + \frac{1}{RS}\right)^2} = \frac{E}{RF \left(\frac{1}{RF} + \frac{1}{RS}\right)}$$

Check Equations

$$\frac{de_2}{dRS} = \frac{E}{RF\ RS^2 \left(\frac{1}{RF} + \frac{1}{RS}\right)^2} = \frac{E\ RF}{(RF + RS)^2}$$

$$e_2 = \frac{E}{RF \left(\frac{1}{RF} + \frac{1}{RS}\right)} = \frac{E\ RS}{(RF + RS)}$$

$$\frac{de_2}{e_2} = \frac{\frac{BA\ dRS'}{RS'^2 \left[A \left(\frac{1}{RF'} + \frac{1}{RA} + \frac{1}{RS'}\right) - \frac{1}{RA^2}\right]^2}}{\frac{B}{\left[\quad\right]}}$$

$$= \frac{A\ dRS'}{RS'^2 \left[A \left(\frac{1}{RF'} + \frac{1}{RA} + \frac{1}{RS'}\right) - \frac{1}{RA^2}\right]}$$

$$= \frac{\left(\frac{1}{RF} + \frac{1}{RA} + \frac{1}{RS}\right) dRS'}{RS'^2 \left[\left(\frac{1}{RF} + \frac{1}{RA} + \frac{1}{RS}\right)\left(\frac{1}{RF'} + \frac{1}{RA} + \frac{1}{RS'}\right) - \frac{1}{RA^2}\right]}$$

Remove 'S

$$\frac{de_2}{e_2} = \frac{\left(\frac{1}{RF} + \frac{1}{RA} + \frac{1}{RS}\right)' dRS}{RS^2 \left[\left(\frac{1}{RF} + \frac{1}{RS} + \frac{1}{RA}\right)^2 - \frac{1}{RA^2}\right]}$$

$$= \frac{\left(\frac{1}{RF} + \frac{1}{RA} + \frac{1}{RS}\right) dRS}{RS^2 \left[\left(\frac{1}{RF} + \frac{1}{RS}\right)^2 + 2\left(\frac{1}{RF} + \frac{1}{RS}\right)\frac{1}{RA}\right]}$$

Variations Due To the Matched Resistors, RF and RF'

Initial tolerance $\pm 0.002\%$

Track 0.1 PPM/^{o}C (40) $\pm 0.0004\%$ $+10^{o}$C to $+50^{o}$C

Track 0.3 PPM/^{o}C 0 + 10^{o}C and 50^{o}C to 70^{o}C

0.3 PPM (20) $\pm 0.0006\%$

Long term drift 0.010%/yr (1/4)

Total variation $\frac{0.0025}{0.0055\%}$

$$\frac{dEo}{Eo} = \frac{\frac{RsExdRF}{(Rs+RF)^2}}{\frac{RsEx}{(Rs+RF)}} = \frac{dRF}{(Rs+RF)}$$

$$dR = \pm 0.0055\% \ (2K) = \Omega \ 0.011 \ \Omega$$

$$\frac{dEo\%}{Eo0} = \frac{0.011}{3K} \ (100)\% = \pm 0.004\%$$

Find the error due to a 1-bit variation in the power measurement.

$$I = (\sigma AT^4) - He$$

$$= K - He$$

$K = 0.18 \text{ w/cm}^2$ for $T = 420^{o}$

$A = 1$ cm

$$dI = \frac{\sigma I}{\sigma K} dK + \frac{\sigma I}{\sigma He} dHe$$

$$= dK - dHe$$

$$\frac{dI}{I} = \frac{dK - dHe}{K - He} = \frac{dK}{I} - \frac{dHe}{I}$$

$I_{max} = 0.15 \text{ w/cm}^2$ Earth solar constant

$I_{min} = 0.055 \text{ w/cm}^2$ Mars solar constant

$He_{max} = K - I_{min} = 0.125 \text{ w/cm}^2$

$He_{min} = K - I_{max} = 0.03$ w

For I_{max}

$$\frac{dI}{I_{max}} = \frac{dK}{K - He_{min}} - \frac{dHe}{K - He_{min}}$$

Assume $\frac{dK}{K - He_{min}} \simeq 0$ For contribution error of power only

$$\frac{dI}{I_{max}} = \frac{-dHe}{I_{max}} = \frac{-dHe}{0.15}$$

$$\% \text{ Error} = \frac{-dHe_{min}}{0.15} \times 100$$

For I_{min} $\qquad \frac{dI}{I_{min}} = \frac{-dHe}{I_{min}} = \frac{-dHe}{0.055}$

$$\% \frac{dI}{I_{min}} = \frac{-dHe}{0.055} \times 100$$

1-Bit Error $He = \frac{He_{max}}{1000} \simeq 0.125 \times 10^{-3}$ w

At I_{max} $\qquad \frac{dI}{dI_{max}} \% = \pm \frac{0.125 \times 10^{-3}}{0.15} \times 100\%$

$\simeq$ 0.08% of I_{max} full scale

For 1-Bit Error He (Power)

At i_{min} $\qquad \frac{dI}{I_{min}} \% = \pm \frac{0.125 \times 10^{-3}}{0.055} \times 100\%$

= 0.227% of I_{min} full scale

or 0.08% of I_{max} full scale

Temperature Error Contribution

$$\frac{dI}{I} = \frac{dK}{I} = \frac{1}{I}\left(4\frac{K}{T}\Delta T\right) \qquad K = \sigma A T^4$$

$$\frac{dK}{dT} = 4\sigma A T^3$$

$$dK = 4\sigma A T^3 \Delta T$$

$$= 4\frac{K}{T}\Delta T$$

At I_{max}

$$\frac{dI}{I} \% = \frac{1}{0.15} \frac{(4x.18)}{420} \Delta T \times 100\%$$

$\simeq +1.14\ \Delta T\ \%$

ΔT	% error I_{max}
0.1°K	0.114%

At I_{min}

$$\frac{dI}{I}\% = \frac{1}{0.055}\frac{(4x.18)}{420}\Delta T \times 100\%$$

$$= 2.38\,\Delta T\,\%$$

ΔT	% Error I_{min}	% Error I_{max}
$^{o}1^{o}K$	0.24%	0.08%

2.2.7 Bandwidth

$\pm$ 1.5% maximum error 5 sec for 0.140 watt/cm^2

Assume settling to 0.1% within 5 sec. Also assume thermal delay of 3 sec.

$$\underline{t} = T \text{ hr } \frac{Ef - Vo}{Ef - (V(t))} \qquad V(t) = \left(\frac{1 - \%}{100}\right) Ef$$

$$\simeq T \text{ hr } \frac{1}{1-(1-0.001)}$$

$$\underline{T} = \frac{5 - 3}{\ln 1000} = 0.29 \text{ sec}$$

$$\omega = \frac{1}{0.29} = 3.5 \text{ cps}$$

$$f = 0.56 \text{ cps}$$

2.2.8 Noise

If the DC approach is used, the primary contribution to noise will be the 1/f noise of the transistors and Johnson noise of the resistors.

$$E_V^2 = 4\,KTRDf$$

$$Df = 1.57 \pm 3 \text{ db}$$

En_K = RMS value of noise voltage

Boltzmann's constant = $1.38 \times 10^{-23} j/^{o}K$

Use $B\omega$ = 1 cps ; R = 1K; T = $410^{o}K$

$$En = \sqrt{4 \times 410 \times 1.38 \times 10^{-23} \times 1 \times 10^{3}}$$

$$= \sqrt{23} \times 10^{-9}$$

$$= 5 \times 10^{-9} \text{ volts}$$

Obviously 1/f noise will predominate.

The μA 709 amplifier proposed does not have a noise spec. A typical figure would be 10μ volts for a 1-cycle bandwidth.

External Noise:

Converter noise will be predominately 2400 cps.

2.2.9 Drift

Current drift = 200 Na max 50 Na typ

Selection required

V diff $= 200^{1-9} \times 1K = 200\ \mu v$

This doubles every $10^{\circ}C$

Offset voltage = $10\mu v/^{\circ}C$

2.2.10 Supply Voltage Registers

150μv/v

2.2.11 Integrated Circuit Selection

Three integrated circuit series were investigated. They were the Signetics 400 series, the TI 51 series, and the Fairchild 9000 series. An estimate of the number of flip-flops and gates used in the system is:

F/F	50
Dual input gates	165
3 Input gates	30
4 ≥ Input gates	5

The basis of the estimate was on the number of chips, which would effect both volume and cost, and the total power. The result of this comparison is shown in Table 2-3. It shows that the Signetics uses the least number of flat packs because of the two flip-flops per package and the quadruple two-input HAND gate. The Fairchild series was the lowest power dissipation and the Signetics was the highest. The Signetics required 88 flat packs to 153 flat packs for the Fairchild units. On this basis it appears that the Signetics is the most desirable.

Table 2-3. Low Power I/C

System Requirements
F/F = 50
Dual input gate = 165
3-Input gate = 30
4-Input gate = 5

Vendor	Type	Unit No.	Power Function	No. Chips	System	
					No. Chips	Power (mw)
Signetics and Sprague (DTL)	(AC) Dual F/F	SE 424J	14 mw AV	2	25	700
	NAND Gate	SE 480J	2.8-9.0 mw 6 Typ	Quad 2 Input	42	990
	NAND Gate	SE 416J	4-9 mw 6 mw	Dual 4 Input Expandable	18 No. 3	108
	Buffer	SE 455J	4-16	Dual 4		
Totals					88	1,798 mw Vol 1
T.I. Series 51	F/F	SN 5111	Typ 5.0 mw 4.5 V	1	50	250
	RTL NOR	SN 5162	Typ 4.5 mw at 4.5 V	Triple 2 Input	55	740
	RTL NOR RTL	SN 513	4.5	6 Input (one) Dual 3 Input	15	68
Totals					125 Vol 48% increase	1,080 mw
Fairchild LPDT	F/F	ML 9040	3.5 mw at 5V	1	50	175
	NAND Gate	ML 9041	1.0 mw	Dual Input	98	195
	NAND Gate	ML 9042	1.0 mw	Dual Input	5	5
Totals					153 Vol 83% increase	375 mw

System Power Estimate

Table 2-4, shows the system power estimate using the Signetics integrated circuits.

Table 2-4. Power Estimate for Signetics Circuits

Subsystem	Power (Watts)
Cone heater	0.25
Guard heater	0.50
Analog bits	2.0
Digital I/C	2.0
Subtotal	4.75
Power supply 60% efficient	2.9
10% Contingency	0.5
Total Power	8.15

3. TRANSDUCER THERMAL ANALYSIS

The thermal control flux monitor (TCFM) transducer consists of an electrically heated conical receiver whose back side is surrounded by a constant temperature guard. Electrical power to the conical receiver (hereafter referred to simply as the cone) is controlled in such a way that the cone temperature is always as nearly equal to that of the thermostatically-controlled guard as possible. As a result, heat transfer between the cone and the guard is minimal. The unknown incident flux is therefore equal to the difference between the thermal energy emitted at the cone aperture and the electrical power required by the cone in order to maintain the null condition.

This report presents a brief analysis of the major modes of heat transfer to and from the guard structure and shows that the required guard temperature ($742^{\circ}R$), can be maintained under all anticipated conditions with a maximum of 0.5 watt of electrical power applied to the guard heating coil.

The main heat transfer paths are listed below:

a. Radiant input on the annular frontal area surrounding the aperture

b. Thermal emission from the annular frontal area to space

c. Thermal emission from the cylindrical side area to space

d. Thermal emission from the cylindrical side area to the spacecraft

e. Thermal conduction to the supporting structure

Each of these forms of heat transfer is discussed individually and analyzed parametrically where possible. The heat balance equation is then solved for the current design configuration with electrical heating

rate and side wall emissivity as variables. By considering this equation for both the maximum and minimum solar intensity, it is shown that the effective emissivity of the side wall should be 0.037 ± 0.007 if 1/4 watt of electrical heating is available or 0.058 ± 0.028 if 1/2 watt of electrical power is available.

3.1 Radiative Heat Addition

Figure 3-1 shows a cross-sectional view of the transducer and its mounting fixture. It can be seen that the incident flux, (mostly solar radiation), will impinge not only on the cone aperture but also on the annular frontal area surrounding the aperture. This annular area is of necessity part of the guard structure. Insulation cannot be applied to the frontal area because such insulation would be "seen" by the sensing cone and would thus cause an error. The guard structure therefore receives radiant heat as follows:

$$Q_1 = (\pi/4)D_1^2 \, E\alpha \left[(D_2/D_1)^2 - 1\right] \qquad (3.1)$$

where:

D_1 = aperture diameter

D_2 = outer diameter of the transducer housing

E = incident flux density

α = absorptivity relative to the spectral distribution of the incident flux

Equation (3.1) is plotted parametrically in Figure 3-2. Radiant heating rates corresponding to an absorptivity of 0.25 (electro-deposited gold) with minimum and miximum flux densities* are indicated in Figure 3-2 for the current geometric configuration, (D_1 = 0.44 inch, D_2 = 1.25 inches).

*Solar flux density ranges from about 0.90 watt/in^2 at Earth to about 0.40 watt/in^2 at Mars. The TCFM is being designed to operate at any flux density between 0.966 watt/in^2 and 0.356 watt/in^2.

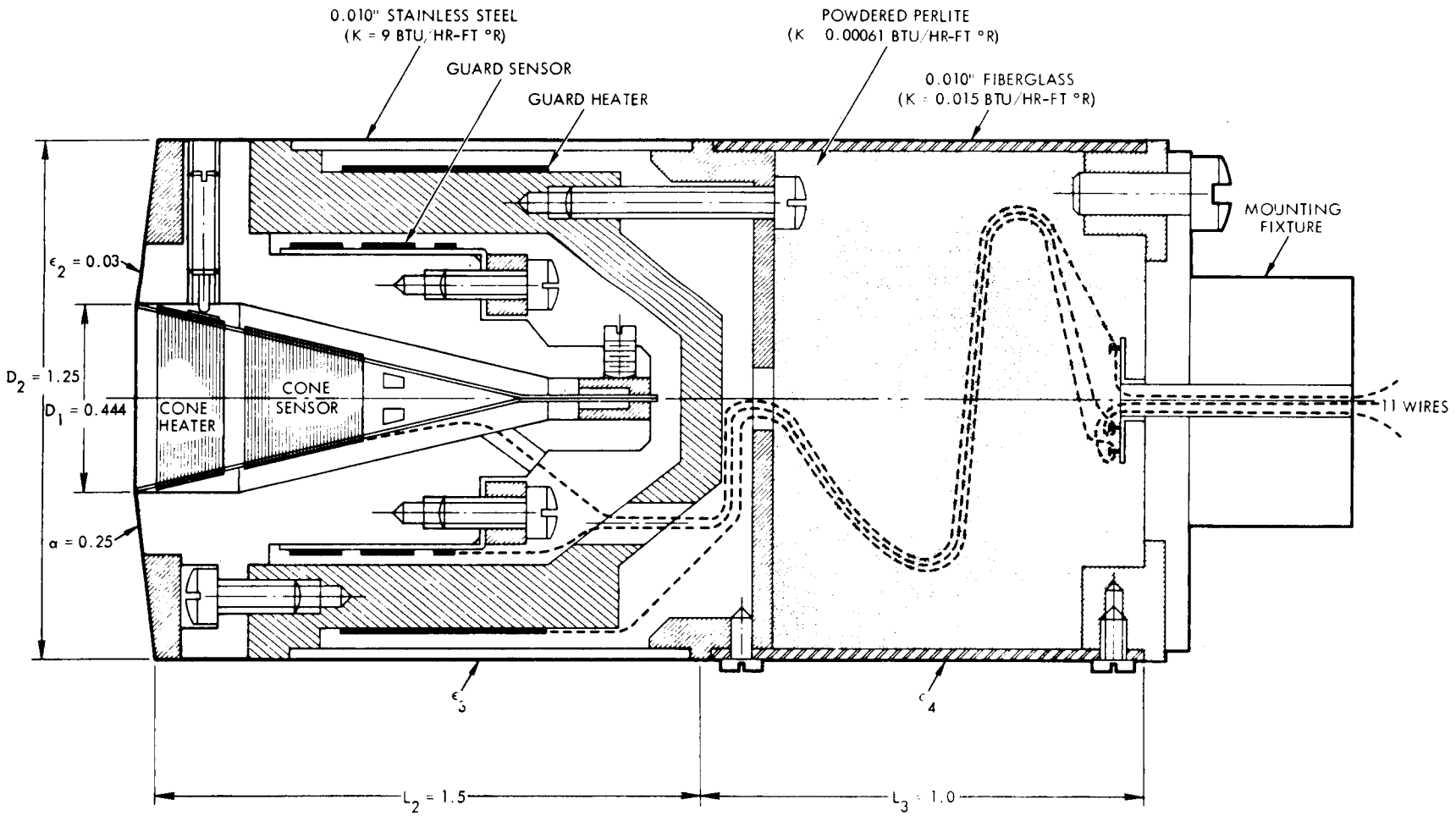

Figure 3-1. TCFM Transducer Preliminary Design

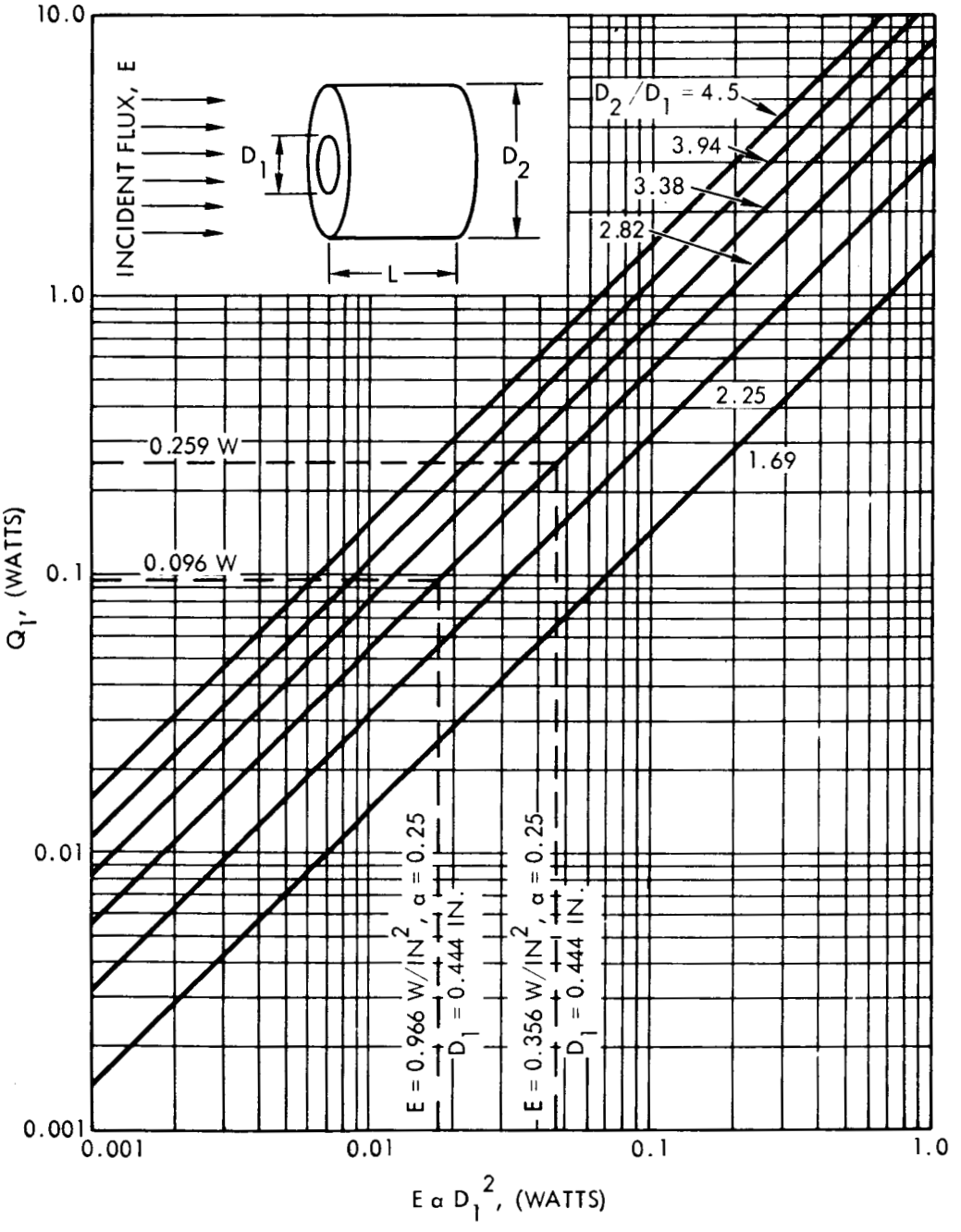

Figure 3-2. Radiative Heating of the Guard

3.2 Radiative Heat Loss

It is convenient to divide the thermal emission from the transducer into two sections according to surface area. The two areas of emission are the annular frontal area surrounding the aperture, and the cylindrical side wall area. Emission from either area depends heavily, of course, on surface temperature. It has already been pointed out that the frontal area cannot be insulated. It therefore will be at essentially the same temperature as the guard structure.

Insulation of the cylindrical area is physically possible. Either multilayer or foam type insulation could be applied. However the small dimensions involved make it extremely difficult to predict, produce, or maintain a specific effective conductance for multilayer type insulation because of the overwhelming edge-effect. Uncertainties of contact-resistance and local foam density make non-radiative insulation equally unattractive. Heat loss therefore will be controlled by providing sufficiently low emissivity on the frontal area and on the outer suface of the metallic cylinder that houses the guard structure.

It can easily be shown that if all of the incident flux absorbed by the frontal area plus 0.25 watt of electrical power were applied at one end of the 10-mil-thick stainless steel housing (see Figure 3-1) and removed at the other end, the end-to-end temperature difference would be only $1.53^{\circ}F$. The housing will therefore be assumed to have an uniform temperature equal to that of the guard.

3.3 Guard Temperature

The guard temperature is by definition equal to the cone temperature. It must, therefore, be high enough so that the flux emitted from the cone aperture is at least as great as the sum of the incident flux absorbed by the cone under maximum solar intensity plus some minimum but measurable heat flux that must be applied electrically to the cone. A simplified heat balance for the cone can be made by noting that the effective emissivity and absorptivity of the cone are by design very close to unity. The result is:

$$T_0 = \left[\frac{E_{max} + \frac{P_{min}}{(\pi/4) D_1^2}}{\sigma} \right]^{1/4} \qquad (3.2)$$

where

P_{min} = minimum measurable electrical heating rate for the cone

E_{max} = maximum incident flux density to be encountered

σ = Stefan-Boltzmann constant

Equation (3.2) is plotted parametrically in Figure 3-3. The dashed line corresponding to the present design configuration indicates that the guard temperature must be at least 742°R. This is based on a minimum electrical heating rate, (on the cone), of 0.015 watt. Since the power measuring equipment is expected to have a resolution of approximately 0.00015 watt, power can be measured to ± 1% under worst-case conditions with the indicated guard temperature.

3.3.1 Frontal Emission

The frontal area "views" no part of the spacecraft. Consequently, frontal emission is given by

$$Q_2 = (\pi/4) D_1^2 \sigma \epsilon_2 T_0^4 \left[(D_2/D_1)^2 - 1 \right] \qquad (3.3)$$

where

ϵ_2 = emissivity of annular frontal area

T_o = guard temperature

This equation is plotted in Figure 3-4 where it can be seen that for the present design configuration the frontal area will emit approximately 0.034 watt.

3.3.2 Side Wall Emission

Thermal emission from the side wall is complicated by the fact that the side wall can "view" other portions of the spacecraft. Fortunately,

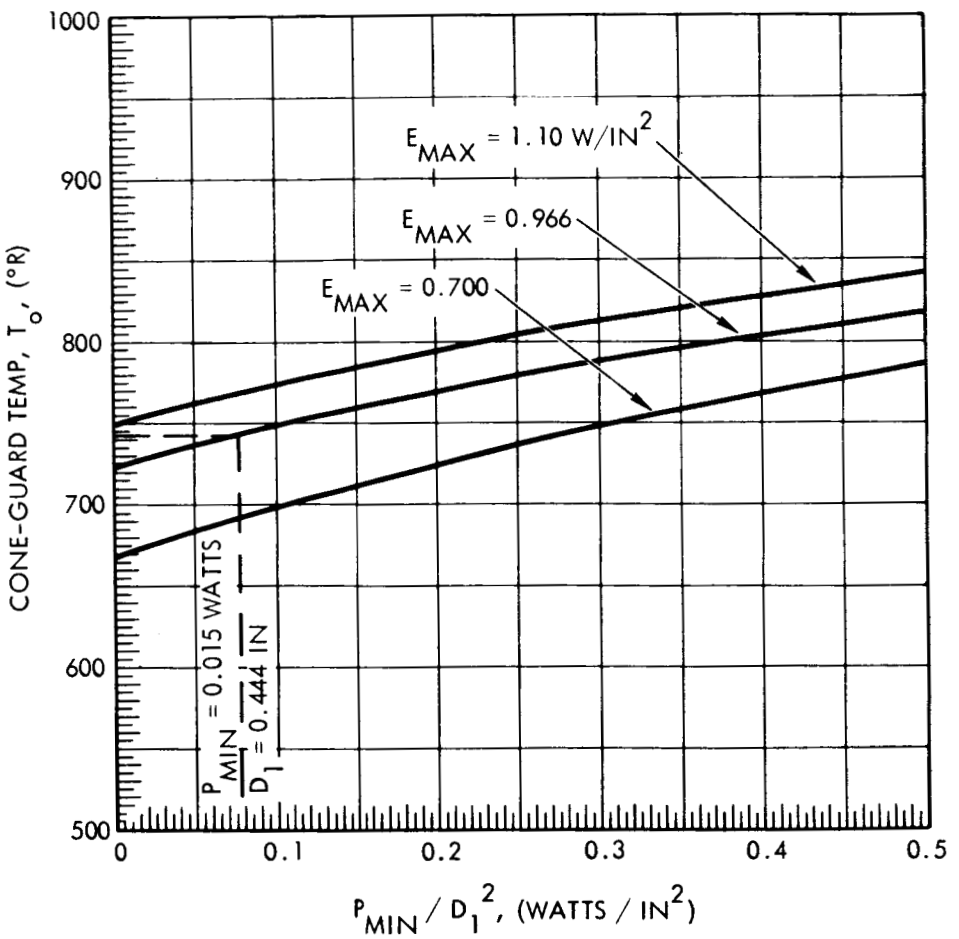

Figure 3-3. Required Temperature as a Function of the Minimum Electrical Heat Flux

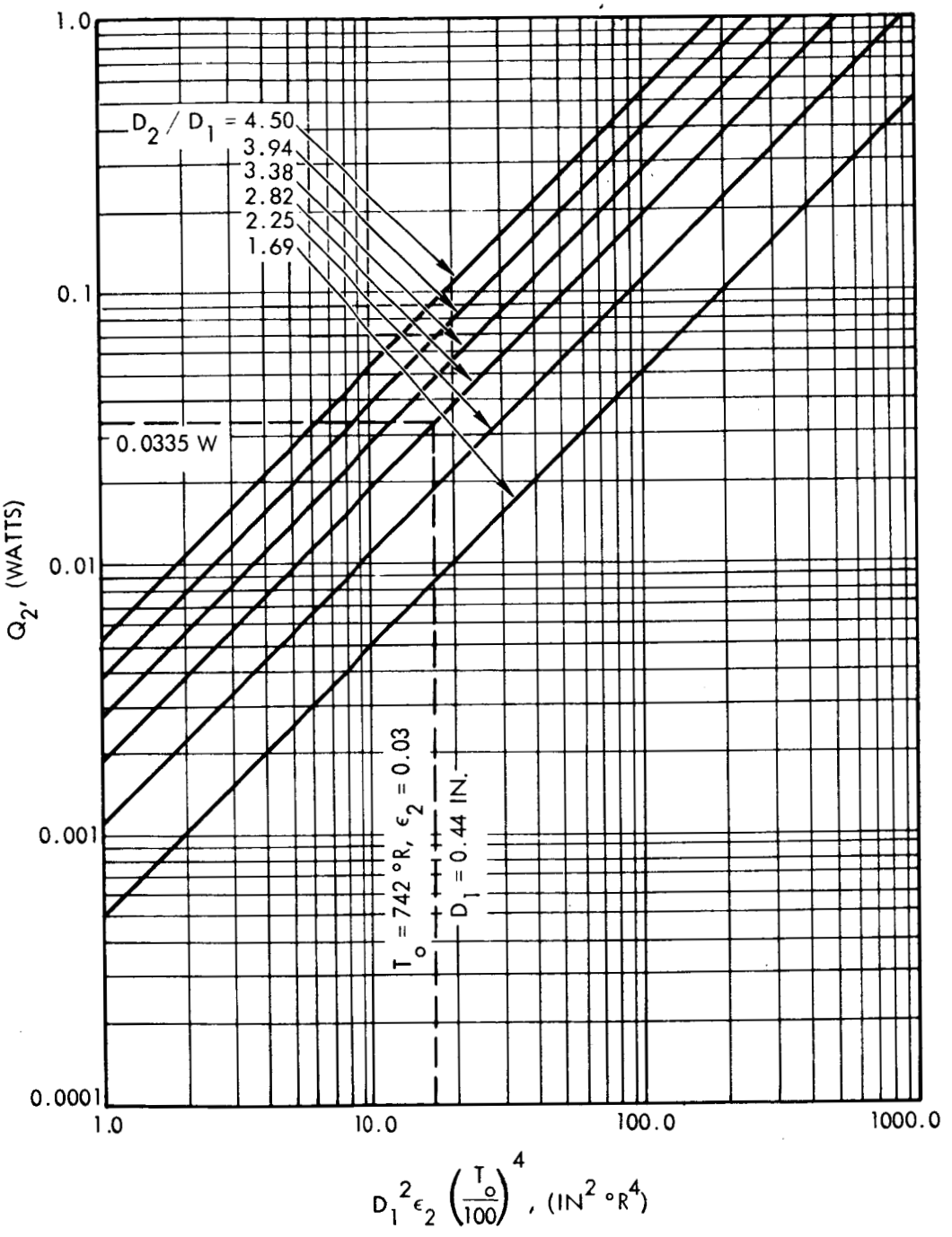

Figure 3-4. Thermal Emission from Annular Frontal Area

the main body of the spacecraft is far enough removed so that it subtends a solid angle (when viewed from the transducer) of only about 0.702 steradian. This is small compared to the total solid angle (4π steradians) to which the side wall emits. Moreover, the generally axisymmetrical orientation of the main body of the spacecraft relative to the transducer, places most areas of the spacecraft at rather shallow angles of incidence for points on the transducer side wall. Heat transfer between the transducer and the main body therefore can be ignored provided no solar radiation is allowed to reflect specularly onto the transducer.

Radiant exchange between the transducer side wall and the adjacent antenna structure is not so easily dismissed. Figure 3-5 shows the orientation of the transducer relative to the conical antenna structure. If multiple reflections between the transducer side wall and the antenna structure are disregarded,* the total thermal emission from the cylindrical side wall can be expressed as follows:

$$Q_3 = A_2\sigma\epsilon_3 F_{21}(T_2^4 - T_1^4) + A_2\sigma\epsilon_3(1 - F_{21})T_2^4 + (\pi D_2 L_2 - A_2)\sigma\epsilon_3 T_2^4 \qquad (3.4)$$

where:

A_2 = that part of the cylindrical area that is within line-of-sight of the conical antenna structure

F_{21} = geometric form factor between surfaces A_2 and A_1, in Figure 3-5

ϵ_3 = emissivity of cylindrical side wall

T_2 = temperature of side wall, (same as guard temperature, T_o)

T_1 = temperature of antenna structure

L_2 = transducer length, (not including fiberglass mount)

D_2 = transducer diameter

The first term on the right is emission from area A_2 to the conical antenna. The second term is emission from A_2 to space, while the third

*Since both surfaces are convex and specular, this assumption seems reasonable.

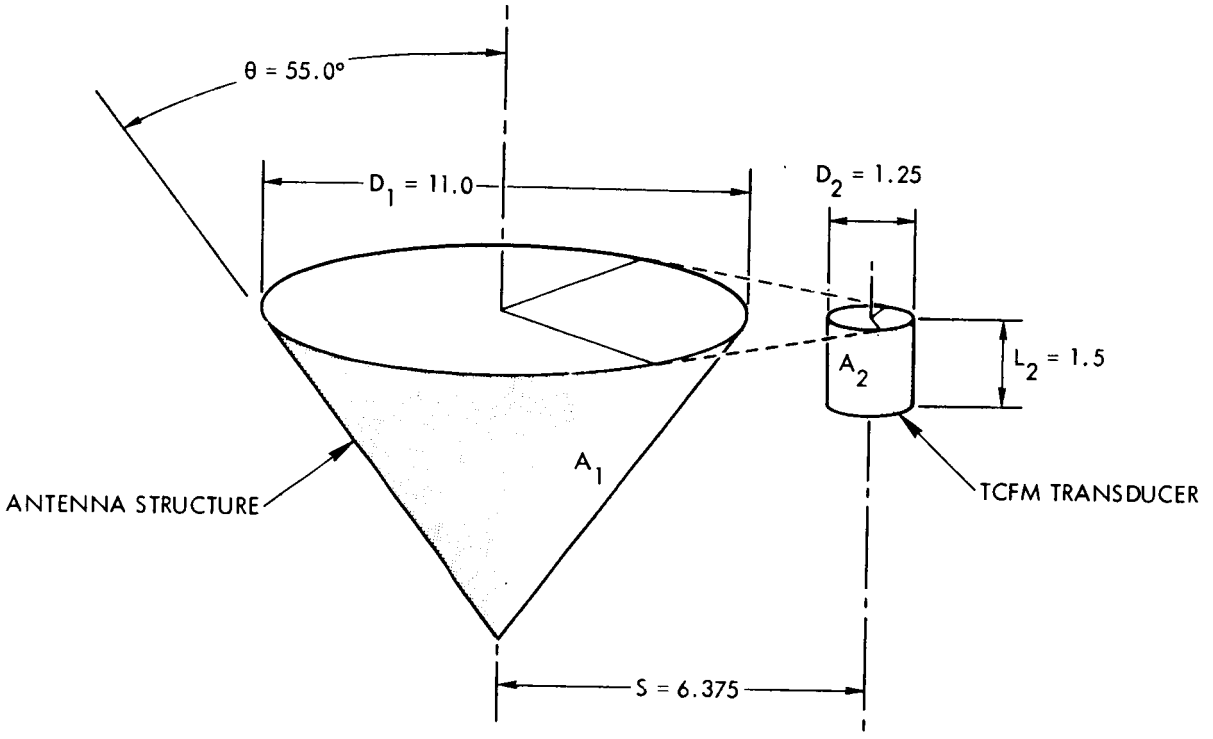

Figure 3-5. Orientation of the Transducer Relative to the Conical Antenna Structure

term is emission from the shaded cylindrical area to space. By collecting terms and simplifying, equation (3.4) can be rearranged to the following, more convenient form:

$$Q_3 = \pi D_2 L_2 \sigma \epsilon_3 T_2^4 \left[1 - (A_2/\pi D_2 L_2) F_{21} (T_1/T_2)^4\right] \qquad (3.5)$$

It is shown in the Section 3.7 that for the configuration drawn in Figure 3-5, $F_{21} = 0.0335$ in^2 and $A_2 = 2.29$ in^2. For such small values of F_{21}, equation (3.4) can be further reduced to the following:

$$Q_3 = \pi D_2 L_2 \sigma \epsilon_3 T_2^4 \qquad (3.6)$$

Equation (3.6) is plotted in Figure 3-6 with Q_3/ϵ_3 as the dependent variable. This was done to avoid the necessity of assigning a numerical value to ϵ_3 until after the rest of the heat balance calculations have been completed. It is seen that for the present configuration and the guard set-point temperature of 742°R, Q_3/ϵ_3 must equal 6.20 watts.

3.4 Conductive Heat Transfer

Since the temperature of the mounting plate is unknown, it is desireable to isolate the transducer from the mounting plate. Three sources of conductive heat transfer between the transducer and the plate have been considered. They are:

- Longitudinal heat transfer along the fiberglass mounting shell
- Conduction through the powder or foam insulation used to fill the fiberglass mounting ring
- Conduction along the electrical leads that necessarily run between the guard structure and the mounting plate

3.4.1 Conduction Along Support Shell

The fiberglass shell acts as a fin drawing heat away from the end of the transducer and emitting it to space. Perfect thermal contact is assumed between the transducer and the support shell. The shell is represented by the following diagram:

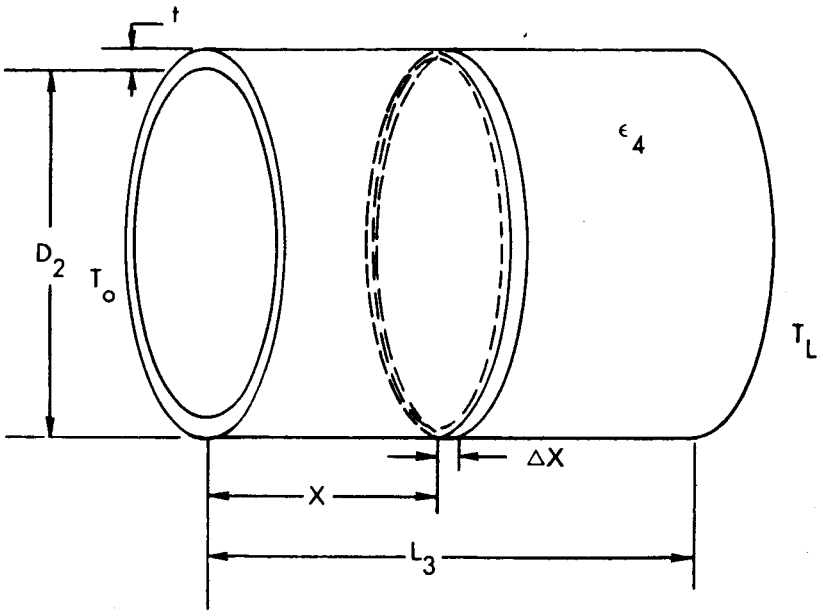

A heat balance for the elemental volume results in the following differential equation:

$$\frac{d^2T}{dX^2} - \frac{\sigma \epsilon_4 T^4}{tK} = 0 \qquad (3.7)$$

where:

T = temperature at any station

t = shell thickness

ϵ_4 = emissivity of outer surface of shell

K = thermal conductivity

X = distance from end fastened to the guard

A linearized solution of this equation is given below for the following boundary conditions:

$$\begin{cases} X = 0, & T = T_o \\ X = L_3, & T = T_L \end{cases}$$

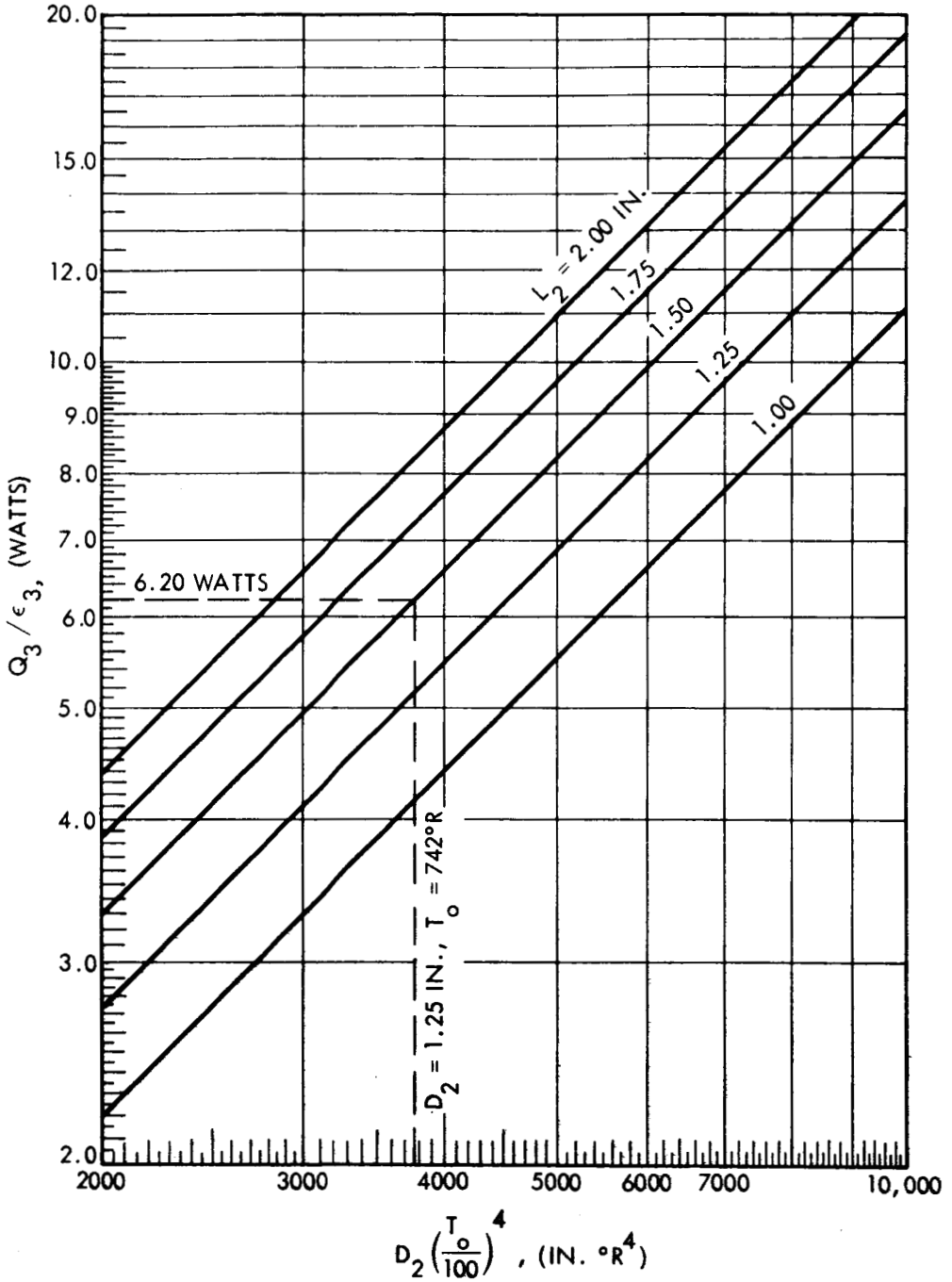

Figure 3-6. Thermal Emission from Cylindrical Side Wall

By evaluating the first derivative at X = 0, the heat conducted away from the guard structure can be determined.

In order to non-dimensionalize the equation, let

$$U = \frac{T - T_o}{T_o} \quad , \quad \xi = \frac{X}{L_3}$$

Then

$$\frac{d^2U}{d\xi^2} - \frac{\sigma \epsilon_4 L_3^2 T_o^3}{tK} (U + 1)^4 = 0 \qquad (3.8)$$

Using only the first two terms of a binominal expansion of $(U + 1)^4$ and taking $(4U + 1)$ as the dependent variable gives the following linearized differential equation:

$$\frac{d^2(4U + 1)}{d\xi^2} = 4\lambda^2(4U + 1) \qquad (3.9)$$

where

$$\lambda^2 = \frac{\sigma \epsilon_4 L_3^2 T_o^3}{tK}$$

The general solution of equation (9) is

$$4U + 1 = A \cosh (2\lambda\xi) + B \sinh (2\lambda\xi) \qquad (3.10)$$

Evaluating the constants A and B for the non-dimensional boundary conditions,

$$\begin{cases} \xi = 0, \quad U = U_o \\ \xi = 1, \quad U = U_1 \end{cases}$$

gives the particular solution.

$$U = \frac{1}{4}\left[\cosh (2\lambda\xi) + \frac{4U_1 + 1 - \cosh 2\lambda}{\sinh 2\lambda} \sinh (2\lambda\xi) - 1\right] \qquad (3.11)$$

The first derivative at $\xi = 0$ is, therefore,

$$\left(\frac{dU}{d\xi}\right)_o = \frac{2\lambda}{4}\left[\frac{4U_1 + 1}{\sinh 2\lambda} - \operatorname{ctnh} 2\lambda\right] \qquad (3.12)$$

The rate of heat conduction at $X = 0$ is given by

$$Q_4 = \pi D_2 t K\left(\frac{dT}{dX}\right)_o = -\pi D_2 t K \frac{T_o}{L_3}\left(\frac{dU}{d\xi}\right)_o \qquad (3.13)$$

Combining equations (3.12) and (3.13) gives the following equation which is plotted in Figure 3-7.

$$\frac{Q_4}{(D_2 t K T_o/L_3)} = \frac{\pi}{4}(2\lambda)\left[\operatorname{ctnh}(2\lambda) - \frac{4U_1 + 1}{\sinh(2\lambda)}\right] \qquad (3.14)$$

In order to determine the heat transfer rate for the present configuration, we first evaluate the dimensionless parameter, λ^2.

$$\lambda^2 = \frac{\sigma\epsilon_4 L_3^2 T_o^3}{tK} = \frac{(0.1714 \times 10^{-8})(0.06)(1/12)^2(742)^3}{(0.010/12)(0.015)} = 23.8$$

Figure 3-7 shows that the heat transfer parameter, $(L_3 Q_4/D_2 t K T_o)$ is independent of the temperature of the mounting plate, (T_L), for such large values of λ^2 and is equal to 7.6 for the present configuration.

Therefore:

$$Q_4 = (7.6)\frac{D_2 t K T_o}{L_3} = (7.6)\frac{(1.25)(0.010)(0.015)(742)}{(12)(1)} = 0.0881 \frac{\text{Btu}}{\text{hr}}$$

or

$$\underline{\underline{Q_4 = 0.0258 \text{ watt}}}$$

3.4.2 Conduction Through Filler Insulation

In order to block radiation heat exchange between the back side of the transducer and the mounting plate, it is recommended that the support shell be filled with some type of lightweight insulation. The rate of heat loss through the insulation has been computed based on the assumption that the cavity would be filled with powder-type Perlite.

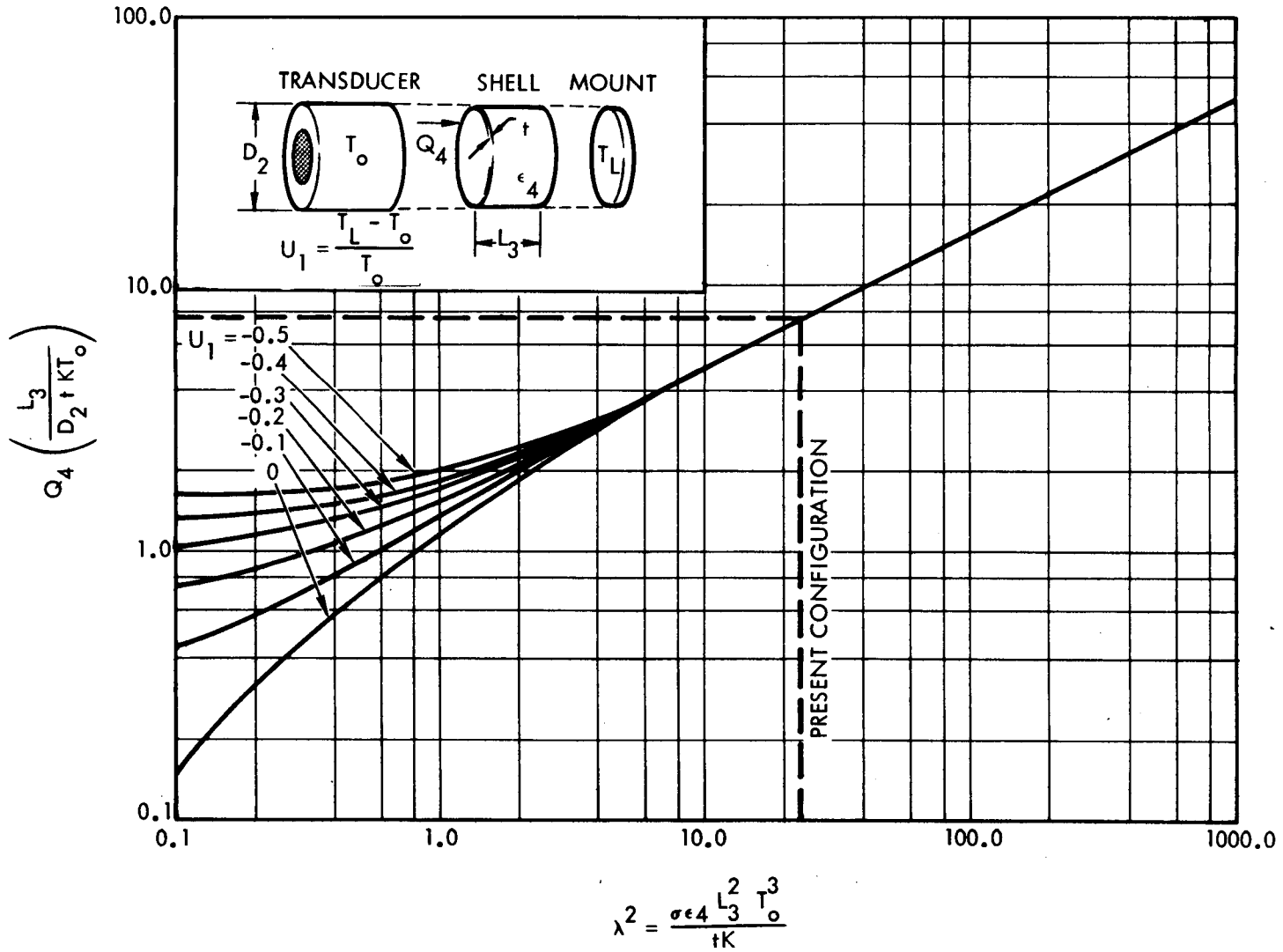

Figure 3-7. Conductive Heat Loss Due to Fin Effect of Support

Other materials such as multilayer aluminized Kapton or silicone foam could be used. The effective conductance of multilayer insulation is difficult to predict for such small dimensions because of lateral conduction and edge-effects. Rigid foam insulation requires that holes be cut for the lead wires. The wire would then have to be fed through with good chance of breakage.

Heat transfer through the filler material is assumed to be one-dimensional. The rate of heat transfer can therefore be represented as follows:

$$Q_5 = \frac{\pi D_2^2 K_f (T_o - T_L)}{4L_3} \qquad (3.15)$$

where

K_f = thermal conductivity of the filler material, (0.00061 Btu/ft-hr^{o}R for 80-mesh powdered Perlite)

The temperature of the mounting plate is unknown but for the purposes of this analysis, it is perhaps sufficient to assume that it is equal to the estimated temperature of the antenna structure (490^{o}R with minimum solar heating or 630^{o}R with maximum solar heating). Then for minimum solar heating and the present configuration

$$Q_5 = \frac{\pi(1.25/12)^2(0.00061)(742-490)}{4(1/12)} = 0.0157 \frac{\text{Btu}}{\text{hr}}$$

or

$$\underline{\underline{Q_5 = 0.00461 \text{ watt}}}$$

And for maximum solar heating

$$Q_5 = (0.0157)\frac{742 - 630}{742 - 490} = 0.00697 \frac{\text{Btu}}{\text{hr}}$$

or

$$\underline{\underline{Q_5 = 0.00205 \text{ watt}}}$$

3.4.3 Conduction Along Lead Wires

Lead wires running between the guard structure and the mounting plate are assumed to be perfectly insulated by the powdered Perlite. The heat transfer rate due to thermal conduction along the wires is, therefore,

$$Q_6 = \frac{n\pi D_w^2 K_w}{4 L_w} (T_o - T_L) \qquad (3.16)$$

where:

n = number of wires
D_w = wire diameter
K_w = thermal conductivity of wire
L_w = lead wire length

It is assumed that eleven 1-foot-long 10-mil-diameter Constantan wires will be used. Using the same mounting plate temperatures as before gives the following heat transfer rates due to wire conduction.
Minimum solar heating:

$$Q_6 = \frac{(11)(\pi)(0.010/12)^2(15.)(742 - 490)}{(4)(1.0)} = 0.0226 \frac{\text{Btu}}{\text{hr}}$$

or

$$\underline{\underline{Q_6 = 0.00663 \text{ watt}}}$$

Maximum solar heating:

$$Q_6 = 0.0226 \frac{(742 - 630)}{(742 - 490)} = 0.0101 \frac{\text{Btu}}{\text{hr}}$$

or

$$\underline{\underline{Q_6 = 0.00295 \text{ watt}}}$$

3.5 Overall Heat Balance

The electrical heating rate required on the guard is determined by summing as follows:

$$Q = Q_2 + Q_3 + Q_4 + Q_5 + Q_6 - Q_1 \qquad (3.17)$$

Substituting the actual heat transfer rates for Q_1 through Q_6 into equation (3.17) and assuming minimum solar heating gives

$$Q = 0.0335 + 6.2\epsilon_3 + 0.0258 + 0.00461 + 0.00663 - 0.259 \sim \text{watts}$$

or

$$Q = 6.2\epsilon_3 - 0.188 \sim \text{watts} \qquad (3.18)$$

Assuming maximum solar heating gives

$$Q = 0.0335 + 6.2\epsilon_3 + 0.0258 + 0.00205 + 0.00295 - 0.096 \sim \text{watts}$$

or

$$Q = 6.2\epsilon_3 - 0.032 \sim \text{watts} \qquad (3.19)$$

Equations (3.18) and (3.19) are plotted in Figure 3-8. It is seen that if the guard heating rate (Q) is limited to 0.5 watt, the transducer side wall emissivity (ϵ_3) must be between 0.03 and 0.086. Limiting heater power to say 0.25 watt places even tighter tolerances on the side wall emissivity.

3.6 Conclusions of Discussion

Conclusions of the foregoing discussion are listed as follows:

1. A guard temperature of at least 742° is required in order to make the minimum cone electric heating rate sufficiently large so that the cone electric power can be measured to an accuracy of ± 1%. This is based on a maximum incident flux density of 0.966 watt/in^2 and an absorptivity of 0.25 on the annular front surface.

2. Thermal emission from the cylindrical side wall of the transducer is the major single source of heat loss from the guard structure. The emissivity of this surface is critical, especially if electrical heating on the guard is limited to less than 0.5 watt.

3. For the present configuration, a guard temperature of 742°R, and a maximum electrical heating rate on the guard of 0.5 watt, the emissivity of the side wall, (ϵ_3), should be 0.058 ± 0.028. This is based on the frontal surface being electro-deposited gold, (α = 0.25, ϵ_2 = 0.03). An emissivity of 0.06 is assumed for the fiberglass support shell.

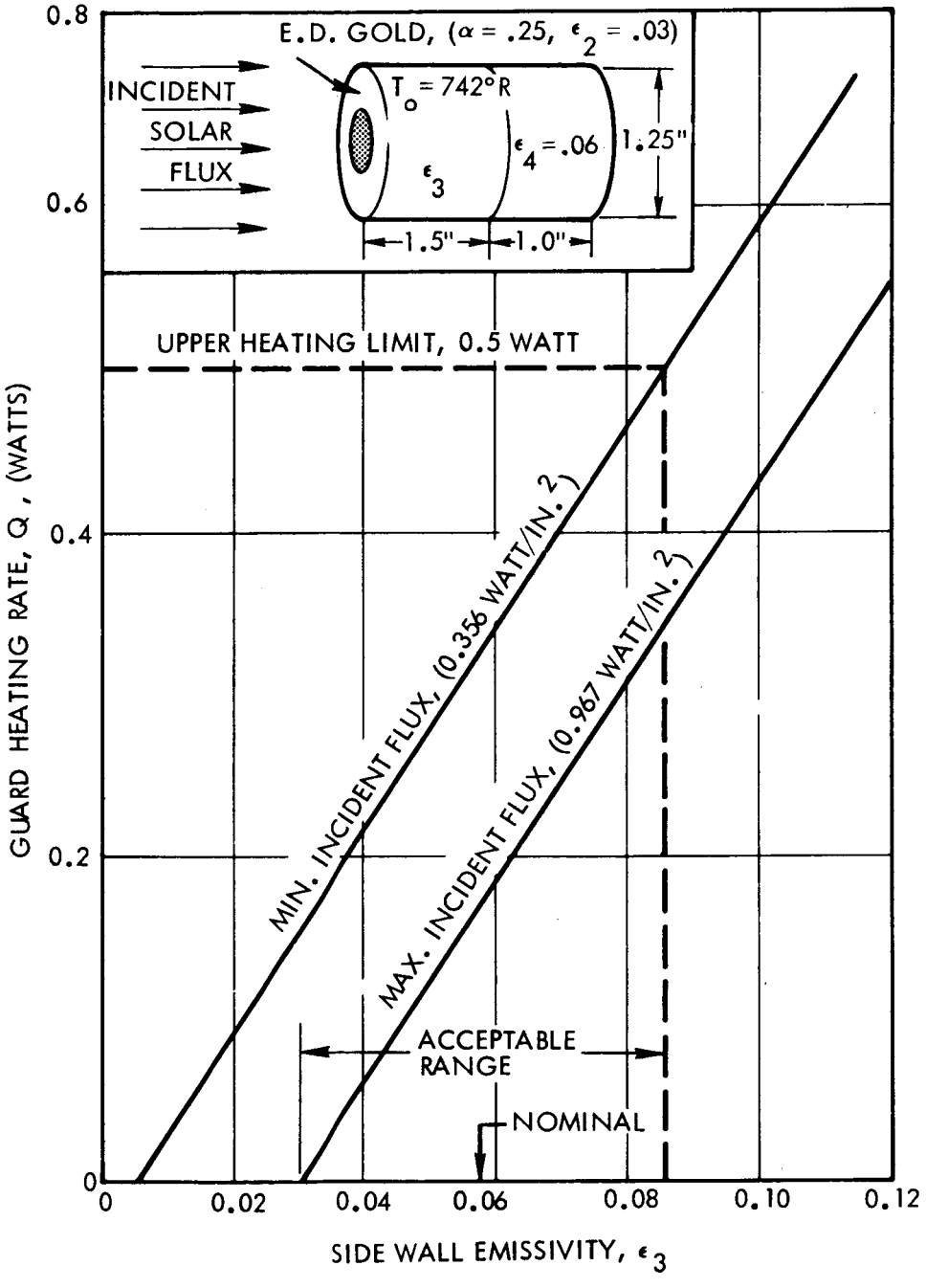

Figure 3-8. Require Guard Heating Rate As a Function of Transducer Side Wall Emissivity

3.7 Appendix to Analysis

Figure 3-9 indicates the geometrical relationship between the transducer and the conical antenna structure. It will serve to define most of the notation used in determining the geometrical form factor between the two bodies.

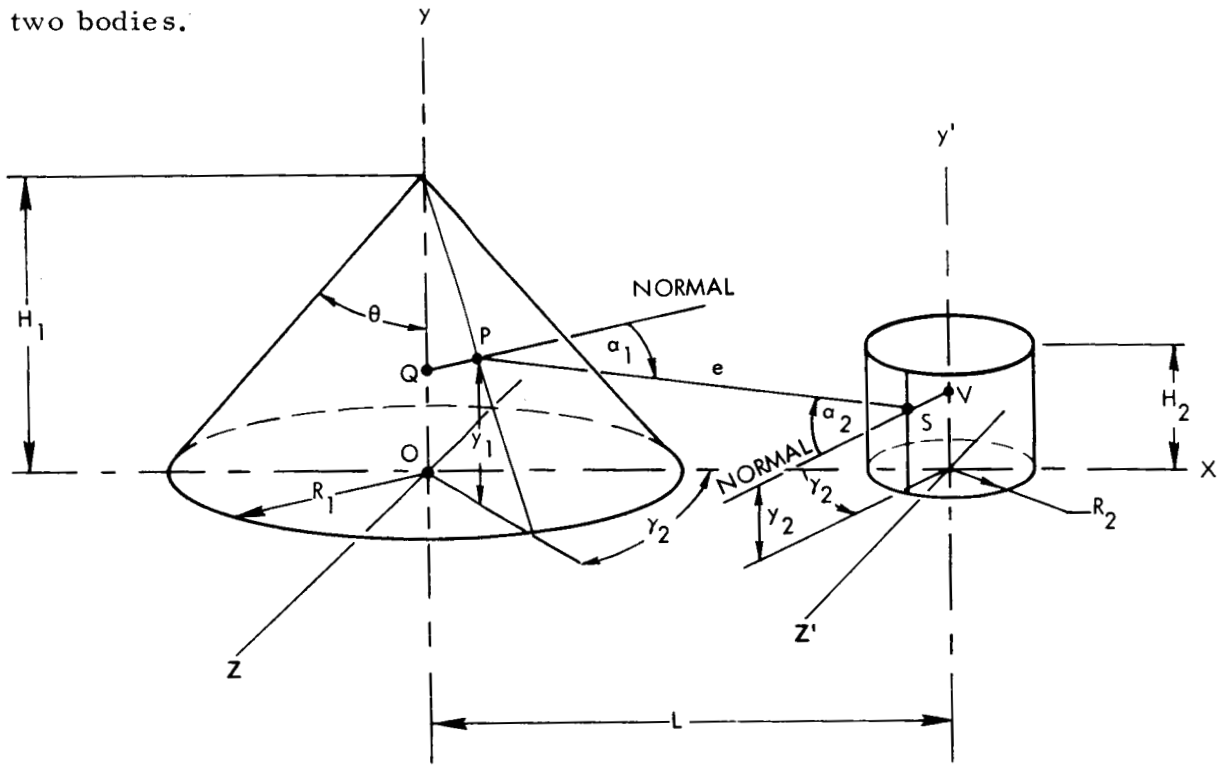

Figure 3-9. Geometrical Notation

The form factor between the transducer side wall and the antenna is given by:

$$F_{2-1} = \frac{1}{\pi A_2} \int_{A_1} \int_{A_2} \frac{\cos \alpha_1 \cos \alpha_2}{\rho^2} \, dA_1 \, dA_2 \qquad (3.20)$$

where:

A_2 is the area of the cylindrical side wall within line-of-sight of the conical antenna

A_1 is the area of the conical antenna within line-of-sight of the transducer wall

In order to perform the integrations, the differential areas are transformed as follows:

$$dA_2 = R_2 (d\gamma_2)(d y_2) \tag{3.21}$$

$$dA_1 = R_1 (d\gamma_1)\left(\frac{H_1 - y_1}{H_1}\right)\left(\frac{dy_1}{\sin\theta}\right)$$

$$= R_1(d\gamma_1)\frac{R_1/\sin(\theta) - y_1}{R_1/\sin\theta}\left(\frac{dy_1}{\sin\theta}\right)$$

$$dA_1 = R_1\left(\text{CSC}\,\theta - \frac{y_1}{R_1}\right)(d\gamma_1)(dy_1) \tag{3.22}$$

For simplicity the angular limits of integration, (γ_{1_L} and γ_{2_L}), will be based on the base-circle of the cone and the cylinder as shown in the following diagram:

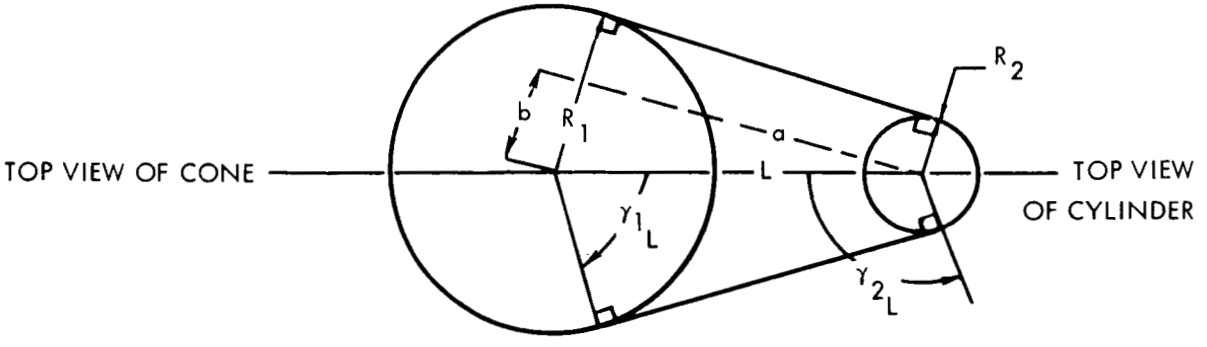

$$\tan\gamma_{1_L} = \frac{a}{b} = \frac{\sqrt{L^2 - (R_1 - R_2)^2}}{R_1 - R_2} \tag{3.23}$$

$$\therefore\ \gamma_{1_L} = \pm\tan^{-1}\sqrt{\left(\frac{L}{R_1 - R_2}\right)^2 - 1} \tag{3.24}$$

$$\text{and:}\quad \gamma_{2_L} = \pm\left(\pi - \left|\gamma_{1_L}\right|\right) \tag{3.25}$$

The receiving and emitting areas then are:

$$A_1 = \gamma_{1_L} R_1^2 \sqrt{1 + (1/\tan\theta)^2} \qquad (3.26)$$

$$A_2 = 2\gamma_{2_L} R_2 H_2 \qquad (3.27)$$

Expressing $\cos\alpha_1$, $\cos\alpha_2$, and ρ^2 in proper terms for integration requires that the coordinates of certain points shown in Figure 3-9 be known. These coordinates are listed in Table 3-1. The denominator of equation (3.20), (ρ^2), can be determined from the equation:

$$\rho^2 = (X_P - X_S)^2 + (Y_P - Y_S)^2 + (Z_P - Z_S)^2 \qquad (3.28)$$

where:

X_P, Y_P, and Z_P are coordinates of point "P" in Figure 3-9.

X_S, Y_S, and Z_S are coordinates of point "S" in Figure 3-9.

Table 3-1. Coordinates of Points

Point	X	Y	Z
Q	0	$2y_1 - R_1 \operatorname{ctn}\theta$	0
P	$(R_1 - y_1 \tan\theta)\cos\gamma_1$	y_1	$(R_1 - y_1 \tan\alpha)\sin\gamma_1$
S	$L - R_2 \cos\gamma_2$	y_2	$L - R_2 \sin\gamma_2$
E	L	0	0
V	L	y_2	0

Substituting coordinates from Table 3-1 into equation (3.28) gives:

$$\rho^2 = \left[(R_1 - y_1 \tan\theta)\cos\gamma_1 - (L - R_2\cos\gamma_2)\right]^2 + \left[y_1 - y_2\right]^2$$

$$+ \left[(R_1 - y_1 \tan\theta)\sin\gamma_1 - (L - R_2\sin\gamma_2)\right]^2 \qquad (3.29)$$

The cosine terms of equation (1) can be determined from the following equations:

$$\cos\alpha_1 = \cos A_{PQ}\cos A_{PS} + \cos B_{PQ}\cos B_{PS} + \cos C_{PQ}\cos C_{PS} \qquad (3.30)$$

$$\cos\alpha_2 = \cos A_{PS}\cos A_{VS} + \cos B_{PS}\cos B_{VS} + \cos C_{PS}\cos C_{VS} \qquad (3.31)$$

where:

$\cos A_{PQ}$, $\cos B_{PQ}$, $\cos C_{PQ}$ are the three direction cosines for line PQ in Figure 3-9. Similarly, lines PS, and VS each have three direction cosines.

The direction cosines are determined from equations of the following form and are listed in Table 3-2 for various lines in Figure 3-9.

$$\cos A_{PQ} = \frac{X_P - X_Q}{\sqrt{(X_P - X_Q)^2 + (Y_P - Y_Q)^2 + (Z_P - Z_Q)^2}} \qquad (3.32)$$

$$\cos B_{PQ} = \frac{Y_P - Y_Q}{\sqrt{(X_P - X_Q)^2 + (Y_P - Y_Q)^2 + (Z_P - Z_Q)^2}} \qquad (3.33)$$

$$\cos C_{PQ} = \frac{Z_P - Z_Q}{\sqrt{(X_P - X_Q)^2 + (Y_P - Y_Q)^2 + (Z_P - Z_Q)^2}} \qquad (3.34)$$

Table 3-2. Direction Cosines

LINE	COS A	COS B	COS C
PQ	$\sin\theta \cos\gamma_1$	$\frac{y_1 \sin\theta}{R_1 - y_1 \tan\theta}$	$\sin\theta \sin\gamma_1$
PS	$\frac{(R_1 - y_1\tan\theta)\cos(\gamma_1) - (L - R_2\cos\gamma_2)}{\sqrt{\rho^2}}$ *	$\frac{y_1 - y_2}{\sqrt{\rho^2}}$ *	$\frac{(R_1 - y_1\tan\theta)\sin\gamma_1 - (L - R_2\sin\gamma_2)}{\sqrt{\rho^2}}$ *
VS	$\frac{R_2\cos\gamma_2}{\sqrt{R_2^2 - 2LR_2\sin(\gamma_2) + L^2}}$	0	$\frac{R_2\sin(\gamma_2) - L}{\sqrt{R_2^2 - 2LR_2\sin(\gamma_2) + L^2}}$

*See equation (3.29) for ρ^2.

Substituting the direction cosines from Table 3-2 into equations (3.30) and (3.31) gives:

$$\cos \alpha_1 = \frac{\sin \theta}{\sqrt{\rho^2}} \left[R_1 - y_1 \tan \theta - (\cos \gamma_1)(L - R_2 \cos \gamma_2) \right.$$

$$\left. - (\sin \gamma_1)(L - R_2 \sin \gamma_2) + \frac{y_1(y_1 - y_2)}{R_1 - y_1 \tan \theta} \right] \qquad (3.35)$$

$$\cos \alpha_2 = \frac{1}{\sqrt{\rho^2}\sqrt{R_2^2 - 2LR_2 \sin \gamma_2 + L^2}} \left[(R_1 - y_1 \tan \theta)(\cos \gamma_1 + \sin \gamma_1) \right.$$

$$\left. + (R_2^2 - 2LR_2 \sin \gamma_2 + L^2) - LR_2 \cos \gamma_2 \right] \qquad (3.36)$$

Equations (3.21, 3.22, 3.27, 3.29, 3.35 and 3.36) can be substituted into equation (3.20) to give:

$$F_{21} = \frac{1}{2\pi \gamma_{2_L} R_2 H_2} \int_{y_1=0}^{y_1=\frac{R_1}{\tan\theta}} 2 \int_{\gamma_2=0}^{\gamma_2=\gamma_{2_L}} \int_{y_2=0}^{y_2=H_2} \int_{\gamma_1=-\gamma_{1_L}}^{\gamma_1=\gamma_{1_L}} f(R_1, R_2, L, \theta, y_1, y_2, \gamma_1, \gamma_2) d\gamma_1 dy_2 d\gamma_2 dy_1$$

This quadruple integration has been performed numerically on the GE 235 digital computer. Rather gross step sizes were required in order to keep the running time within reason. γ_1 and γ_2 were stepped $\gamma_{1_L}/5$ and $\gamma_{2_L}/5$, respectively. y_1 and y_2 were stepped $H_1/5$ and $H_2/4$, respectively. The results are plotted in Figures 3-10 and 3-11.

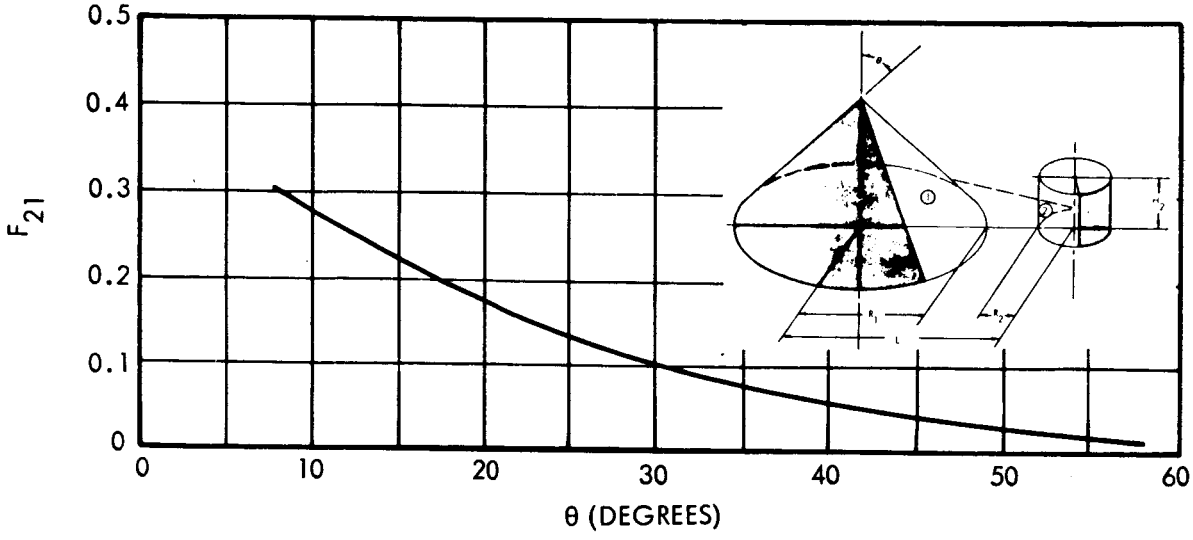

Figure 3-10. Form Factor as a Function of Apex Half Angle

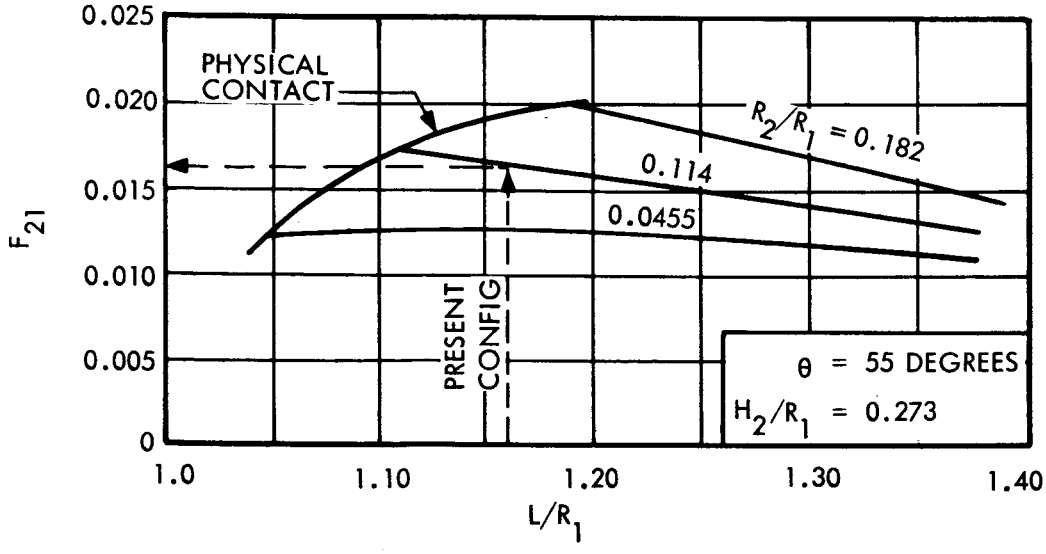

Figure 3-11. Form Factor as a Function of Separation Ratio With Cylinder-Cone Radius Ratio as a Parameter

4. ERROR ANALYSIS

4.1 Aperture Area

The basic aperture diameter (cone base) is 0.4350 inch (1.11 cm). The diameter dimension can be controlled during fabrication to $\pm$ 0.0005 inch; this tolerance represents an uncertainty in the area of the aperture of 0.2%. If, however, the actual diameter is measured optically to within 0.0002 inch, the uncertainty in the area can be reduced to $\pm$ 0.1%.

The measurement of the cone base diameter, however, will be in error if the measurement is made at room temperature since at the operating temperature (140°C) the diameter will increase by 0.0010 inch due to the thermal expansion of the silver cone. The thermal coefficient of expansion of silver is 18×10^{-6} in/in/°C and the temperature increase is 120°C so that $(18 \times 10^{-6})(0.435/\pi)\ \pi\ (120) = 1000 \times 10^{-6}$ inches. Since this represents a significant increase in the aperture area (0.4%), either the measurement must be made at the operating temperature or a corresponding correction must be applied to the room temperature area measurement.

4.1.1 Annular Gap

The annular gap between the cone rim and the thermal guard represents an additional opening through which the cone may exchange radiation with the external environment. This is accomplished by reflection from the inner surface of the thermal guard. Tentatively, the minimum gap width which can be maintained in assembly is estimated to be 0.0005 inch. The annular area of such a gap represents 0.45% of the cone aperture area.

An increase in the annular gap width with temperature is anticipated due to the difference in the thermal expansions of the cone and thermal guard materials. Aluminum and magnesium alloys have thermal expansion coefficients of approximately 26×10^{-6} in/in/°C or about 50% greater than silver; so that as the cone diameter increases 0.001 inch, the guard opening diameter increases by 0.0015 inch. This increases the annular gap area to about 0.6% of the cone aperture area.

Means for reducing the annular gap loss effect, such as aluminizing the exterior of the cone, will require consideration since it is important that this loss be reduced. In lieu of this, the best approach will be to adjust the aperture area to an effective area value to account for the incremental increase due to the gap. The resulting area uncertainty should not be greater than $\pm$ 0.2%.

4.2 Effective Cone Thermal Properties

The effective thermal properties of the conical cavity are determined analytically. Although the analysis is rigorous and the mathematics exact, some uncertainty in the effective results from the uncertainty in the basic flat plate properties of the coating material (hemispherical emissivity, absorptivity, specularity). More precise analyses are currently being pursued by JPL. At present the uncertainty in the effective emittance and absorptance is of the order of $\pm$ 0.1% (0.995 - 0.997).

4.3 Ohmic Power to Cone (E^2/R)

The accuracy to which the ohmic power to the cone is measured depends on the accuracy of the heater resistance and the voltage measurement.

4.3.1 Cone Heater Resistance

A basic resistance of 1000 ohms is used for analysis (0.22 watt = $15V^2/1000\Omega$). A practical limit of error of 0.05% ($\pm$ 0.5 ohm) is readily achieved with precision laboratory equipment for this measurement.

It is important however that the heater resistance be measured at the operating temperature. For example, even Constantan wire, with a temperature coefficient of $0.00004^{\circ}C/\Omega/^{\circ}C$, (or $0.004^{\circ}C/o/^{\circ}C$), would incur an increase in its resistance of 0.5% from room temperature to $150^{\circ}C$.

4.3.2 Cone Heater Voltage (E^2)

A voltage stability and accuracy of 0.1% is well within the state-of-the art for a fixed voltage-fixed load application, such as the TCFM.

4.4 Cone Absolute Temperature

The cone temperature on an absolute basis is only indirectly known since it is based on the thermal guard set point temperature and the cone/guard temperature balance. The absolute temperature of the cone is probably the greatest source of uncertainty on the absolute reference basis since the overall flux measurement error is based on $(T_{cone})^4$.

4.4.1 Guard Set Point Temperature

The primary temperature sensor may be calibrated in the laboratory by comparison to a certified platinum temperature standard over an anticipated range of temperatures about the set point. The resistance of the guard sensor at the operating temperatures must be determined to an accuracy of at least $\pm$ 0.5 ohm.

A sensor of 1000-ohm nominal resistance of Pt wire (TC = 0.004 ohm/ohm/^{o}C) will have a sensitivity of 4 ohms/^{o}C. An uncertainty in its resistance calibration of $\pm$ 0.05% (or $\pm$ 0.5 ohm) at the operating temperature will result in an effective guard temperature measurement uncertainty of $\pm$ 0.12^{o}C (or $\pm$ 0.08% of the operating temperature) due to sensor resistance uncertainty only.

4.4.2 Guard Temperature Measurement

The errors in this measurement are identified in detail in the section dealing with the TCFM Electronic Assembly errors. It is estimated that the resultant error for the set point temperature will be 0.1%.

4.4.3 Cone-Guard Temperature Equality

To assure the minimum difference between the cone and guard temperatures at the set point operating temperature, it is necessary to match the resistances of the two sensors in the cone/guard differential bridge. To provide the maximum tracking accuracy, the resistances of the sensors should be matched at the set point. It would appear that the resistance matching accuracy is dependent on the physical limit in trimming the length of one of the windings—this is judged to be about 0.05 inch. For Pt wire with a nominal resistance of 60 ohms/foot, (5 ohms/inch) the trimming resolution would be 0.25 ohm. Since the Pt sensor has a temperature coefficient of 0.004 ohm/ohm/^{o}C, the 0.25-ohm mismatch of the two sensors will result in a tracking error of 0.025%/^{o}C about the set point.

4.4.4 Cone/Guard Temperature Deviation Measurement

The specific errors or uncertainties in this measurement are identified in the section dealing with the TCFM electronic assembly errors. The resultant error in the cone-guard temperature equality is computed to be 0.2%.

The overall cone temperature error, therefore, will be the summation of the set point temperature error and the cone-bridge temperature difference, or 0.3%.

4.5 Stefan Boltzmann Constant

The computed value for σ differs from the mean of the best experimental values by 0.6%. Some workers in the field of precision absolute radiometry utilize one value, some the other. There is therefore a disagreement in the value of σ to be utilized. It would appear that a basic uncertainty exists for any experiment in absolute thermal radiometry where the order of precision is such that the exact value of σ is significant.

4.6 Radiant—Ohmic Power Non-Equivalence

There is a difference between the two modes of heating since absorption of radiation takes place in an absorbing layer of black paint on the inner surface of the conical cavity, and electrical heating occurs on the outer surface. The two sources planes of energy are therefore separated by the effective paint layer thickness, the cone metal thickness and the electrical heater insulation layer thickness. Since there is heat flow through the layers, the temperature gradient which results, represents a degree of non-equivalence in the two heating modes.

An actual thickness of black optical lacquer of 0.003 inch (0.0076 cm) is probable. If it is considered to be a "body" emitter and absorber, an effective thickness of 1/2 the actual thickness should obtain. The epoxy insulating layer applied to the exterior surface of the cone is judged to be 0.001 inch (0.0025 cm) thick; additionally the insulation of the wire itself is judged to be 0.0005-inch thick (0.0012).

A typical thermal conductivity for both the optical lacquer and the epoxy insulation is 0.004 watt/cm^2/^oC/cm. The thermal conductivity of silver is about three orders of magnitude greater than this so that the thermal resistance of the 0.005-inch metal thickness of the cone is negligible in comparison.

For a net outgoing flux of 0.1 watt/cm^2, the flux near the cone aperture will be 0.05 watt/cm^2. Under this condition the temperature drop across the 0.0062-cm thickness of insulation (lacquer + epoxy) will be 0.08°C, or a temperature error at 150°C of 0.05%. The resulting radiation error (σT^4) therefore will be 0.2%. The non-equivalence becomes greater when there is a great difference in the fraction of energy supplied by each heating mode, i.e. at zero incident radiation when all the energy is supplied electrically, then the radiation error would be 0.4%.

The placement of the temperature sensing winding relative to the heating winding, fortunately tends to reduce the sensing error. If the sensor and heater windings were closely interwound, the sensor would sense the temperature of the heater, which would be the worst case. If the two coils are positioned side by side, then the sensor assumes the temperature (by lateral conduction along the cone) of the metal element, thereby reducing the non-equivalence error to half the value, or 0.1%.

At maximum incident flux or when all the energy is supplied by incoming radiation, the error reduces to insignificance since there is only minor heat flow (parasitic losses only) through the cone/insulation thickness.

4.7 Temperature Sensor Self Heating

The conical element contains a wound-on resistance temperature sensor. The ohmic power generated by this winding represents a fraction of energy supplied to the cone which not accounted for in the cone heater power measurement and therefore represents an error.

A Pt sensor of 1000-ohm resistance in a half-symmetrical bridge with 20K-ohm ratio legs, with an excitation of 6 volts (RMS) will provide a signal of 0.00154V/°C. The current through each half of the bridge will be 0.00026A. The resulting I^2R heating of the cone due to the sensing current will be 67 microwatts. This represents 0.06% additional power to the cone in the nominal range of 0.100 watt.

4.8 Lead Wire Conduction—Cone

Thermal conduction by means of the lead wires attached to conical element and the inner thermal guard represent unaccounted for energy to or from the cone. Six copper wires, 0.005 inch-diameter by approximately 1.0-inch long, are attached to the cone. The heat conduction through each wire is 0.000050 watt/^{o}C or about 0.00030 watt/^{o}C total. It is computed that the temperature difference between the apex of the cone and the end of the inner guard may be 0.3^{o}C. If such is the case the loss from the cone will be 0.00009 watt or about 0.04% of the total energy supplied to the cone.

4.9 Cone Support Conduction

Thermal conduction from the cone through the apex support to the thermal guard also represents unaccounted for energy loss. An apex support consisting of 0.030-OD x 0.015-ID glass tubing will conduct 0.000085 watt/^{o}C or about 0.04% of the cone power. If this were to be replaced by 0.014-OD x 0.007-ID stainless steel tubing the loss would be 0.000136 watt/^{o}C or about 0.07% of the cone power.

The aperture centering support losses are difficult to assess. The contact with the cone is a point contact with glass-tipped screws. Further, the temperature of the cone is estimated to be somewhat less at the aperture than the thermal guard so that some heat addition to the cone rather than a loss would be experienced. In any event the heat transfer is judged to be less than that experienced through the glass apex support, i.e. less than 0.04% of the cone power.

If the glass-tipped centering screws are adjusted so that they just contact the cone at room temperature, the contact pressure will be relieved at the higher operating temperature of the transducer due to the differential thermal expansion of the cone and guard materials, thereby further reducing the conduction loss.

4.10 Error Analysis for the Thermal Control Flux Monitoring System

The operating principle of the thermal control flux monitor system (TCFM) in the measurement of incident thermal radiation is given by the basic thermal balance relationship.

$$G = \frac{A \epsilon \sigma T^4 - \frac{E^2}{R}}{A\alpha} = \alpha^{-1} \epsilon \sigma T^4 - E^2 A^{-1} \alpha^{-1} R^{-1} \qquad (4.1)$$

where:

A = cavity aperture area
α = absorptance of cavity
G = source irradiation
E = heater voltage
R = heater resistance
ϵ = emittance of cavity
σ = Stefan-Boltzmann constant
T = temperature of cavity

The uncertainty in the measurement of (G), the incident irradiation, is a function of the accuracies with which each of the component terms in the relationship is known. The effective uncertainty in each term is, in turn, a function of the various other uncertainties related specifically to that term.

This analysis treats only the accidental errors or uncertainties to determine the probable error in the measurement. The accidental error of a single determination is the difference between the true value of the quantity and a determination that is free from blunders or systematic errors. Accidental errors represent the limit of precision in the determination of a value. They obey the laws of chance and, therefore, must be handled according to the mathematical laws of probability. The proper treatment of these accidental errors is not complex; however the fundamental theory depends upon mathematical derivations.

4.10.1 Computation Rules Involving Measures of Precision

When a measurement, M, consists of the product of several measurements, a, b, c, ..., having different standard errors, σ_a, σ_b, σ_c, ..., the standard error of the measurements σ_p is found as follows: Let Δa, Δb, Δc, ..., represent increments in the measurements a, b, c, ..., and let ΔM represent the resulting increment in M. Thus

$$M + \Delta M = (a + \Delta a)(b + \Delta b)(c + \Delta c) \tag{4.2}$$

Algebraically we can determine ΔM.

In the general case, M is any function whatever of the measured quantities a_1, a_2, a_3, ..., and is expressed by $M = f(a_1, a_2, a_3, \ldots,)$. An increment in M caused by various increments in a_1, a_2, a_3, ..., expressed by X_1, X_2, X_3, ..., can be computed as follows:

$$\Delta M = \frac{\partial M}{\partial a_1} X_1 + \frac{\partial M}{\partial a_2} X_2 + \frac{\partial M}{\partial a_3} + \ldots + \ldots \tag{4.3}$$

If the increments are caused by accidental errors, we have

$$\sigma M^2 = \left(\frac{\partial M}{\partial a_1} \sigma_1\right)^2 + \left(\frac{\partial M}{\partial a_2} \sigma_2\right)^2 + \left(\frac{\partial M}{\partial a_3} \sigma_3\right)^2 + \ldots + \ldots \tag{4.4}$$

The error analysis below for the TCFM is a detailed treatment using equations (4.1), (4.3), and (4.4) based upon the data obtained

$$G = \frac{A \epsilon \sigma T^4 - \frac{E^2}{R}}{A\alpha} = \alpha^{-1} \epsilon \sigma T^4 - E^2 A^{-1} \alpha^{-1} R^{-1} \tag{4.5}$$

Using equation (4.5) with the following values for Case I where

a) $A = 0.14896\ in^2 = 0.961024\ cm^2$

b) $\alpha = 0.9950$

c) $\epsilon = 0.9950$

d) $T = 140^{\circ}C = 413^{\circ}K$

e) $R = 1{,}000$ ohms

f) $\sigma = 5.6686 \times 10^{-12}$ watts/$cm^2 - {}^{\circ}K^4$

g) $E = 3.969886$ volts

$$G = (0.995)^{-1}(0.995)(5.6686 \times 10^{-12})(413)^4 - \frac{(3.969886)^2}{(0.961024)(0.995)(1000)}$$

$$= (5.6686 \times 10^{-12})(29,093,783,761) - \frac{15.76}{956.2145} \qquad (4.6)$$

$$= 0.16492 - 0.016481$$

we obtain

$$G = 0.148439\ \frac{watt}{cm^2} \qquad (4.7)$$

Using the same values for Case II, except $T = 433^{\circ}K$

$$G = (5.6686 \times 10^{-12})(35,152,125,121) - \frac{19.070}{956.2145} \qquad (4.8)$$

$$= 0.199263 - 0.019933$$

We obtain

$$G = 0.179330\ \frac{watt}{cm^2} \qquad (4.9)$$

To determine ΔG we proceed as follows:

given

$$G = \alpha^{-1}\epsilon\sigma T^4 - E^2 A^{-1}\alpha^{-1}R^{-1} \qquad (4.10)$$

a) $$\frac{\partial G}{\partial \alpha} = -\alpha^{-2}\epsilon\sigma T^4 + E^2 A^{-1}\alpha^{-2} R^{-1}$$

b) $$\frac{\partial G}{\partial \sigma} = \alpha^{-1}\epsilon T^4$$

c) $$\frac{\partial G}{\partial T} = 4\alpha^{-1}\epsilon\sigma T^3$$

d) $$\frac{\partial G}{\partial E} = 2 E A^{-1}\alpha^{-1} R^{-1}$$

e) $$\frac{\partial G}{\partial \epsilon} = \alpha^{-1}\sigma T^4$$

f) $$\frac{\partial G}{\partial A} = E^2 A^{-2}\alpha^{-1} R^{-1}$$

g) $$\frac{\partial G}{\partial R} = E^2 A^{-1}\alpha^{-1} R^{-2}$$

Using the above partial derivatives and the given deltas (Δ's) shown below, and from equation (4.4) we obtain

$$\Delta G = \sqrt{\left(\frac{\partial G}{\partial \alpha}\Delta\alpha\right)^2 + \left(\frac{\partial G}{\partial \sigma}\Delta\sigma\right)^2 + \left(\frac{\partial G}{\partial T}\Delta T\right)^2 + \left(\frac{\partial G}{\partial \epsilon}\Delta\epsilon\right)^2 + \left(\frac{\partial G}{\partial E}\Delta E\right)^2 + \left(\frac{\partial G}{\partial A}\Delta A\right)^2 + \left(\frac{\partial G}{\partial R}\Delta R\right)^2} \qquad (4.11)$$

To obtain values for ΔG, we use equation (4.11) and the data based on the precision of each component for Case I where

a) $\Delta A = 0.092\%$ of area $= 0.0008819\ cm^2$

b) $\Delta\alpha = 0.2\% = 0.0020$

c) $\Delta\epsilon = 0.2\% = 0.0020$

d) $\Delta T = 0.2\% = 0.826^{\circ}K$ guard temperature delta

e) $\Delta T = 0.10\% = 0.413^{\circ}K$ cone temperature delta

$\Delta T = 0.30\% = 1.239^{\circ}K$

f) $\Delta R = 0.05\% = 0.5000$

g) $\Delta\sigma = 0.0000\% = 0.0000$

h) $\Delta E = 0.1\% = 0.003969886$

And from equation (4.10) (a-g), we have

$$\frac{\partial G}{\partial \alpha} = -0.1491856 \qquad \frac{\partial G}{\partial \alpha}\Delta\alpha = -0.1491856\ (0.0020) = -0.0002984$$

$$\frac{\partial G}{\partial \sigma} = 29,093,783,761 \qquad \frac{\partial G}{\partial \sigma}\Delta\sigma = 29,093,783,761\ (0.0) = 0.0$$

$$\frac{\partial G}{\partial T} = 0.0015972 \qquad \frac{\partial G}{\partial T}\Delta T = 0.0015972\ (1,239) = 0.001978$$

$$\frac{\partial G}{\partial E} = -0.0329600 \qquad \frac{\partial G}{\partial E}\Delta E = 0.0329600\ (0.0039689) = -0.000130$$

$$\frac{\partial G}{\partial E} = 0.1657500 \qquad \frac{\partial G}{\partial E}\Delta\epsilon = 0.1657500\ (0.0020) = 0.0003320$$

$$\frac{\partial G}{\partial A} = 0.0171500 \qquad \frac{\partial G}{\partial A}\Delta A = 0.0171500\ (0.0008849) = 0.00001512$$

$$\frac{\partial G}{\partial R} = 0.00001648 \qquad \frac{\partial G}{\partial R}\Delta R = 0.00001648\ (0.5000) = 0.00000824$$

Hence,

$$\Delta G = \sqrt{(-0.002984)^2 + (0.0)^2 + (0.001978)^2 + (-0.000130)^2 + (0.0003320)^2 + (0.0000824)^2}$$

$$= \sqrt{0.000004128945} \tag{4.12}$$

$$\Delta G = \pm 0.0020 \frac{\text{watt}}{\text{cm}^2} \tag{4.13}$$

$$\frac{\Delta G}{G} = \frac{0.0020}{0.148439} = 0.01347 \tag{4.14}$$

ΔG shows an error of $\pm$ 1.347% in the measurement of G for Case I.

Using the same procedure to obtain ΔG for Case II, we obtain

$$\Delta G = \sqrt{(-0.000360)^2 + (0.0)^2 + (0.0022881)^2 + (-0.0001583)^2 + (0.000401)^2 + (0.0000183)^2 + (0.00000995)}$$

$$= \sqrt{0.0000055130} \tag{4.15}$$

$$\Delta G = \pm 0.002356 \tag{4.16}$$

From equation (4.9) for Case II

$$G = 0.17933000 \tag{4.17}$$

Therefore

$$\frac{\Delta G}{G} = \frac{0.002356}{0.1793300} = 0.013137 \tag{4.18}$$

ΔG shows an error of $\pm$ 1.314% in the measurement of G for Case II.

The objective of the above error analysis was to determine the error in the dependent variable (G) resulting from errors of the independent variables (A, ϵ, σ, T, E, R and α) where

$$G = \frac{A \epsilon \sigma T^4 - \frac{E^2}{R}}{A \alpha}$$

and using the multivariate normal distribution. Considering

$$G = K_1 T^4 - K_2 E^2$$

where

$$K_1 = \frac{\epsilon \sigma}{\alpha}$$

and

$$K_2 = \frac{1}{A \alpha R}$$

The above analysis was completed assuming $K_1 T^4 = 1.1G$ with T = 140°C for Case I, and T = 160°C for Case II.

5. ANALOG SYSTEM STUDY
(Figures 5-1 through 5-7)

5.1 Temperature Control

This control system consists of a pulsed bridge which has a variable set point. The bridge is interrogated only when the error exceeds a preset limit (greater than detector dead band). The bridge error output is AC amplified through a high gain amplifier (low DC gain) and converted to a DC level by a sample and hold circuit. The DC error controls the output level of a DC power amplifier which supplies the heater.

No stability problems are anticipated, as the pole due to the thermal transfer rate (approximately 200 sec time constant for cone) will be sufficiently low to roll of the required loop gain. The required loop gain is apparently in the order of 5000 ($\simeq$ 72 db). The protect circuit is for provision of effectively reducing cone (or guard) temperature when required and decouples during the normal operation.

5.2 A/D Converter Operation

At the 303 data command, the converter will make a conversion of the heater voltage. The conversion will be complete before the rise of the bit synch pulse immediately following the rise of the 303 data command pulse.

The information register will be 13 bits long, the format being as shown below.

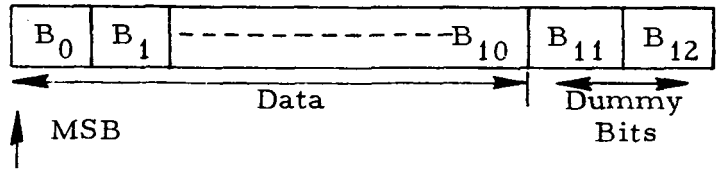

B_{11} and B_{12} will have zeros inserted during the convert period and the two telemetry 7-bit words will be shifted out under control of the bit synch clock in the following format:

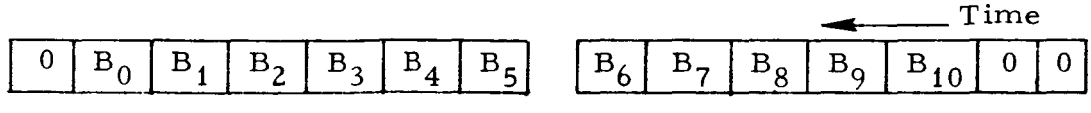

2nd Word
Data Command 304

1st Word
Data Command 303

The converter data register is locked out of a conversion cycle from the rise of the 1st bit synch pulse after 303 data command until the next 303 data command.

The converter is a conventional successive bit comparison type. The binary weighter control switches are FET's ($< 50\ \Omega$).

For the comparator, a chopper-stabilized-type amplifier is used, the grounded input for same being obtained by grounding the comparator input during the zero correct mode.

It is intended to use the Fairchild μA 709 and μA 711 in the comparator. Although the μA 709 will saturate in the proposed topology, this will be no problem as the saturation time is short compared to the bit time of conversion.

5.2.1 Accuracy and Limitations

The converter accuracy is ≃ 0.1% full scale, (full scale = 10 V) and it should be noted that this refers to minimum flux. If the flux ratio is 3:1 (max:min), then the accuracy at maximum flux will be $0.1\% \times 3^2 = 0.9\%$, and for a 2:1 ratio the accuracy at maximum flux is 0.4%. For the above accuracy, the input rate change is limited to approximately 0.05 solar constant/sec for a 2-solar constant max scale.

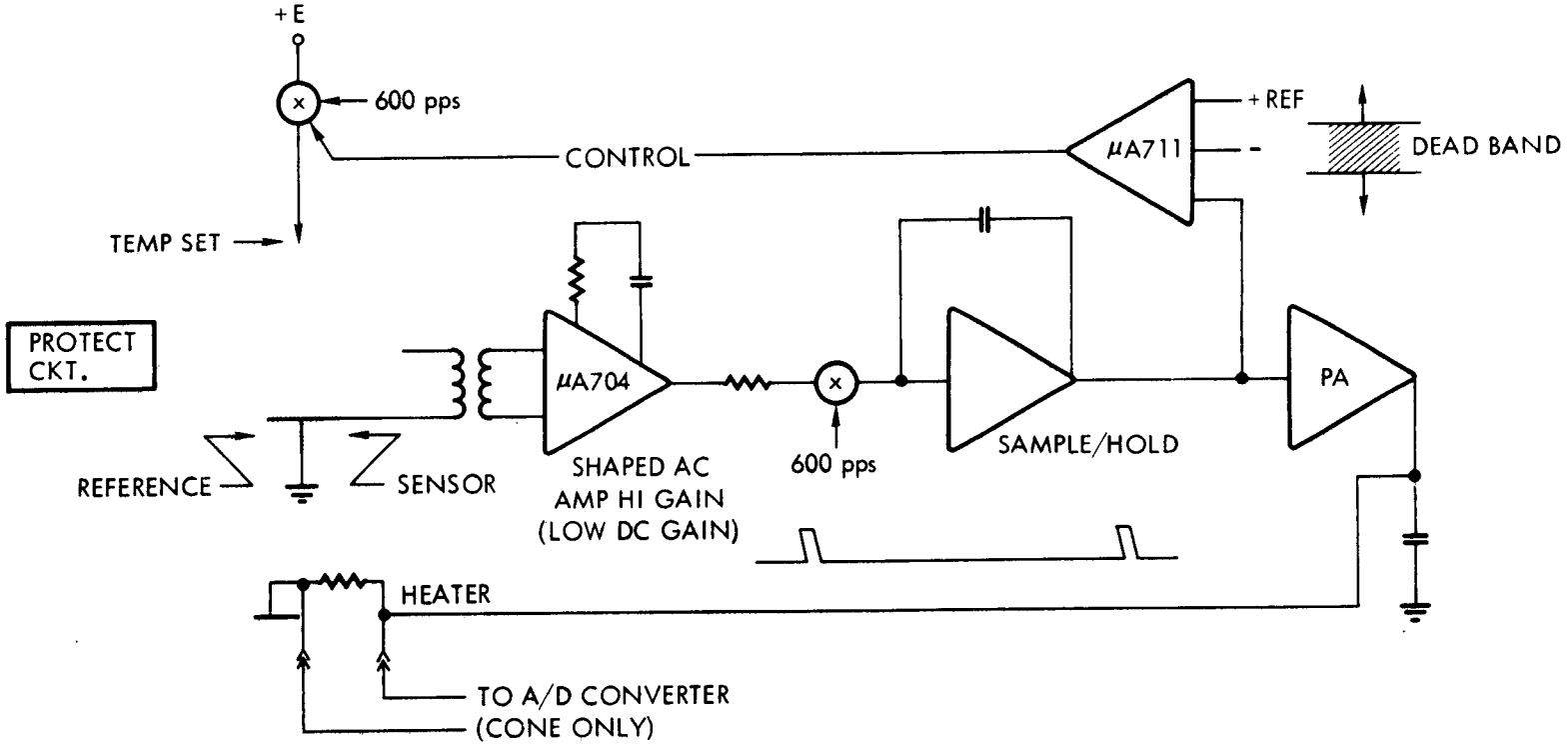

Figure 5-1. Temperature Control

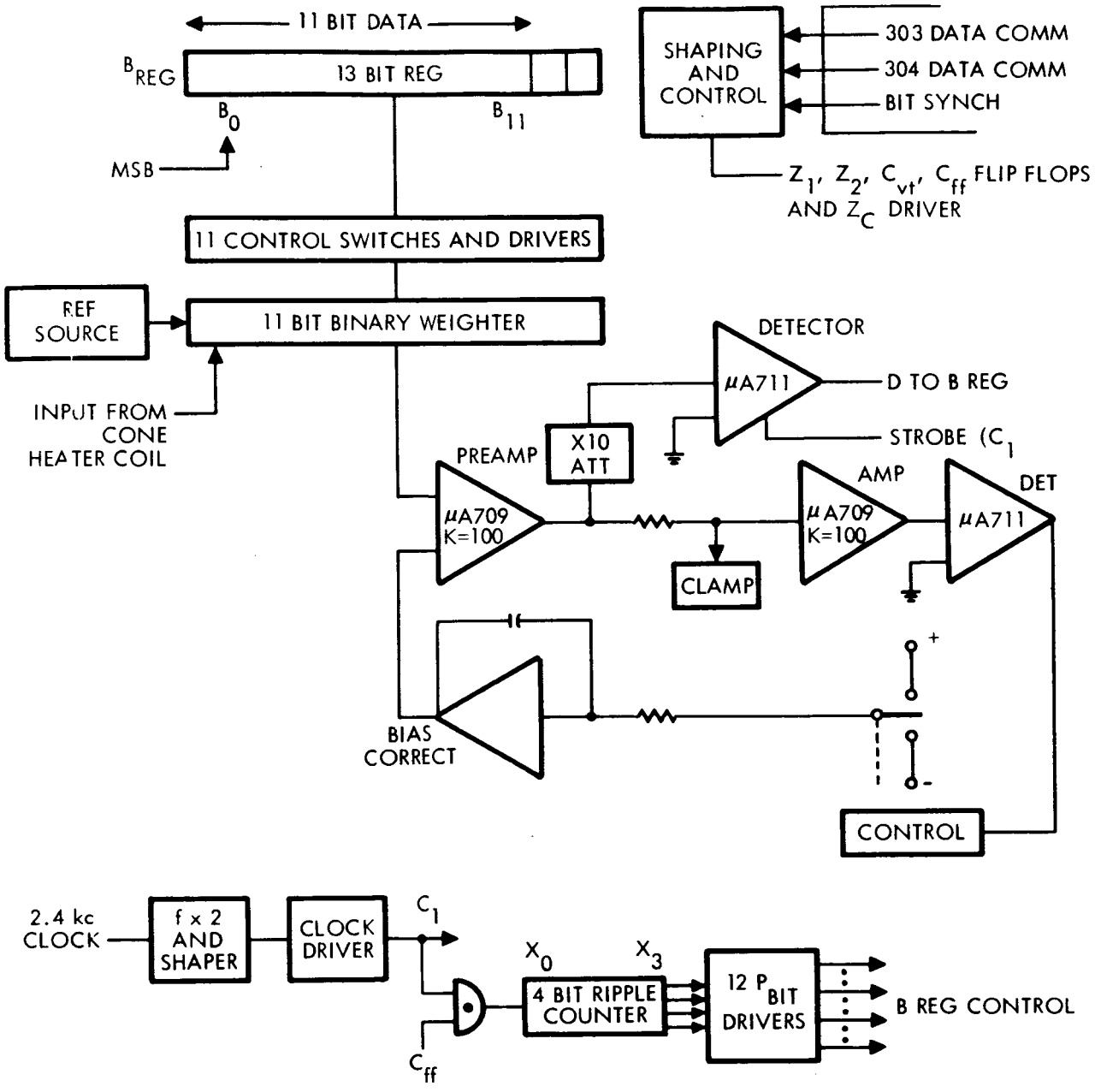

Figure 5-2. A/D Converter

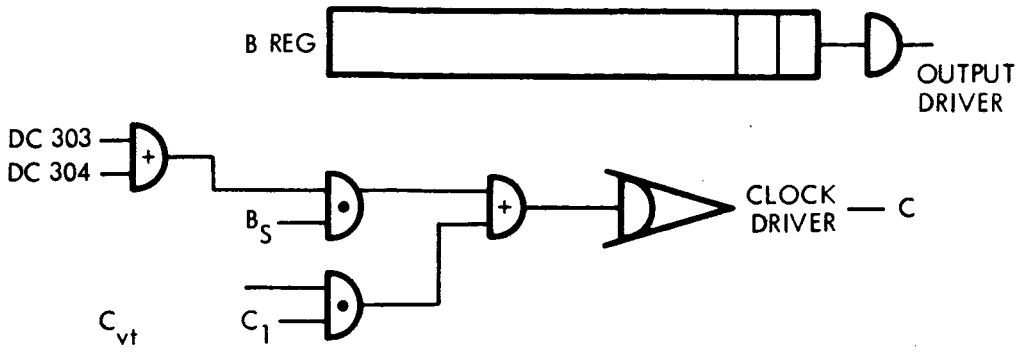

TYPICAL B REG CELL B_5

$$B_{5S} = \left(Z_1 Z_2 DC_{303} + B_4\, C_{vt}'\right) C$$

$$B_{5R} = \left(P_5 D + B_4'\, C_{vt}' + Z_C\right) C$$

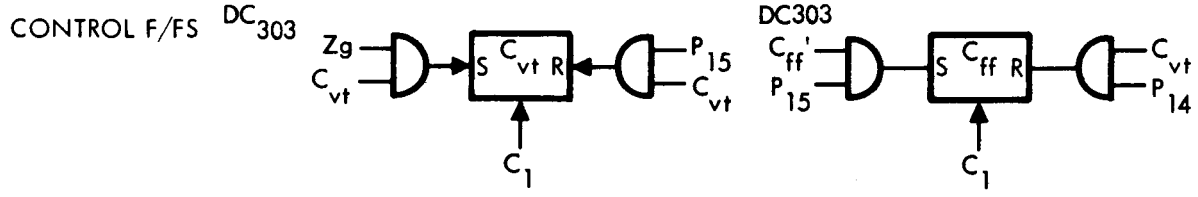

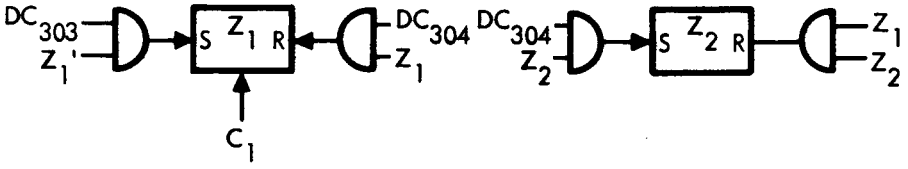

ZERO CORRECT DRIVER $\quad Z_C = \left(Z_1 + DC_{304}\right)'$

Figure 5-3. Control

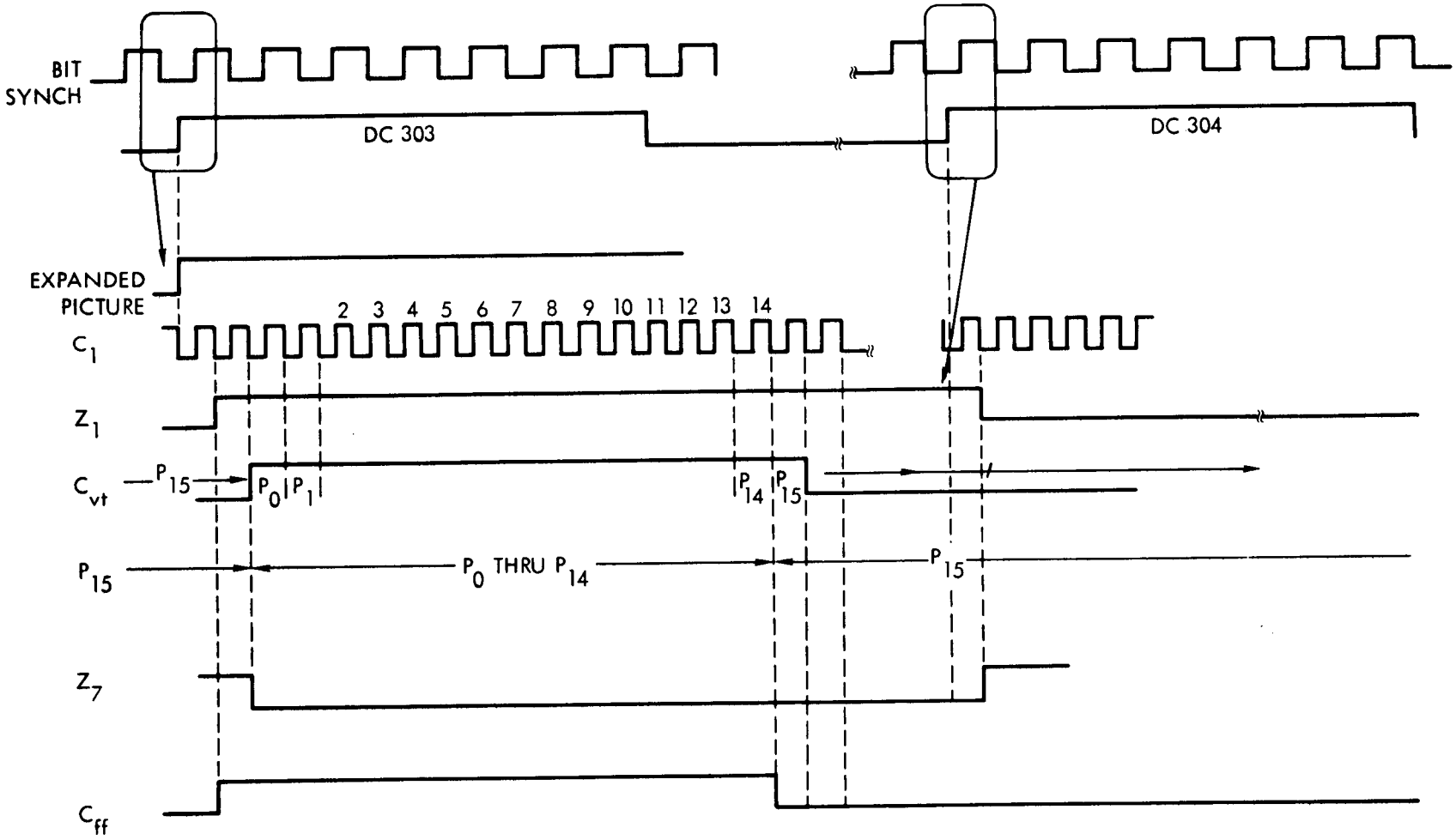

Figure 5-4. Data Register

Ripple Counter

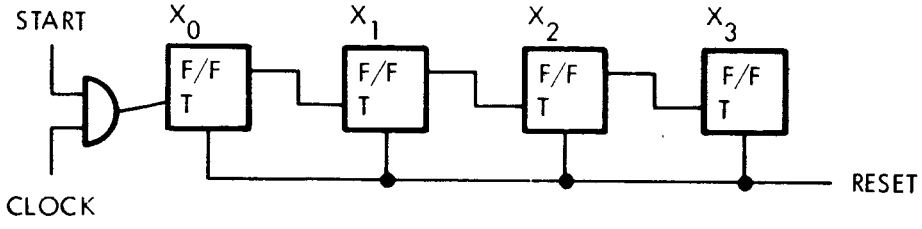

X_3	X_2	X_1	X_0	
0	0	0	0	$P_0 = X_0'X_1'X_2'X_3'$
0	0	0	1	$P_1 = X_0X_11X_2'X_3'$
0	0	1	0	$P_2 = X_0'X_1X_2'X_3'$
0	0	1	1	
0	1	0	0	
0	1	0	1	
0	1	1	0	
0	1	1	1	
1	0	0	0	
1	0	0	1	P_9
1	0	1	0	$P_{10} = X_0'X_1X_2'X_3$
1	0	1	1	
1	1	0	0	↑
1	1	0	1	P_{11} thru $P_{15} = X_3X_2+X_3X_1X_0 = P_Z$ Driver
1	1	1	0	↓
1	1	1	1	

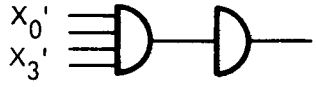

P Count Decoding — 12 of 4 inp gates(3) 11 of 2 inp gates(3)
2 of 2 inp gates(1/2) 4 buffers(2) (P_Z, P_Z')

Total 8-1/2 flat packs

Flat Pack Count

	FFS	Flat Packs
Control FFS	4	2
Control FF GTS	2-4 input 14-2 input	2 3-1/2
Zero correct driver	2-2 input	1/2
B register	13	6-1/2
B register GTS	2-4 input 5-2 input x 13 = 32-1/2 + 13	45-1/2
Ripple counter	4	2
Input gate		1/4
P count drivers	12 gates (4-input)	6
B register clock control	6-2 input	1-1/2
Comparator (strobe gate and zero correct)		1
Extra gating		
Used in f multiplier or in ripple counter to change it to Mod 11 count	6 gates	1-1/2
		72
Amplifiers and integrator including reference source		6
	Total	78

A/D Converter—Discrete Count

	FET	Xstr	R
Weighter switches	11	22	44
Weighter network	34 res	Approx size = 3-1/2 x 2 x 3/8 in.	

References source	R	C		Xstr	Diode	FET
		Small	Large			
	7	3	4	1	1	
Comparator	30	6	6	2	6	1

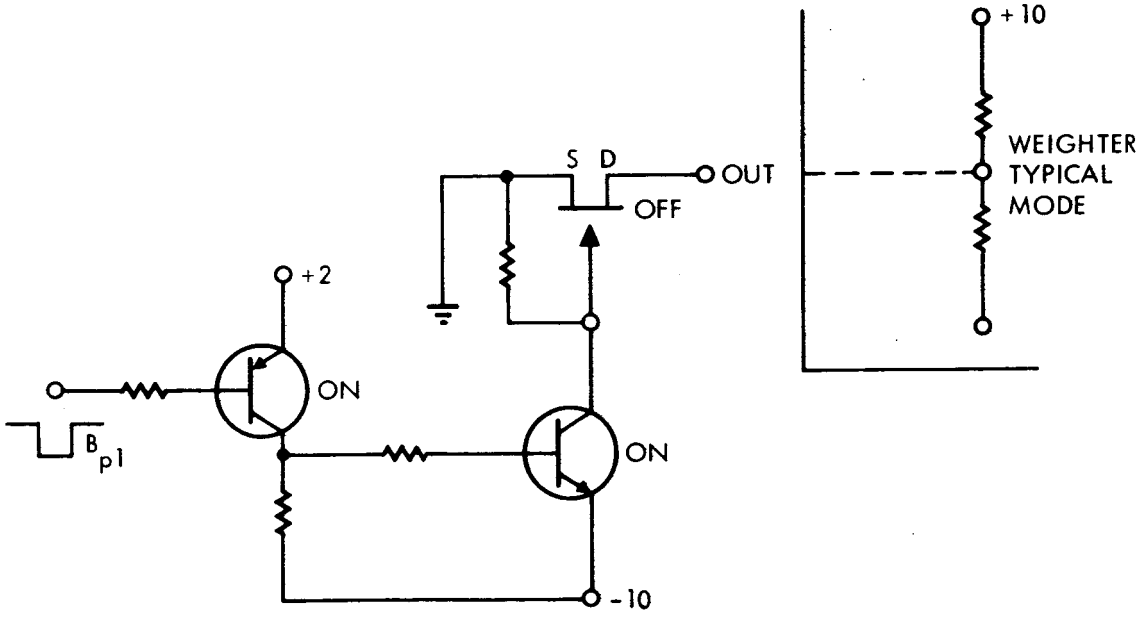

Figure 5-5. Weighter Switch

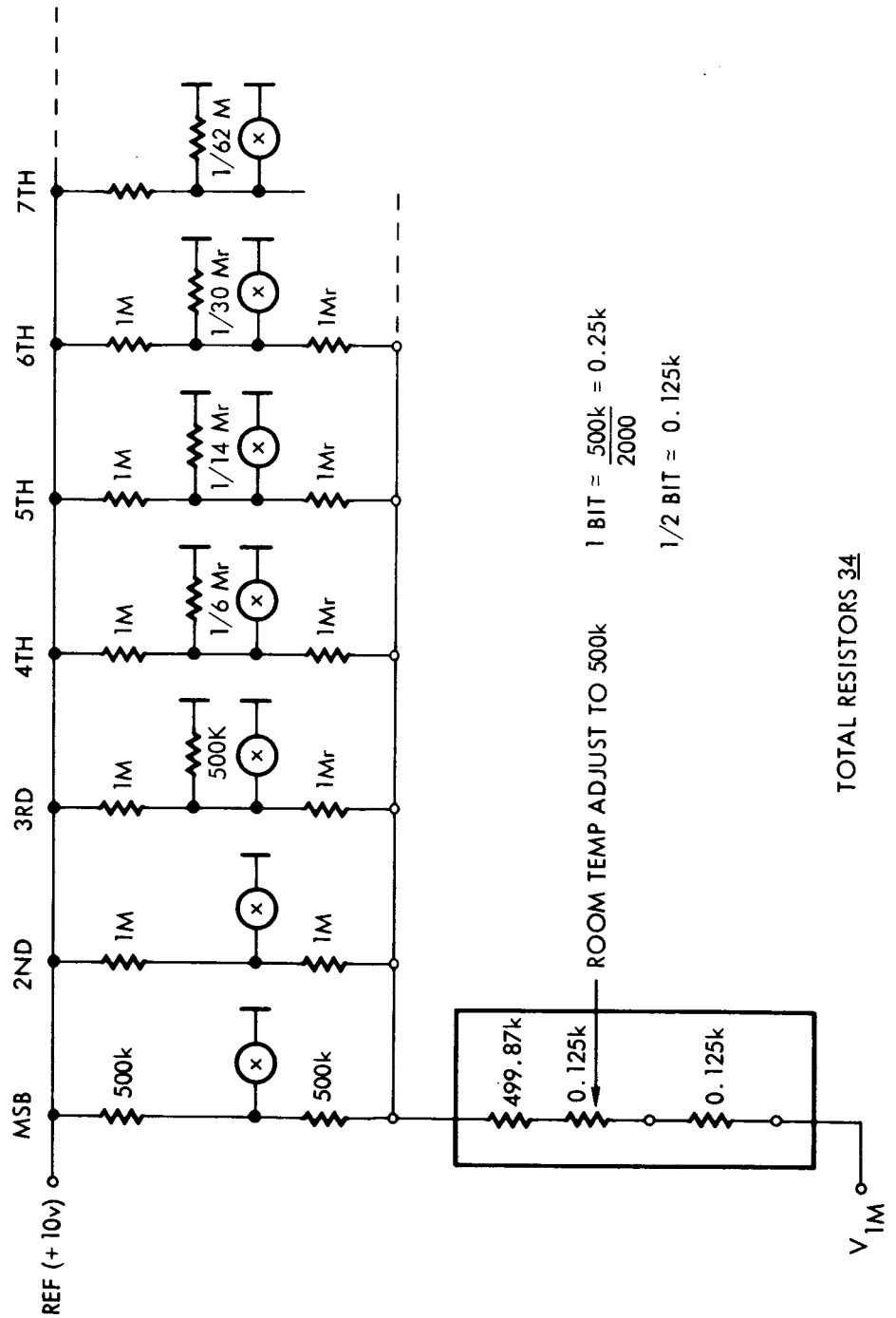

Figure 5-6. Weighter Network

Weighter

1st Bit $V/1$

2nd Bit $V/2$

3rd Bit $\dfrac{\frac{V}{1.5}\ 0.5}{1+\frac{0.5}{1.5}} = \dfrac{V/3}{1+1/3} = V/4$

4th Bit $\dfrac{\frac{V}{(1+R)}\ R}{1+\frac{R}{1+R}} = V/8 \qquad \dfrac{R}{1+R} = \dfrac{1}{8}\left(1+\dfrac{R}{1+R}\right) = \dfrac{(1+2R)}{1+R}\ 1/8$

$8R = 1 + 2R$

$6R = 1 \quad R = 1/6$

Check $\dfrac{\frac{V\ 1/6}{1+1/6}}{1+\frac{1/6}{1+1/6}} = \dfrac{V\ 1/6}{1+2/6} = V/8$

5th Bit $\dfrac{\frac{VR}{1+R}}{1+\frac{R}{1+R}}$ or $R = (1+2R)\ \dfrac{1}{X} \qquad X = 16$

$16R = 1 + 2R$

$R = 1/14$

Check $\dfrac{\frac{1/14}{1+1/14}}{1+\frac{1/14}{1+1/14}} = \dfrac{1/14}{1+2/14} = 1/16$

6th Bit $R = \dfrac{1m\Omega}{30}$

$32R = 1+2R$

$R = 1/32$

7th Bit $R = \dfrac{1m\Omega}{62}$

$64R = 1+2R$

$R = 1/64$

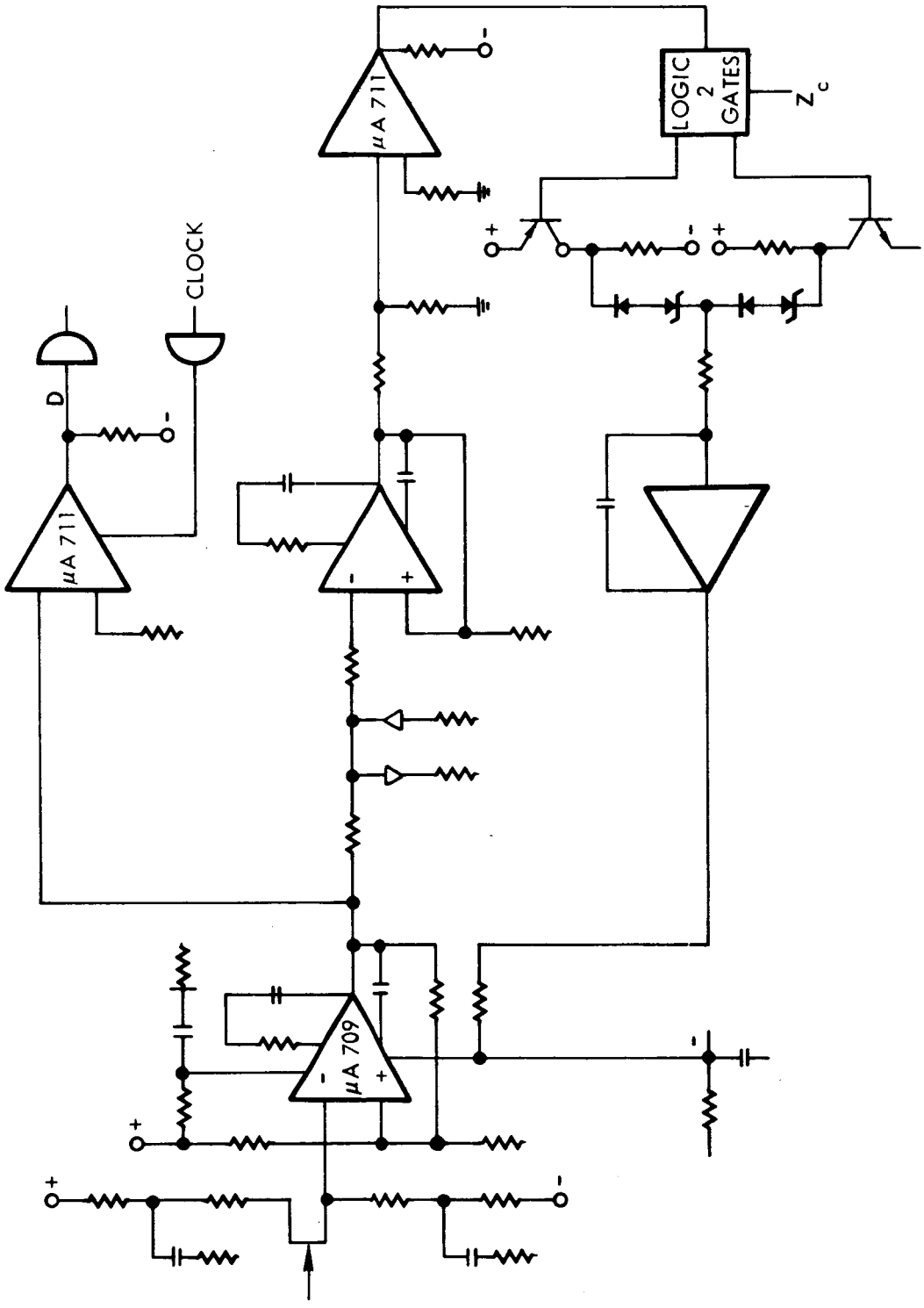

Figure 5-7. Comparator

A/D Converter

Accuracy — Power 0.2%
Voltage 0.1%

No. of bits = 11 $\pm$1 bit $\leq$ .05%

Full scale = 10V 1 bit = $\frac{10 \times 10^3}{2046} \simeq 5$ mv

Error Allocation		Error
Weighting network R = 500k	0.005% resistors 2 ppm 0.01%	0.02%
Switches (FET offset = 0; R = 50Ω) Leakage current		0.01% 0.015%
Reference Source (RSS error)		0.03%
Comparator		0.01%

$$\text{RSS error} = 10^{-2}\sqrt{2^2+1^2+1.5^2+3^2+1^2}$$

$$= 10^{-2}\sqrt{17}$$

$$\simeq .04\% \text{ or } .085\% \text{ WC}$$

Converter error = 0.04% $\pm$ 1/2 LSB $\simeq (0.04 + 0.025)\%$
$\simeq 0.065\%$ for voltage

Reference Source

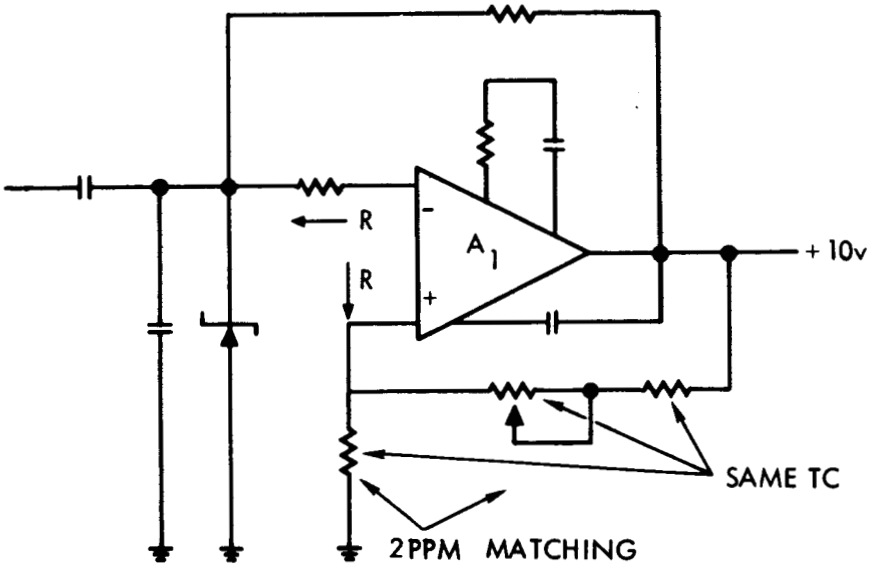

Zener Drift 0.0005%/°C

For ΔT = 50°C error = 0.0005 x 50% = 0.025%

For A_1 = μA 709 ΔV_{off} = 6μv/°C

$$\% \Delta V_{off} \text{ for 6.8v Zener} = \frac{6\times10^{-6}\times50\times100\%}{6.8}$$

$\not\Delta T$ = 50°C = 0.004%

$\Delta I_{offset} \simeq 25 \times 10^{-9}$ 0 to 75°C

For R ≤ 10k $\% \Delta V_o \simeq \frac{25\times10^{-9}\times10^{4}\times1.5\times100\%}{10}$ (-Gain) = 0.0037%

Scaling Resistor Drift $\frac{2}{10^6}$ x 100% x 50°C = 0.01% = 0.01%

Set up Accuracy 0.005%

RMS Error = $10^{-2}\sqrt{0.05^2 + 2.5^2 + 0.4^2 + 37^2 + 1^2}\%$

$\leq 10^{-2}\sqrt{9} \leq 0.03\%$

Present Bridge Information

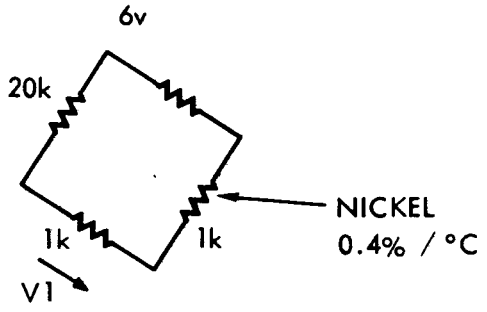

$$V_1 = \frac{6x1}{20} \simeq 300 \text{ mv/1k}$$

$$u_v = \frac{300}{1000} \times AR = \frac{300}{1000} \times 0.4 \simeq 120 \text{ μv/o.1°C} \quad (0.4\text{r}/0.1\,^\circ\text{C})$$

Resistor Network Information (Converter)

$$2 \text{ ppm} = \frac{2}{10^6} \times 100 = 0.0002\%/^\circ\text{C}$$

For ΔT = 50°C Error = 0.01%

Match Error $\frac{0.005\%}{0.015}$

RSS Error $\simeq 15^2 \sqrt{1.5^2 + \frac{1.5^2}{4} + \text{-----}}$

$= 0.021\%$

Comparator Error

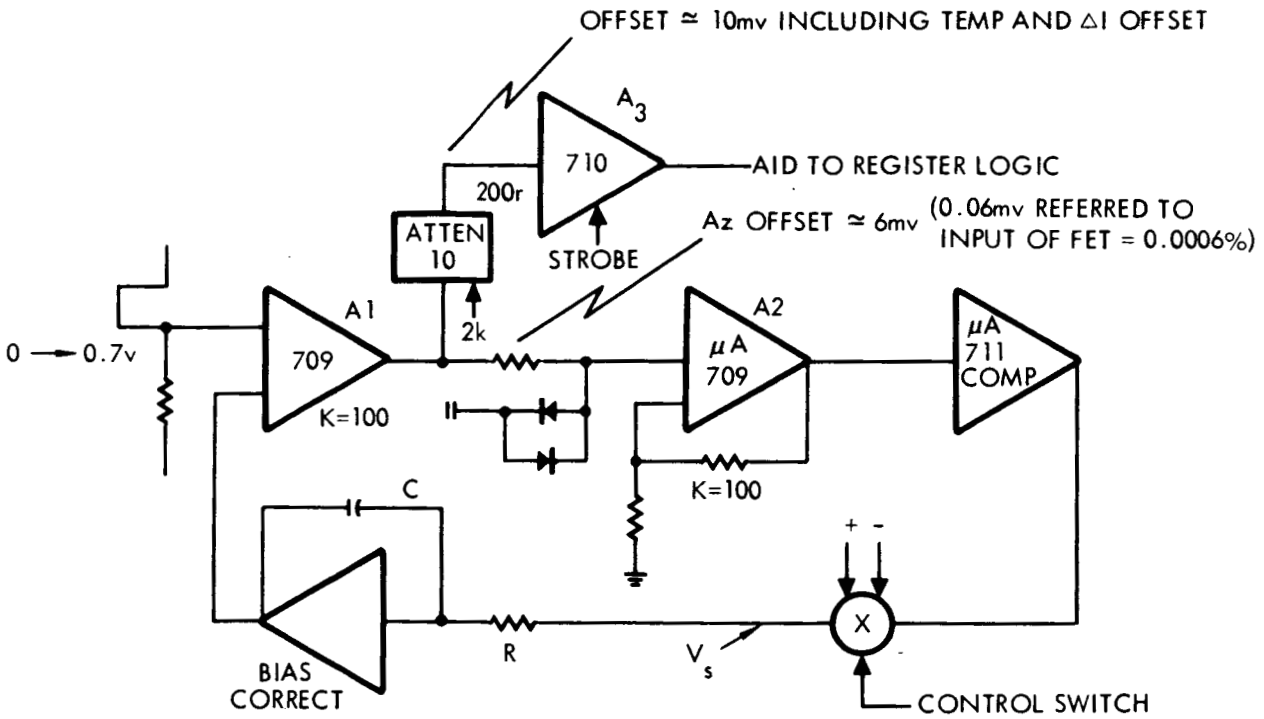

$A_1 + A_2$ saturation time is ≃ 4μsec + 4μsec

Limit cycle error $e_{LC} = \frac{Vs}{RC} \times t$

For V_s = 10v say t = 4 μsec and $e_{LC} \leq 0.1$ mv

$$RC \geq \frac{10 \times 8 \times 10^{-6}}{.1 \times 10^{-3}} \geq 400 \times 10^{-3}$$

For $C \simeq 0.1 \times 10^{-6}$ $\quad R \geq \frac{800 \times 10^{-3}}{0.1} \geq 8M$

Required slew rate $\geq \frac{dV}{dT}\frac{dT}{dt}$ $\qquad \frac{dT}{dt} \leq 1°/sec$

$\geq 2 \times 10^{-3} \times 1$ $\qquad \frac{dV}{dT} = 2 \times 10^{-3}/°C$

$\geq 2 \times 10^{-3} V/sec$

With slew time say ≤ 400 μsec (actually 5 x 200 μsec) $\qquad \frac{Vs}{RC} > 2 \times 10^{-3}$

$$RC < \frac{10}{2 \times 10^{-3}} \leq 5 \times 10^{3} V/S$$

Switch Leakage Current

ASSUME WEIGHTING NETWORK AS SHOWN

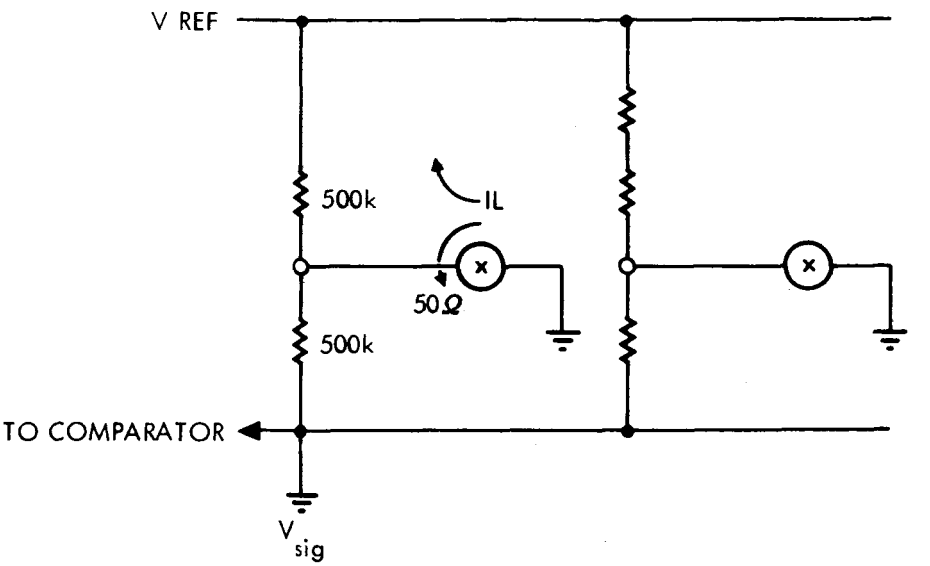

For 10v pinch off (eg 2N4092) 2ηa at 75°C worst case

$$\text{equivalent input} \simeq 2 \times 10^{-9} \times \frac{500}{2} \times 2 \times 10^{3} = 10^{-3}\text{v} = 1\text{ mv}$$

$$= 0.01\%$$

$$\Sigma \text{Tss Error} \simeq 0.015\%$$

Drift Error (Comparator) During Convert Time

Assume bit rate = 1/2400 cps ≃ 400 μsec

11 bit convert time ≃ $400 \times 10 \times 10^{-6}$

Drift = 2mv/sec x 0.004 sec — negligible

$$\text{Total comparator error} \simeq \frac{\text{A3 offset}}{10} \simeq \frac{10}{10} = 1\text{ mv}$$

$$= 0.01\%$$

6. DESIGN REQUIREMENTS

The design requirements are outlined in Exhibits I, II, and III which follow:

EXHIBIT I

PRELIMINARY-DESIGN REQUIREMENTS OF THE TEMPERATURE CONTROL FLUX MONITOR ELECTRONIC CONTROL ASSEMBLY

1. SCOPE

These requirements establish the performance requirements and physical characteristics of a thermal flux radiometer suitable for the accurate absolute measurement of radiation in the range of 0.2 to 40 microns with a maximum intensity of 0.2 watt per cm^2. The complete radiometer consists of a conical cavity-type thermal flux sensor, termed the TCFM Transducer Assembly, and a companion electronic control unit, termed the TCFM Electronic Control Assembly (ECA). The TCFM transducer assembly is described in Applicable Document No. 1. The within document delineates the requirements of the TCFM ECA as well as the performance of the complete system when the TCFM ECA and the TCFM Transducer Assembly are interconnected.

2. APPLICABLE DOCUMENTS

The following documents are applicable to and form a part of these requirements:

(1) TRW Document No. 6988.000-67-3346.12-02, Exhibit III, "Preliminary-Design Requirements of the Temperature Control Flux Monitor Transducer Assembly," 24 January 1967.

(2) California Institute of Technology, "Cost Plus a Fixed Fee Type Research and Development Contract," (Subcontract under NASA Contract NA7-100), Task Order No. RD-29, Contract No. 951726, 30 September 1965, Exhibits 1, 2 and 3.

(3) TRW Document No. 06988-6002-R000, Exhibit II, "Preliminary-Design Requirements of the Temperature Control Flux Monitor Operational Support Equipment (TCFM OSE)," January 1967.

(4) JPL Document No. MM69-3-260, "MM69 Electrical Interface and Electrical Grounding."

(5) JPL Document No. 30250B, "Mariner C Flight Equipment. Type Approval Environmental Test Procedure," 15 March 1963. (Also Amendments 2 and 3.)

(6) JPL Document No. 30236A, "Environmental Test Specifications, RFI Control for Spacecraft and Ground Control Equipment," 20 October 1961.

3. REQUIREMENTS

3.1 General Requirements

3.1.1 Compatibility

The TCFM ECA shall be physically and functionally compatible with Mariner Mars 1969 Spacecraft systems requirements as defined in Applicable Document No. 2. The TCFM ECA shall also be functionally and electrically compatible with the TCFM Transducer Assembly and the TCFM OSE as defined in Applicable Documents No. 1 and 3.

3.1.2. Components

The TCFM ECA shall consist of the following components:

a) Guard temperature control circuit

b) Radiometer cone temperature control circuit

c) Telemetry control and interface circuit

d) OSE buffer circuit

e) Power supply

3.2 Design Requirements

The functions of the TCFM ECA are three-fold, namely, (1) to maintain the radiometer guard and cone temperatures at a preset value, (2) to generate telemetry system compatible electrical signals which represent the amount of power required to maintain the cone at the constant preset temperature, and (3) to generate digital signals which indicate whether or not the cone is in a stable condition. The digital signals shall represent and be proportional to cone heater power within an accuracy of 0.5 percent under all conditions defined in Section 3.5.

3.2.1 Guard Temperature Control Circuit

The guard temperature control circuit shall maintain the guard temperature at 140°C ± 0.1°C. The guard shall stabilize at this temperature within 30 minutes after power turn-on under all conditions defined in Section 3.5.

3.2.2. Radiometer Cone Temperature Control Circuit

The radiometer cone temperature control circuit shall maintain the cone temperature to within 0.1°C of the guard temperature. The cone temperature shall return to within 1 percent of its final equilibrium value within 5 seconds after experiencing a positive step change of not less than 0.140 watt per cm^2 in incident flux. The cone temperature control circuit shall generate a 10-bit binary number that is proportional to and represents the required cone heater power within an overall accuracy of 0.5 percent. This binary number shall be transferred to the telemetry storage register and shall at all times be ready for transfer to the TM system upon receipt of shift commands. The telemetry

storage register shall be updated at lease once per second, unless an output shift is in progress. In addition to the 10-bit cone heater power word, a word of 4 binary bits or less shall be generated, defining the cone temperature deviation from equilibrium. The formatting of these data in the telemetry storage register is specified in Section 3.2.3.

3.2.3 Telemetry Control and Interface Circuits

The 10-bit cone heater power data word and the 4-bit error status word shall be made available in a 14-bit TM register for serial transfer to the TM system upon command by the TM system. The ECA shall be compatible with the following applicable system characteristics and requirements:

a) The TM word is 7 bits long. At least 1 bit in each TM must be a zero.

b) The TM system presents a separate alert command for each of the two TM words to be received. The alert commands are presented on separate lines and occur alternately.

c) A continuous bit sync signal is presented on a third line. The bit sync rate can be either 8-1/3 or 33-1/3 pulses per second. The data transfer from the TM register to the TM system is in synchronism with the bit sync, provided an alert command is present.

d) Each alert command starts a nominal 5.1 milliseconds before the start of a bit sync pulse and ends a nominal 5.1 milliseconds after 7-bit sync pulses have been presented.

e) The alert commands and bit sync have rise and fall times of 10 microseconds maximum. The true level for the alert commands is 0 volt $\begin{smallmatrix}+5\ \text{volt}\\-0\ \text{volt}\end{smallmatrix}$ and the false level is + 4.5 volt ± 1 volt. The bit sync is transformer-coupled, but has the same peak voltage excursion and sense as the alert commands.

f) The termination requirement on the alert command lines shall be 2 K ohms minimum to the ECA +4.5 volts supply voltage.

g) The termination requirement on the bit sync line shall be 1.8 K ohms minimum to ECA common.

The 10-bit cone heater power data word and the 4-bit error word shall be transferred to the TM register at least once each second, unless data are being shifted from the TM register to the TM system. One of the alert commands, herein called R1, shall cause the serial shift of 7 bits of the 14 stored data bits, and the other alert command, herein called R2, shall cause the serial shift of the remaining 7 data bits. The 14-bit TM register shall not be updated during the time interval from the start of the R1 alert command to the termination of the R2 command, regardless of the elapsed time. The TM register output shall be delivered to the TM system through buffer circuits in a manner to be defined at a later time. These buffer circuits shall insure that shorter or open lines

do not have a permanent adverse effect on the operation of the TM system or the ECA.

3.2.4 OSE Buffer Circuit

The function of the TCFM OSE buffer circuit is to supply certain signals to the OSE and to provide isolation of the signal lines between the ECA and the OSE.

The following signals are to be supplied to the OSE through the OSE cable on individual lines:

a) The buffered output of the TM 14-bit shift register.

b) The shift pulses used to transfer the error data into the TM register.

c) The shift pulses used to transfer the cone power register data into the TM register.

d) The resistance of the guard temperature sensor, supplied by the four wires from the Kelvin-connected temperature sensing element in the TCFM transducer assembly.

The shift register output and shift pulse signals shall be isolated from the OSE cable by means of buffer amplifiers with the following characteristics:

a) The buffers shall receive their operating power from the OSE.

b) The power return shall be connected to the ECA circuit common but not to the ECA frame or the OSE common.

c) The output true logic level shall be +4 volts ± 1 volt and the false level shall be 0 volt $^{+5}_{-0}$ volts.

d) The rise and fall times of the buffer circuit outputs shall be less than 2 microseconds when the outputs are loaded with a capacitance to TCFM common of 2000 picofarads and a resistance of 1000 ohms. For test purposes the tolerances on the capacitance and resistance are to be determined at a later date.

e) Each output shall be accompanied by a separate return wire connected to TCFM common.

3.2.5 Power Supply

The operating power for the TCFM ECA shall be derived from an AC power source having the following characteristics:

a) Frequency - 2400 Hz ± 0.01 percent

b) Waveform - 50 volts peak ± 2.0 percent
square-wave rise and fall times of 5 microseconds ± 4 microseconds
overshoot: 5 volts maximum, 5 microseconds maximum duration

The peak recurrent power supply input line current shall not exceed 1.5 times the maximum average line current. Current limiting or over-current protection shall be employed to prevent a failure in the ECA from affecting the power source or other portions of the spacecraft.

The power supply shall operate from either the spacecraft AC power source or the OSE multiple DC power source without the need for switching devices. The power supply shall be designed such that the two sources are mutually isolated. The OSE buffer circuits shall receive their operating power from the OSE. The AC input lines shall not have a direct current connection to the ECA circuitry or common.

3.3 Performance Requirements

Limits are placed on the following parameters to insure that the ECA will meet the performance requirements stated herein, namely,

a) Servo error - to be established.

b) Preamplifier drift - to be established.

c) Bridge sensitivity - to be established.

d) Output voltage stability - to be established.

e) Power level measurement range - to be established.

3.4 Interface Requirements

The TCFM ECA shall meet the performance requirements stated herein with the TCFM transducer assembly connected to the ECA by means of a 10-foot long interconnecting electrical cable.

The ECA shall meet the interface requirements defined in Applicable Document No. 4.

3.5 Environmental Requirements

The TCFM ECA shall meet the environmental requirements defined in Applicable Document No. 5 in the following fields:

a) Temperature

b) Vacuum

c) Shock

d) Vibration

3.6 Radio Interference

The TCFM ECA shall meet the radio interference requirements defined in Applicable Document No. 6.

3.7 Reliability

The TCFM ECA shall have a minimum lifetime under continuous use in space of 280 days. The failure of the TCFM transducer assembly,

the ECA or the interconnecting cable shall in no way affect the spacecraft or any component thereof.

3.8 Size and Weight

3.8.1 Size

The TCFM ECA shall be contained in two standard 6 inch by 6 inch by 1.5 inch thick Mariner subchassis.

3.8.2 Weight

The weight of the TCFM ECA shall not exceed 4.75 pounds.

3.9 Power Consumption

The TCFM system shall consume not more than 8 watts.

4. QUALITY ASSURANCE PROVISIONS

4.1 Acceptance Tests

A test procedure shall be devised at a later time to cover the requirements of Section 3 of this document. The test procedure shall define inspections, functional test procedures, test conditions, and test equipment and equivalents to be used.

5. PREPARATION FOR DELIVERY

Not Applicable.

6. NOTES

6.1 Intended Use

These preliminary design requirements are the result of an instrument definition study and are not intended for final equipment procurement purposes.

EXHIBIT II

TCFM OPERATIONAL SUPPORT EQUIPMENT PRELIMINARY-DESIGN REQUIREMENTS

1. SCOPE

These preliminary-design requirements establish the functional requirements and physical characteristics of the operational support equipment (OSE) to be used for the pre-launch checkout of the Thermal Control Flux Monitor (TCFM) system as defined in Applicable Document No. (1). The TCFM system consists of the TCFM Transducer Assembly and the TCFM Electronic Control Assembly (ECA) as defined in Applicable Document No. (1). The TCFM system consists of the TCFM Tansducer Assembly and the TCFM Electronic Control Assembly (ECA) as defined in Applicable Documents Nos. (2) and (3).

2. APPLICABLE DOCUMENTS

The following documents are applicable to and form a part of these requirements:

(1) California Institute of Technology, "Cost Plus a Fixed Fee Type Research and Development Contract," (Subcontract under NASA Contract NA7-100), Task Order No. RD-29, Contract No. 951726, 30 September 1965, Exhibits 1, 2 and 3.

(2) TRW Document No. 6988.000-67-3346.12-02, Exhibit III, "TCFM Transducer Assembly Preliminary-Design Requirements," January 1967.

(3) TRW Document No. 06988-6002-R000, Exhibit I, "TCFM Electronic Control Assembly Preliminary-Design Requirements," January 1967.

(4) JPL Document No. OSE/MC-3-110, "Functional Specification, Mariner C, Operational Support Equipment, Design Characteristics and Constraints," 17 June 1966.

3. REQUIREMENTS

3.1 General

3.1.1 OSE Functions

The OSE shall perform the following functions when connected to the TCFM ECA by means of a multiconductor cable not exceeding 100 feet in length, namely,

a) Acquire and display cone heater power measurement.
b) Acquire and display cone control loop error measurement.
c) Acquire and display TCFM guard temperature measurement.

d) Provide standby command to operate the TCFM at lower than operational temperature.
e) Provide a test flux stimulus to the TCFM transducer assembly.
f) Provide operating power for the TCFM and OSE buffer circuit.

3.2 Design and Performance Requirements

3.2.1 Cone Heater Power Measurement

The design requirements of the OSE consist of the implementation of the general requirements enumerated in Section 3.1.1. These implementations must be compatible to the characteristics and design requirements of the TCFM ECA and TCFM Transducer Assembly as defined in Applicable Documents Nos. (2) and (3).

3.2.1.1 TCFM Data Output Characteristics

The cone heater data consist of a 10-bit pure binary number. The data are delivered serially the OSE through the OSE cable, least significant bit first. Ten shift pulses accompany the data on a separate wire. The timing of the data and shift pulses are in accordance with Figure 1. Each input line has a separate return line tied to the TCFM ECA circuit common.

3.2.1.2 OSE Data Input Requirements

Cable terminator circuitry is to be employed in the OSE to receive and condition the data shown in Figure 1. The design of the cable terminators shall be such that the resistive load from each data line to its return wire will not be less than 1000 ohms. Neither the data lines nor the returns shall be connected to the OSE common through a resistance of less than 10 k ohms or a capacitance of greater than 200 picofarad Common mode signals of up to 1 volt peak amplitude referred to OSE common shall not affect the proper operation of the equipment of cause errors in the readings.

3.2.1.3 Cone Heater Power Display

The cone heater power 10-bit binary number is to be displayed on a single horizontal row of 10 lamps. Lighted lamps are to indicate one bits and unlighted lamps are to indicate zero bits. The least significant bit is to be positioned at the right-hand end of the row as viewed facing the front panel of the OSE.

The lamps may be either neon or incandescent. If incandescent lamps are used, they must be replaceable from the front panel without the use of special tools. The data and shift pulses are presented to the OSE every 0.213 second unless data are being shifted from the TCFM ECA to the TM system. It should be noted that in the latter case the OSE shift pulses are inhibited by the TCFM ECA for periods as long as 120 seconds. In no case, however, are the shift pulses inhibited during

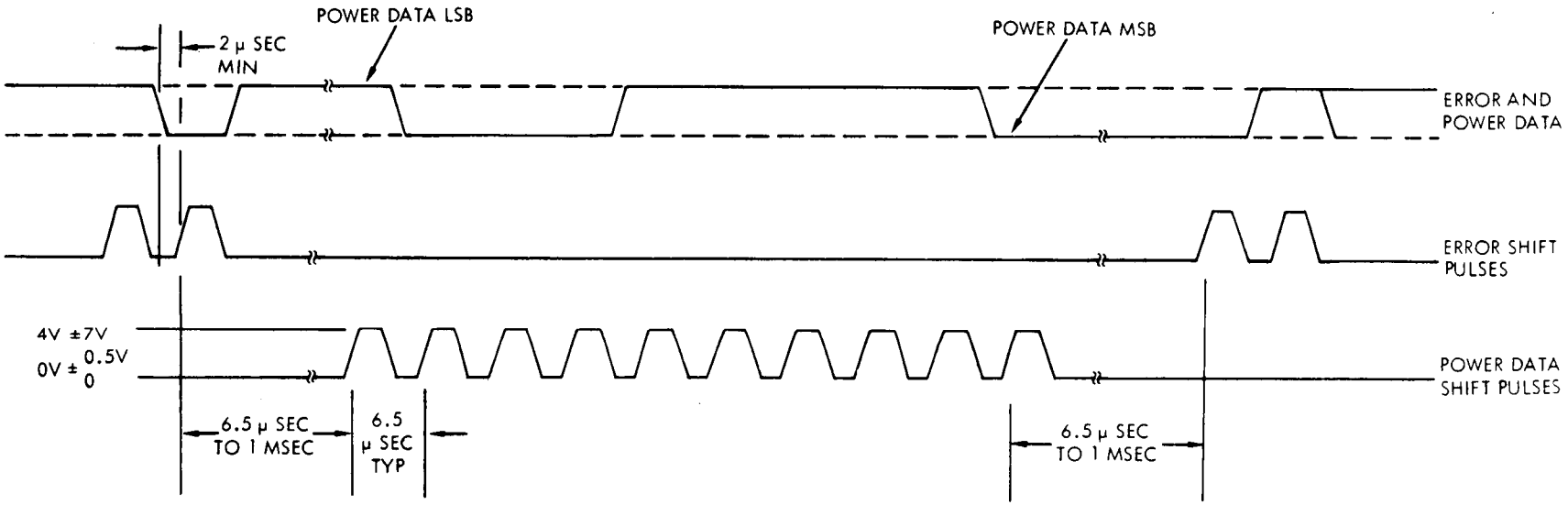

NOTES:

1. ALL RISE AND FALL TIMES ARE 2 μ SEC MAX
2. TIMING BETWEEN PULSES IS MEASURED FROM 50% AMPLITUDE POINTS
3. TRUE LOGIC LEVEL IS +4V
4. ONE FRAME OF DATA SHOWN. DATA FRAME REPEATS EVERY 0.213 SEC UNLESS TM READOUT IS IN PROGRESS

Figure 1. TCFM Data Output Waveforms

an ECA to OSE transfer frame. Provision shall be made to alter the display change form 0.213 second to a variable display change rate at the discretion of the operator. The variable display time shall be continuously adjustable from 10 to 60 seconds.

3.2.2 Cone Heater Control Loop Error Measurements

3.2.2.1 TCFM Data Output Characteristics

The error data are presented to the OSE on the same wire as the power data. The four shift pulses associated with the error data are delivered on a separate line. The timing of the waveforms is shown in Figure 1. The least significant error bit appears first. The 4-bit error code is a variable weight code as shown in Table 1. The least significant bit is in the right-hand column.

Table 1. Error Code

Code	Significance
0001	no error
0000	1 bit error
1000	2 bit error
0100	4 bit error
1001	8 bit error
0010	16 bit error
1010	32 bit error
0110	64 bit error
0101	128 bit error

3.2.2.2 OSE Data Input Requirements

Same as Section 3.2.1.2.

3.2.2.3 Cone Heater Error Display

The cone heater error 4-bit number is to be displayed on a single horizontal row of four lamps. The number is to be displayed in the order shown in Table 1, except that the bits in the right-hand row shall be complemented in order to have all zeros indicate no error. Lighted lamps are to indicate one bits and unlighted lamps are to indicate zero bits. The last paragraph of Section 3.2.1.3 is applicable here also.

3.2.3 Guard Temperature Measurement

3.2.3.1 TCFM Data Output Characteristics

The guard temperature sensor consists of a platinum wire element with a nominal temperature coefficient of resistance of 3000 PPM/^{o}C and a nominal resistance of 100 ohms at a guard temperature of 0^{o}C. The sensor is Kelvin connected and the four wires are connected to the OSE through the OSE cable.

3.2.3.2 OSE Data Input Requirements

Not applicable.

3.2.3.3 Guard Temperature Display

The resistance of the sensor element shall be sensed and displayed in temperature units on a 4-inch mirrored scale panel meter. The range of the meter shall be $0^{o}C$ to $150^{o}C$. The readability and accuracy shall be such that the meter indication can be read to an absolute accuracy of $\pm 1^{o}C$.

3.2.4 Standby Temperature Command

A front panel toggle switch shall be provided to control the standby temperature mode. The switch closure shall short a pair of wires in the OSE cable which in turn causes the guard temperature to be reduced from the normal operating temperature of $130^{o}C$ to approximately $40^{o}C$. The exact set point is determined by components within the ECA and cannot be controlled by the OSE.

3.2.5 Test Flux Stimulus

The OSE shall control a lamp source to be used to provide a test flux input to the transducer. The lamp shall be connected to the OSE by means of a detachable cord 100 feet in length. An on-off switch shall be provided to control the lamp. The type of lamp to be used is to be determined at a later time.

3.2.6 TCFM Operating Power

The OSE shall provide operating power for the TCFM. When operating from the spacecraft power system the TCFM is powered by 2.4 KH, 50 V peak square wave power.

The OSE shall provide multiple DC voltages which are connected into ECA power supply circuitry after the transformer and rectifiers. The number of different voltages and the characteristics of each are to be compatible with the ECA power requirements and are to be determined at a later time.

The OSE shall also provide operating power for the OSE buffer circuit in the ECA. The buffer power supply return shall be connected to the ECA common, but not to the ECA frame or OSE common.

3.3 Mechanical Requirements

3.3.1 Racks and Panels

An 8-3/4 inch panel, suitable for mounting in a rack, as specified in OSE/MC-3-110.

3.3.2 Paint

Paint type and color are as specified in OSE/MC-3-110. All equipment in the TCFM OSE requiring painting shall be in conformance with this specification.

3.3.3 Construction Methods

To be determined.

3.3.4 Weight

To be determined.

3.4 Environmental Requirements

3.4.1 Vibration and Shock

Per OSE/MC-3-110.

3.4.2 Operating Temperature and Humidity

Per OSE/MC-3-110.

3.4.3 Storage Temperature

Per OSE/MC-3-110.

3.4.4 Sand, Dust, Salt Spray, Rain and Fungus

Per OSE/MC-3-110.

3.4.5 RF Environment

Per OSE/MC-3-110.

3.4.6 RFI

Per OSE/MC-3-110.

4. QUALITY ASSURANCE PROVISIONS

4.1 Environmental Tests

A test procedure shall be devised to cover the requirements of Section 3.4 of this specification. This procedure shall define inspections, functional test procedures, test conditions, and test equipment and equivalents to be used.

4.2 Performance Tests

A test procedure shall be devised to cover the requirements of Section 3.2 of this specification. This procedure shall define inspections, functional test procedures, test conditions, and test equipment and equivalents to be used.

5. PREPARATION FOR DELIVERY

Not applicable.

6. NOTES

6.1 Intended Use

These preliminary design requirements are the result of an instrument definition study and are not intended for final equipment procurement purposes.

EXHIBIT III

PRELIMINARY-DESIGN REQUIREMENTS FOR THE TEMPERATURE CONTROL FLUX MONITOR TRANSDUCER ASSEMBLY

1. SCOPE

This preliminary-design document establishes the requirements for the Mariner Mars 1969 Temperature Control Flux Monitor (TCFM) Transducer Assembly as defined in Applicable Document No. (1).

1.1 Classification

The TCFM transducer assembly is classified as a constant temperature, guarded cavity, absolute thermal radiation detector.

2. APPLICABLE DOCUMENTS

The following documents are applicable to and form a part of this design requirement.

(1) California Institute of Technology, "Cost Plus A Fixed Fee Type Research and Development Contract," (Subcontract under NASA Contract NA7-100), Task Order No. RD-29, Contract No. 951726, 30 September 1965, Exhibits 1, 2 and 3.

(2) TRW Document No. 06988-6002-R000, Exhibit I, "TCFM Electronic Control Assembly Preliminary-Design Requirements," January 1967.

(3) TRW Document No. 06988-6002-R000, Exhibit II, "TCFM Operational Support Equipment Assembly Preliminary-Design Requirements," January 1967.

(4) JPL Specification No. 20045/200E, "Detail Specification - D Series, Mark 1 Connectors, Miniature, High Reliability," 6 November 1962.

(5) JPL Document No. MM69-3-260, "MM69 Electrical Interface and Electrical Grounding."

(6) JPL Document No. 76, "2D0800 Project, S/C System Environmental Test Program Requirements," 6 May 1966.

(7) JPL Document No. 30236A, "Environmental Test Specifications, RFI," 20 October 1966.

3. REQUIREMENTS

3.1 General Requirements

3.1.1 Compatibility

The TCFM transducer assembly shall be physically and functionally compatible with Mariner Mars 1969 Spacecraft system requirements as defined in Applicable Document No. (1). The TCFM transducer assembly shall also be functionally and electrically compatible with the TCFM Electronic Control Assembly and TCFM Operational Support Equipment Assembly, as defined in Applicable Documents No. (2) and (3).

3.1.2 Components

The TCFM transducer assembly shall consist of the following components:

a) Receptor Subassembly

b) Thermal Guard Subassembly

c) Case and Mount Subassembly

3.1.3 Functional Requirements

3.1.3.1 Functional Concepts

The TCFM transducer conical receptor and receptor thermal guard shall both be maintained at a preset reference temperature ranging from 10°C to 140°C. The reference temperature shall be such that thermal radiation emitted from the receptor shall be greater than that absorbed by the receptor from incident thermal radiation. The energy required to maintain the receptor at the reference temperature in addition to that absorbed from incident radiation shall be supplied by means of an electrical heater. The transducer shall sense any temperature deviation of its receptor and thermal guard greater than 0.1°C from the preset reference temperature.

3.2 Design Requirements

3.2.1 Receptor Subassembly

3.2.1.1 Receiver Element

The thermal radiation receiver shall be of the conical cavity type, having a base aperture with a diameter of 0.435 inch ± 0.005 inch, and an included apex angle of 23.5°C ● 0.5°. The cone material shall be C. P. Silver with a uniform wall thickness of 0.005 inch ± 0.001 inch.

3.2.1.2 Heater

The conical receptor shall be provided with an electrical heating element wound on its outer surface. A close spaced bifilar winding shall be utilized which shall have a resistance ± of 1000 ohms ± 10 ohms. The material shall have a temperature coefficient of not greater than 0.00004 ohms per ohm-°C. The winding shall be located within the first 25 percent of the cone slant length measured from base to apex.

3.2.1.3 Temperature Sensor

The conical receptor shall be provided with an electrical resistance temperature sensing element would on its outer surface. A close spaced bifilar winding of C. P. Nickel wire shall be utilized. The resistance of the winding shall be 600 ohms at 20°C and shall be matched in resistance to the thermal guard temperature sensor (Section 3.2.2.3.3) to within ± 0.5 ohm at 150°C. The temperature sensor winding shall be located within the first half of the cone slant length measured from base to apex.

3.2.1.4 Thermal Coating

The internal surface of the conical receptor shall be coated with a high-emissivity material. The material and method of application shall be separately specified at a later time.

3.2.2 Thermal Guard Subassembly

3.2.2.1 Thermal Guard

The thermal guard shall be designed to enclose and support the receptor subassembly in such a manner that the thermal energy exchange between the two shall be a practical minimum. The thermal guard shall be designed to provide a temperature gradient of less than 0.5°C throughout its structure under all conditions of steady-state operation. The surfaces of the thermal guard shall be gold electroplated to minimize radiant energy interchange between the guard and the conical receptor and between the guard and the exterior case subassembly.

The thermal guard shall be designed to provide a uniform annular gap width of no greater than 0.0005 inch between the conical receptor base rim and the adjacent surface of the thermal guard at the aperture of the transducer.

3.2.2.2 Heater

The thermal guard shall be provided with a wound-on resistance heating element to maintain its temperature uniformly at the present reference temperature. A uniformly-spaced bifilar winding shall be utilized, which shall have a resistance of 1000 ohms ± 1 ohm at 20°C. The temperature coefficient of resistance of the material shall be not greater than 0.00004 ohm per ohm-°C.

3.2.2.3 Temperature Sensor

The thermal guard subassembly shall be provided with electrical resistance temperature sensing elements. Three independent sensors are required, performing, respectively, the following three functions:

a) Guard reference temperature measurement

b) Guard reference temperature control

c) Guard cone temperature deviation control

The sensors shall be wound on a single cylindrical spool of 0.005 inch ± 0.001 inch thickness of C. P. Silver, which shall be designed to fit the thermal guard and be attached to it with minimum practical thermal resistance.

3.2.2.3.1 Guard Reference Temperature Measurement Sensor

The guard reference temperature measurement sensor shall utilize close spaced bifilar windings of C. P. Platinum wire. The resistance of the sensor shall be 100 ohms ± 1 ohm at $0^{o}C$.

3.2.2.3.2 Guard Reference Temperature Control Sensor

The guard reference temperature control sensor shall utilize close spaced bifilar windings of C. P. Nickel wire. The resistance of the sensor shall be 600 ohms ± 1 ohm at $20^{o}C$.

3.2.2.3.3 Guard Cone Temperature Deviation Control Sensor

The guard cone temperature deviation control sensor shall be wound on a silver spool of 0.005 inch ± 0.001 inch thickness. The sensor shall utilize close spaced bifilar windings of C. P. Nickel wire. The resistance of the sensor shall be matched to the resistance of the temperature sensor described in Section 3.2.1.3 to within 0.5 ohm at $150^{o}C$.

3.2.3 Case and Mount Subassembly

3.2.3.1 Case and Mount

The TCFM transducer case and mount subassembly shall be designed to mechanically support and enclose the thermal guard subassembly. The subassembly shall be provided with a mounting flange to attach the transducer to an external bracket and shall be designed to thermally isolate the case from the supporting bracket. The mounting flange shall be fitted with an electrical connector receptacle and shall conform to the dimensional requirements of Section 3.4.1.

3.2.3.2 Electrical Connector

The TCFM transducer case and mount subassembly shall be equipped with an electrical receptacle of the quick disconnect variety. The receptacle shall contain provision for no less than 15 pin connectors, shall be compatible with the requirements of Applicable Document No. 4 and shall be commensurate in weight and dimensions with the TCFM transducer design.

3.2.3.3 Thermal Design

The case and mount subassembly shall be designed to control the loss of power from the thermal guard to the space environment. The thermal guard shall not require electrical power in excess of 0.400 watt nor less than 0.050 watt to be maintained at a reference temperature of $140^{o}C$ when subjected to solar irradiation in the range of 0.055 to 0.150

watt per square centimeter. Thermal conduction through the structural support and electrical leads to the mounting flange shall be reduced to the practical minimum.

3.3 Performance Requirements

3.3.1 Operational Temperature Range

The TCFM transducer assembly shall be capable of sustained operation over a temperature range of 10°C to 140°C.

3.3.2 Incidental Thermal Flux Range

The TCFM transducer shall be capable of sensing incident flux levels of from 0.055 to 0.150 watt per cm^2.

3.3.3 Resolution

The TCFM transducer shall be capable of sensing an incremental change of 0.1 percent in the incident flux level.

3.3.4 Accuracy

The TCFM transducer shall be capable of measuring the incident flux within its operational range to an absolute accuracy of ± 1.0 percent.

3.3.5 Spectral Sensitivity

The sensitivity of the TCFM transducer shall be uniform to within 0.5 percent for all wavelengths of incident radiation between 0.2 micron and 40 microns.

3.3.6 Angular Sensitivity

The response of the TCFM transducer shall be proportional, within 0.5 percent, to the cosine of the angle of incident radiation.

3.3.7 Time Constant

Upon the application of a positive step change in incident flux of not more than 0.140 watt per cm^2, the TCFM transducer, in conjunction with the TCFM electronic control assembly, shall require a period of not more than 5 seconds to reach within 1 percent of the final new power value.

3.4 Interface Requirements

3.4.1 Mechanical

The TCFM transducer assembly shall be provided with a mounting flange of the following dimensions: 1.750 inch ± 0.010 inch outside diameter; 1.000 inch ± 0.010 inch inside diameter; 0.050 inch ± 0.002 inch material thickness. The flange shall contain four equally spaced holes of 0.115 + 0.004/ - 0.001 inch diameter on a basic diameter of 1.500 inch ± 0.010 inch.

3.4.2 Electrical

All electrical interface requirements of the TCFM transducer assembly shall be governed by Applicable Document No. 5.

3.4.3 Remote Operation

The TCFM transducer assembly shall be capable of operation when connected to the TCFM electronic control assembly with a 10 foot long interconnecting electrical cable.

3.5 Reliability

The TCFM transducer assembly shall be capable of operation in space at temperatures up to 140°C for a minimum period of 150 days. Failure of the assembly shall in no way affect the spacecraft or any of its components.

3.6 Dimensions and Weight

3.6.1 Dimensions

The TCFM transducer assembly shall have dimensions not greater than the following quantities:

a) Outside diameter (less mounting flange) - 1.25 inches

b) Length (less connector) - 2.50 inches

3.6.2 Weight

The weight of the TCFM transducer assembly, including electrical receptacle, shall not exceed 0.25 pound.

4. QUALITY ASSURANCE PROVISIONS

4.1 Environmental Tests

The TCFM transducer assembly shall be subjected to the environmental tests defined in this section. Immediately after subjection to any of these environmental tests, the assembly shall operate satisfactorily under the performance test conditions defined in Section 4.2.

4.1.1 Thermal

The TCFM transducer assembly shall be capable of operation, within the specified performance requirements of Section 3.3, during and after having been exposed to the following time-temperature test:

Operation at temperatures up to 170°C for a continuous period of 288 hours (12 days) at a reduced pressure of 10^{-5} torr or lower.

4.1.2 Dynamic

4.1.2.1 Vibration

The TCFM transducer assembly shall be subjected to the three-part vibration test specified below while positioned so as to receive vibrational energy inputs in a direction parallel to the launch vehicle axis of thrust and in the two other orthogonal directions. The assembly shall operate during the tests in the launch mode and shall function in accordance with the specified performance requirements of Section 3.3.

Part 1: The assembly shall be subjected to sinusoidal vibration at frequencies from 1 to 15 cps in each axis. The magnitude of the vibration shall be ± 1.5 inches double amplitude displacement from 1 to 4.4 cps, and 2.1 g rms (3.0 g peak) from 4.4 to 15 cps. The sweep from 1 to 15 cps shall require 1.5 minutes and be repeated twice.

Part 2: The assembly shall be subjected to sinusoidal vibration at frequencies between 10 and 2000 cycles per second. The sweep rate shall be logarithmic at 1 minute/octave. The amplitudes over the frequency range are shown in Figure 1 for the various axes.

Part 3: The assembly shall be subjected to random vibration consisting of a shaped spectrum for one minute. The vibration shall be of Gaussian amplitude distribution except that instantaneous peak amplitudes of greater than 3 sigma shall be suppressed. The spectral shape is defined in Figure 2. If the exact spectrum specified is obtained the wideband level shall be 6.4 g rms. However, the controlling test parameters shall be the specified power spectral density (PSD) levels at the indicated frequencies.

4.1.2.2 Acoustic

The TCFM transducer assembly shall be subjected to an acoustic environmental test while in the three orthogonal positions described in the first paragraph of Section 4.1.2.1. The assembly shall operate during the test in the launch mode and shall function in accordance with the performance requirements of Section 3.3. The assembly shall be mounted in the test chamber with a low frequency suspension system whose lowest frequency shall be 20 cps or less. The assembly shall be subjected to a reverberant (random incident) sound field within the test chamber. The test shall consist of shaped acoustic noise for 60 seconds. The special shape shall be as specified in Figure 3. If the exact spectrum specified is obtained, the overall sound pressure level (SPL) will be approximately 151 db (ref 2×10^{-4} dynes/cm^2); however, the controlling test parameters shall be the specified spectral levels within each 1/3 octave band.

Test tolerances shall be as defined in Applicable Document No. 6. No shock test shall be performed, since there are no pyrotechnics in the vicinity of the TCFM transducer assembly.

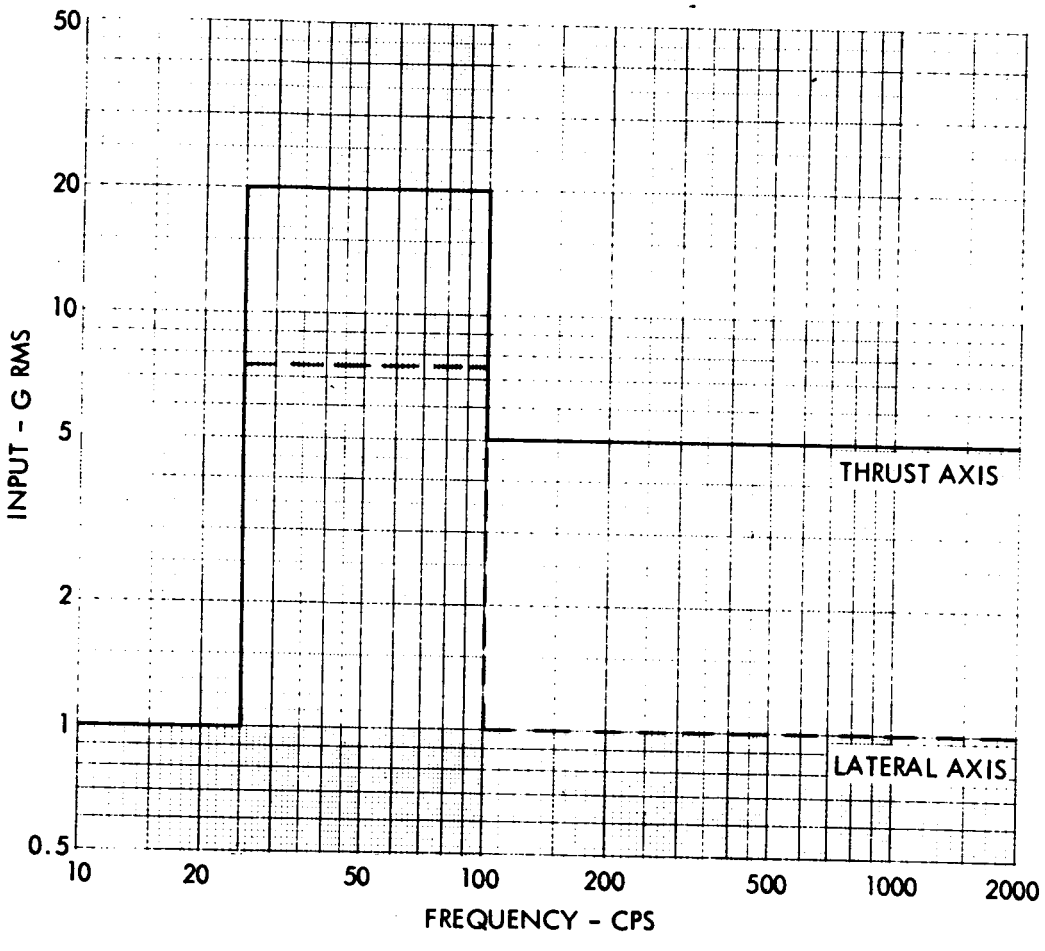

Figure 1. Preliminary TCFM TA Sine Test

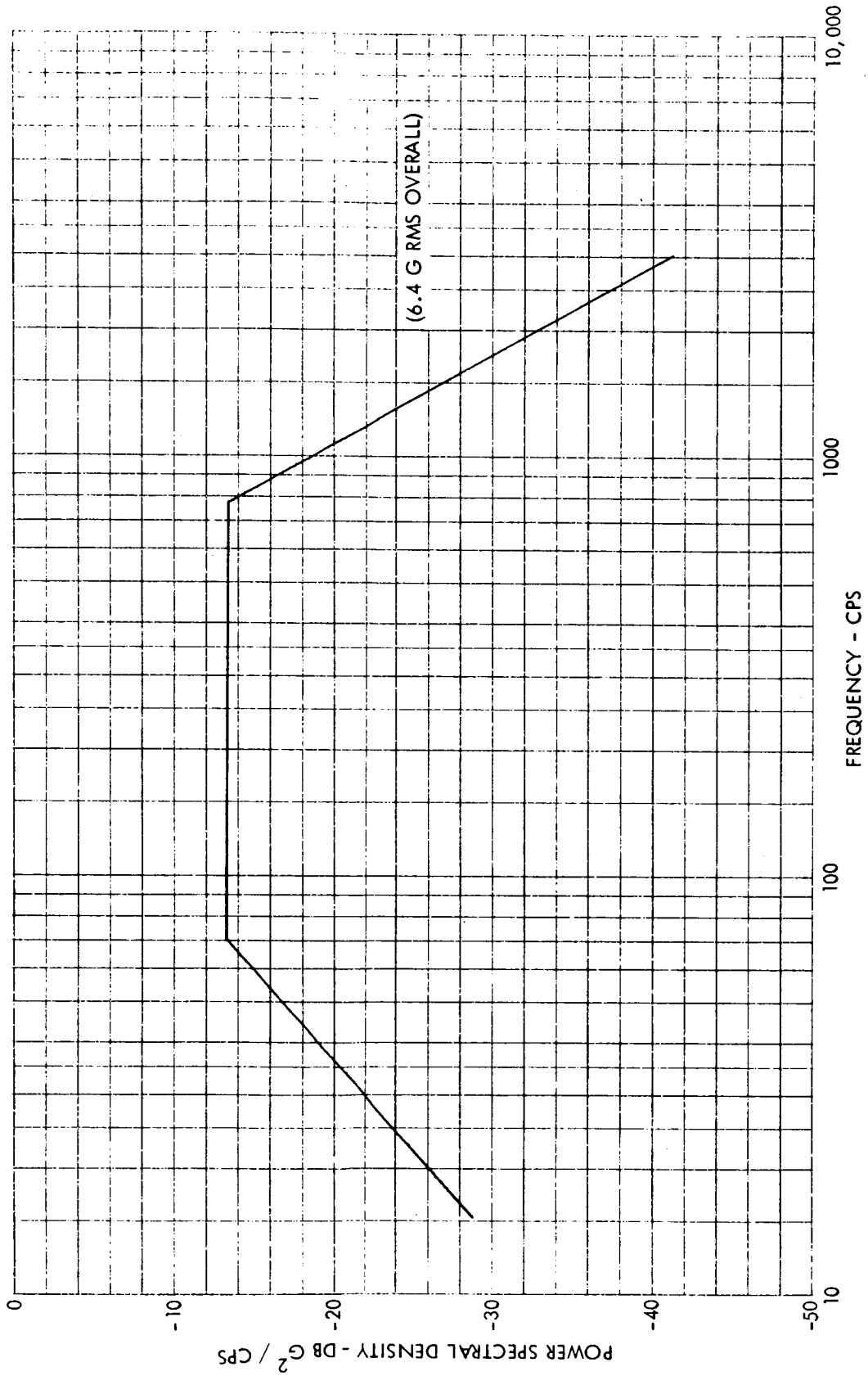

Figure 2. Preliminary TCFM TA Noise Test

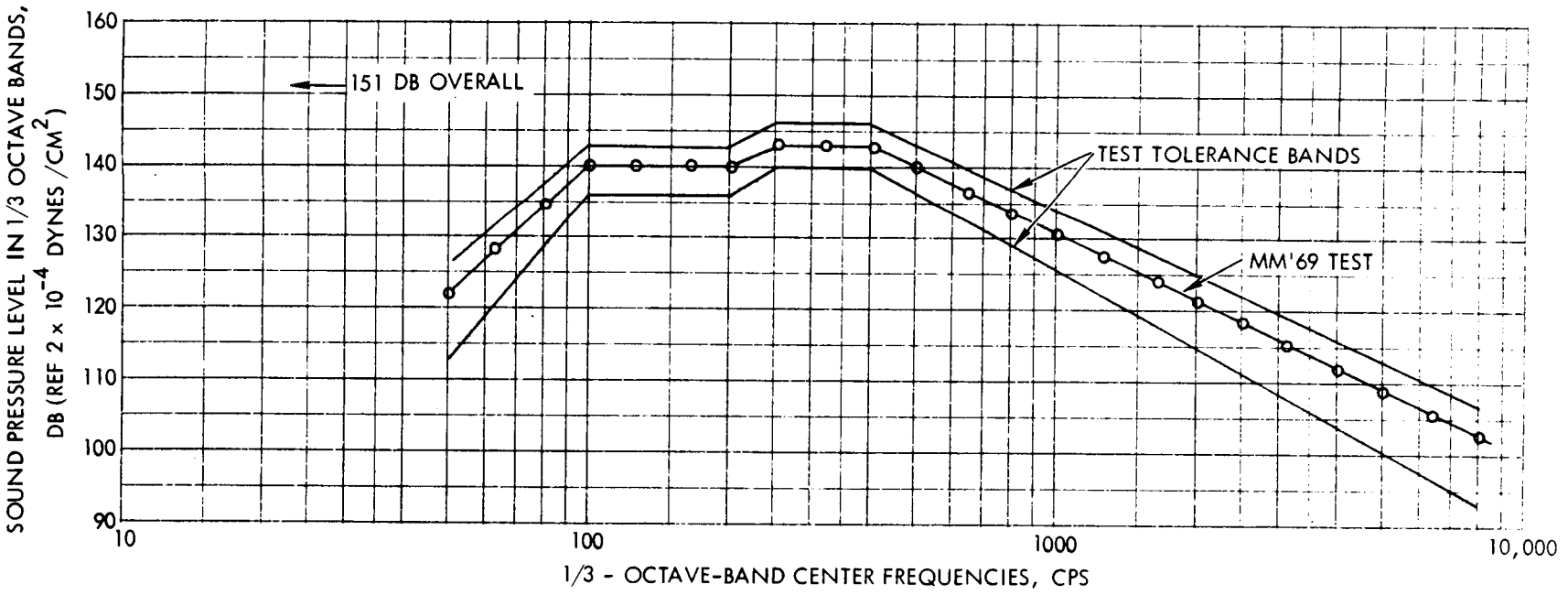

Figure 3. MM'69 TA Acoustic Test Requirements

4.1.3 Radio Interference

All radio-interference test requirements of the TCFM transducer assembly shall be governed by Applicable Document No. 7.

4.2 Performance Tests

The TCFM transducer assembly, connected to a properly adjusted TCFM electronic control assembly, shall be mounted in a hohlraum which is evacuated to a pressure of not greater than 10^{-6} torr.

a) The hohlraum temperature and the TCFM reference temperature shall be set to a nominal test temperature of 140°C. The exact value of this test temperature shall be determined to within ± 0.1°C. When thermal equilibrium is reached, the TCFM electronics control assembly shall be adjusted, if necessary, so that the electrical power to the receptor heater of the TCFM transducer assembly shall be zero.

b) The hohlraum temperature shall then be decreased to a value such that its emitted flux shall be approximately 75 percent of that emitted in Step a) above. An equilibrium the indicated electrical power to the receptor heater shall be within 1.0 percent of the value computed by the following relationship:

$$W_{electrical} = (\epsilon\sigma T^4)_{transducer} - (\epsilon\sigma T^4)_{hohlraum}$$

where the two effective emissivity values shall be determined to an accuracy of 0.2 percent.

c) The procedure of Step b) shall be repeated for levels of approximately 50 percent and 25 percent of the initial value of hohlraum flux specified in Step a).

d) The specified performance test shall be conducted in accordance with a detailed procedure to be outlined at a later time in an approved document.

5. PREPARATION FOR DELIVERY

Not applicable

6. NOTES

6.1 Intended Use

These preliminary-design requirements are the result of an instrument definition study and are intended to control the detailed design of the TCFM transducer assembly.

7. DESIGN REVIEW MINUTES

Subject: Minutes of Conceptual Design Review - Thermal Control Flux Monitor (TCFM)

From: C. Saunders

To: Distribution

The design review was held on January 12, 1967, in R1/1096c. Participants are listed in Attachment 1.

The following subjects were discussed:

1. Purpose of the design review
2. Background and systems requirements
3. Alternate approaches
4. JPL design
5. TRW design

Questions, alerts, and action items resulting from the design review are listed below:

1. Yamasaki - Proposed to use thermistors instead of wires around the heater and sensor to achieve greater sensitivity.

   Answer

   The transducer is not part of this design review, but the mechanical configuration does not allow for this.

2. Hamilton - Suggested using bronze or platinum wire instead of nickel wire as in the present design.

   Answer

   Question referred to R. Clifford.

3. Yamasaki - Questioned if the number of bits in the register are sufficient to handle the dynamic range and accuracy.

   Answer

   Moede - Yes, however this question was considered as an alert.

4. Ettinghoff - Questioned the possibility of noise pickup between error amplifier and power gates if the noise level is sufficiently large.

Answer

Moede - This possibility has been investigated. Synchronous detection technique eliminates this problem.

5. Nicklas - Questioned the possibility of distortion of the square power wave which would reduce accuracy.

Answer

Moede - This could be a problem, but this error appears to be on the order of 0.08%.

6. Ettinghoff - Open-loop technique presently used requires a large quantity of hardware. Would an analog loop controlling the heater power with AD converter for TM interface reduce the quantity of hardware and design time?

Answer

This question will be answered after completion of a study requested at this design review (item 8).

7. Moede - Questioned if integration is required using analog approach; if so, how can this be accomplished.

Answer

This question will be answered after completion of a study requested at this design review (item 8). Integration is required.

8. Ettinghoff - Requested a study to be conducted of the system using the analog approach.

This is an action item for K. Hamilton. This study should be accomplished in approximately 1 week.

9. Nicklas - Suggested that stability compensation may be required for digital or analog system.

This item is considered as an alert and will be determined during the system design phase.

10. Yamasaki - Suggested using synchronous demodulator with band width filters to eliminate the square wave.

Answer

Saunders - This approach would only be justified in a continuous system. More hardware required.

11. Yamasaki - Stated that in an analog system it would be difficult to know the error accompanying each data measurement. The digital system has this feature automatically.

Distribution:

A. Rosen
M. Ettinghoff
R. Yamasaki
J. Nicklas
M. Valkass
L. Moede
R. Clifford
H. Suer
R. Endara
K. Hamilton

ATTACHMENT 1

RECORD OF ATTENDANCE AT DESIGN REVIEW MEETING

MEETING PLACE - Bldg. R1 Room 1096

EQUIPMENT: JPL Temperature Control Flux Monitor for Mariner Mars 1969

DESIGN REVIEW NUMBER: 1 DATE: December 12, 1966

ASSIGNED SPECIALTY	NAME OF PARTICIPANT	SIGN-IN	BLDG & ROOM
1. Chairman	C. Saunders	C. Saunders	R1/1078
2. Technical Secretary	M. Valkass	M. Valkass	R1/1058
3. Sr. Design Engr	K. Hamilton	K. Hamilton	
4. Design Specialist	M. Ettinghoff	M. Ettinghoff	R1/1070
5. Control Specialist	Dr. J. Nicklas	J C Nicklas	R2/1144
6. Sr. Design Engr	R. Endara	R Endara	R1/1078
7. Design Consultant	R. Yamasaki	R.G. Yamasaki	R1/2028
8. Program Management	Dr. H. Suer	H S Suer	R1/1196
9.			
10.			
11.			
12.			
13.			
14.			
15.			
16.			
17.			
18.			
19.			
20.			
21.			
22.			
23.			
24.			
25.			
26.			
27.			
28.			
29.			
30.			

Sheet ____ of ____